ROLE OF SPONTANEOUS BURSTS IN FUNCTIONAL PLASTICITY AND SPATIOTEMPORAL DYNAMICS OF DISSOCIATED CORTICAL CULTURES

A Thesis
Presented to
The Academic Faculty

by

Radhika Madhavan

In Partial Fulfillment
of the Requirements for the Degree
Doctor of Philosophy in the
Interdisciplinary Bioengineering program
Department of Biomedical Engineering

Georgia Institute of Technology
August 2007

ROLE OF SPONTANEOUS BURSTS IN FUNCTIONAL PLASTICITY AND SPATIOTEMPORAL DYNAMICS OF DISSOCIATED CORTICAL CULTURES

Approved by:

Dr. Steve M. Potter, Advisor
School of Biomedical Engineering
Georgia Institute of Technology

Dr. Stephen P. DeWeerth
School of Biomedical Engineering
Georgia Institute of Technology

Dr. Rober J. Butera
School of Electrical and Computer Engineering
Georgia Institute of Technology

Dr. Eric Schumacher
School of Psychology
Georgia Institute of Technology

Dr. Peter Wenner
Department of Physiology
Emory University, School of Medicine

Date Approved: May 24th, 2007.

To my parents, my pillars of strength

ACKNOWLEDGEMENTS

My years in graduate school can be described as a constant process of learning and unlearning and numerous people have seen me through these exciting years. I would like to start by acknowledging my advisor Dr. Steve Potter for his continuous and active support in all my projects. Steve's open mindedness about science and encouraging spirit allows for the free exchange of ideas and continues to be an inspiration. His undying enthusiasm infuses vigor and motivates one to excel. In particular, I would like to thank him for teaching me to adhere to scientific integrity, to check and recheck for errors; this is something I will carry with me for the rest of my academic career. In spite of various demands on his time, Steve has always made time for me. On the multiple occasions when I have called him up on weekends with scientific or personal problems, he has readily obliged me with answers. Working with him has been a rewarding experience and I hope that we will continue to discuss and collaborate on various projects in the future.

It has been a pleasure working with the Potter group. I would like to recognize the assistance of all the present and past members of the group; Tom, Peter, Mark, Komal and John who have contributed to create a lively and collaborative atmosphere in the lab. I would like to thank my colleagues, Zenas Chao and Douglas Bakkum, who have literally shared my life at graduate school. We have discussed and deliberated about several ideas and techniques, many that have turned into successful collaborative projects. A special thanks to Daniel Wagenaar; my work with him formed the beginnings of my research work at the lab. I would also like to acknowledge the work of several very smart undergraduate students, whom I have had the pleasure of mentoring. Particularly,

Bhavesh Mehta's assistance in the immunostaining studies and Yi Xiao's input in the burst-quieting project have helped further my research goals. Various technical assistants and lab staff have made my work proceed smoothly. I would like to acknowledge Bryan Williams for being an excellent laboratory manager, Eno Ekong for helping me through immunohistochemistry and Douglas Swehla for dissection and other cell culture related problems.

The collaborative atmosphere of the Neuroengineering laboratory (Neurolab) allows for the exchange of expertise between various groups. During my graduate work, I have had the opportunity to work and interact with many members of the Neurolab and have benefited immensely from their advice. In particular, I would like to acknowledge Kacy Cullen for providing prompt answers to any questions related to cell culture, Jim Ross for helping me with electrode testing and Dr. Michelle Laplaca's group for sharing tissue and cell culture equipment with me.

The Georgia tech community provides state-of-the-art facilities and an excellent environment conducive for scientific endeavor. I would like to thank the staff of the Biomedical and Bioengineering departments for efficiently managing all my administrative issues. Specially, I would like to thank Chris Ruffin, Amber Burris, Sandra Wilson and Beth Bullock for promptly attending to all my queries.

I would like to thank my thesis committee members for their guidance and creative ideas that have helped shape my thesis work. A special thanks to the Schlumberger Foundation for awarding me with the *Faculty of the Future* grant to support me during my graduate study. Other funding agencies include the National

Institutes of Health, Center of behavioral neuroscience, the National Science Foundation, Georgia Research Alliance and the Whitaker foundation.

This work is dedicated to my parents, whose undying faith in my abilities has always brought out the best in me. I know that they have missed me a lot during these years (and so have I) and I would like to specially thank them for their immense patience and understanding. I would also like to thank my sister for always being there for me and literally holding my hand through these five years. Also, I am grateful to my extended family and friends for their constant support and encouraging words.

Radhika Madhavan

April, 2007.

TABLE OF CONTENTS

LIST OF TABLES

Page

LIST OF FIGURES

Page

LIST OF ABBREVIATIONS

ASDR	Array-wide spike detection rate
APV	2-amino-5-phosphonovaleric acid
BAM	Burst activity matrix
BF	Burstiness factor
BMI	Bicuculline methiodide
CAT	Center of activity trajectory
CNQX	6-cyano-7-nitroquinoxaline-2,3-dione
DIV	Days *in vitro*
GABA	Gamma-amino butyric acid
IBI	Inter-burst interval
I/O	Input-output
IPI	Inter-probe interval
MAP2	Microtubule associated protein
MEA	Multi-electrode array
MCS	Multichannel systems
PTX	Picrotoxin
spsa	Spikes per second array-wide
TTX	Tetrodotoxin

SUMMARY

What changes in our brain when we learn? This is perhaps the most intriguing question of science in this century. In an attempt to learn more about the inner workings of neural circuitry, I studied cultured 2-dimensional networks of neurons on multi-electrode arrays (MEAs). MEAs are ideal tools for studying long-term neural ensemble activity because many individual cells can be studied continuously for months, through electrical stimulation and recording. One of the most prominent patterns of activity observed in these cultures is network-wide spontaneous bursting, during which most of the electrodes on the MEA show elevated firing rates. Unlike *in vivo*, global bursting *in vitro* persists for the lifetime of the culture. We view the persistence of spontaneous bursting *in vitro* as a sign of arrested development due to deafferentation. Substituting distributed electrical stimulation for afferent input transformed the activity in dissociated cultures from bursting to more dispersed spiking, reminiscent of activity in the adult brain. Additionally, electrical burst suppression reduced the variability in neural responses making it easier to induce and detect functional plasticity caused by tetanic stimulation. This suggests that spontaneous bursts interfere with the effects of external stimulation and that a burst-free environment leads to more stable connections and predictable effects of tetanization. Moreover, this culture model continuously receives artificial sensory input in the form of background electrical stimulation, and so better resembles the intact brain than isolated (non-continuously stimulated) cultures. The proportion of GABAergic neurons in the cultures was significantly increased ($p<1e-2$, paired t-test) after 2 days of burst-quieting, suggesting that burst suppression operated

through the homeostatic control of inhibitory neurotransmitter levels. We also studied the role of spontaneous bursts as potential carriers of information in the network by clustering these spatiotemporally diverse bursts. Spontaneous burst clusters were stable over hours and tetanic stimulation significantly reorganized the distribution of the clusters. The plastic nature of spatiotemporally diverse bursts together with their stability in the absence of external stimulation recommends these recurring patterns as memory substrates in cortical networks. In summary, this body of work explores the rules of network-level functional plasticity and provides the input (electrical stimulation) – output (spatiotemporal neural activity patterns) mappings for behavioral studies in embodied hybrid systems. The results of this study may also have clinical implications in the development of sensory prostheses and treatment of diseases of aberrant network activity such as epilepsy.

CHAPTER 1

INTRODUCTION

The brain is perhaps the most complex structure in the universe; complex enough to create a 3-dimensional landscape from light that falls on a pair of 2-dimensional retinae. The human brain consists of 10^{11} neurons, intricately connected to each other through ~10^{15} synapses. While we are born with a practically complete set of neurons, the connections between them are determined by learning; external stimuli from sensory neurons cause patterns of nerve impulses that can alter the strength of coupling between the neurons. This process of dynamically changing connection strengths was described in a simple rule by Donald Hebb in 1949: 'When an axon of cell *A* is near enough to excite a cell *B* and repeatedly or persistently takes part in firing it, some growth process or metabolic change takes place in one or both cells such that *A*'s efficiency, as one of the cells firing *B*, is increased' [1]. While this rule describes the process of 'learning' at a single synapse, it does not however explain how such subtle changes in synaptic strength can cause modifications at the network level to result in changes in behavior.

1.1 Dissociated cultures on Multi-electrode arrays

Storage of information as long term modification is commonly studied as a synapse-centric mechanism [2]. These studies provide the necessary insight into understanding how the precise timing of spikes at the pre-synaptic and post-synaptic terminals of two neurons interacts to strengthen or weaken connections between them. However, they provide insufficient information about how these synaptic rules could

extend to the storage of information in an ensemble of neurons in the brain. Thus, a better understanding of the memory mechanisms may require a shift from exclusive focus on isolated synapses. Knowledge about how, when and where **networks of neurons** allow synaptic modifications might be essential.

This work provides evidence for network plasticity by mapping the changes in the spatiotemporal firing patterns of thousands of cells in highly interconnected, 2-dimensional cortical cultures. Such network-level studies could provide tools to fill the gap between cellular level synaptic plasticity and higher-level interactions in the brain that result in behavior. Many disorders of the brain involve malfunctions in the mechanisms of learning, storing and recalling memories. By enabling a deeper understanding of the fundamental mechanisms by which plasticity changes the ability of cortical networks to store memories, this work offers new methods for potential treatments of these disorders.

Over the last couple of decades, technology for neuronal monitoring has been focused on recording from a population of neurons simultaneously using multi-channel electrode arrays [3-5]. Multi-electrode arrays (MEAs) allow for the sampling of activity dynamics of a small network of cortical neurons through simultaneous stimulation and recording while preserving the resolution to measure single cell activity. Developed in late 1970's by Jerry Pine [4] and Gunter Gross [6], MEAs consist of a grid of substrate-embedded electrodes on which a network of neurons can be cultured (Figure 1.1). Since the electrodes are addressable through electrical stimulation and recording, they provide a unique 2-way interface for studying functional neural plasticity; continuous stimulation patterns (input) can be fed to the cultured network and the stimulus-evoked responses of

the network (output) can be simultaneously examined. In addition, MEAs can be also used in conjunction with more conventional methods of recording electrical activity like patch-clamp or functional imaging. Thus, the study of cultured neuronal networks on MEAs provide for influencing and monitoring, long term activity of neuronal networks, in the time scales of milliseconds to months and with the resolution from individual synapses to ensemble connectivity.

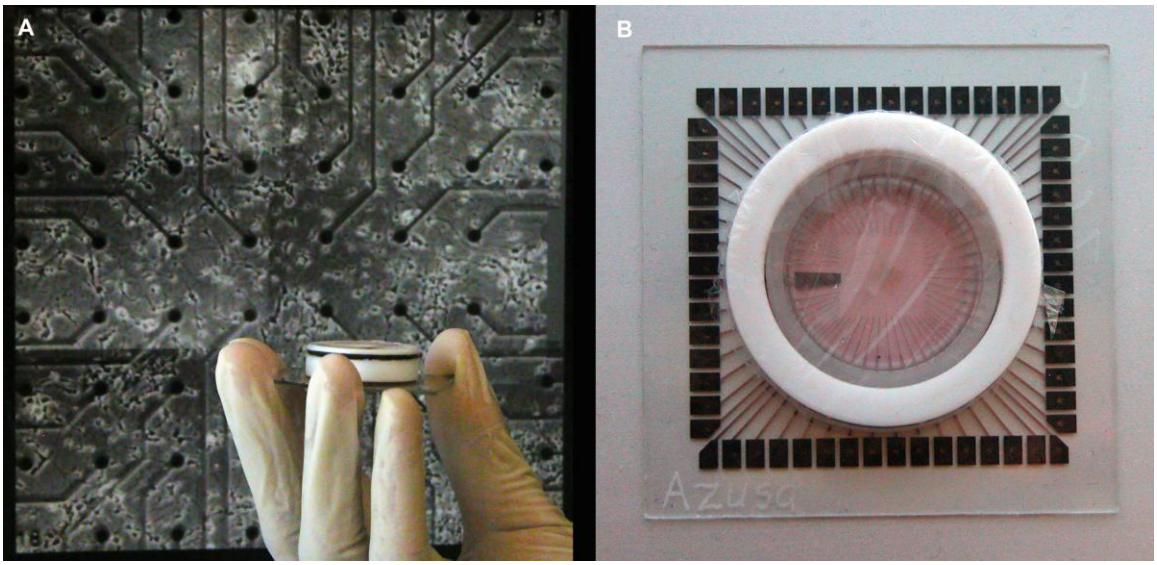

Figure 1.1: Multi-electrode arrays (MEAs) A. MEA held up with a background image of neurons on the array. **B.** MEA, with Teflon membrane covering and neurons plated on the center of the array (~1.5mm^2 area of electrodes, typically 200µm spacing between electrodes).

Dissociated cortical networks cultured *ex vivo* have proven to be extremely helpful in the study of neural function by reducing the complexity of the *in vivo* brain. Studies on cultured networks have formed the basis of our understanding of ion channels, receptor molecules and synaptic plasticity [2, 7-10]. Most of our knowledge about the mechanisms involved in long-term potentiation (LTP) has been derived from studies using *in vitro* networks [2, 8]. Though animal models are in abundant use, *in vitro* networks continue to be important tools for understanding neuronal functions due to their

enhanced accessibility for detailed electrophysiology, imaging, pharmacology and genetic manipulations.

Studying network-level learning and memory in cultured networks *in vitro* has many advantages over *in vivo* studies. *In vitro* networks allow for enhanced accessibility to the networks being studied compared to the *in vivo* brain. Detailed electrophysiology and imaging *in vivo* requires the animal being studied to be immobilized or anaesthetized [11-14] but these techniques may have adverse effects on the phenomenon being studied [15, 16]. As an example, motility of dendritic spines was reversibly blocked by anesthetics at concentrations at which they are clinically effective [17]. In awake animals, *in vivo* recordings suffer from motion artifacts even in the best of conditions. In addition, the insertion of electrodes in the brain can cause damage to neural tissue and finally post mortem analysis of brain tissue from experiments *in vivo* provide only one time-point per animal making it difficult to study dynamics over longer time-scales. In contrast, *in vitro* cultured networks afford for detailed observation and manipulation at cellular as well as network levels over different timescales from milliseconds to months [18, 19], while providing complete control over the inputs to the network. Extracellular recordings from dissociated cortical networks *in vitro* using substrate-embedded electrodes on MEAs offer a non-invasive method to track the dynamics of the emergent properties of an ensemble of neurons over months.

Alternate *in vitro* models, like brain slices, retain the organization of the brain but it is difficult to maintain these cultures for long periods due to cell death caused by insufficient diffusion of nutrients in the slice. This reduces the utility of this model in studies involving long term (> couple of weeks) monitoring of network activity. Though

dissociated monolayer networks do not possess the 3-dimensional architecture of the brain, they retain many of the electrical and morphological properties of cortical networks *in vivo* [20, 21]. These networks demonstrate extensive functional connectivity and sensitivity of that connectivity to activity. Dissociated networks *in vitro* are unlike the brain in that they lack the functional architecture of connections in the brain, where neurons reside in specific regions and project their processes in a specific manner. But the connectivity in these networks is not random; dissociated cultures develop physiological responses to neurotransmitters and self-organize into spontaneously active networks. Moreover, dissociated cultures can be maintained for months [22] making them ideal models for the study of the emergence, organization and dynamics of neuronal groups over months, without the presence of uncontrolled interfering input variables.

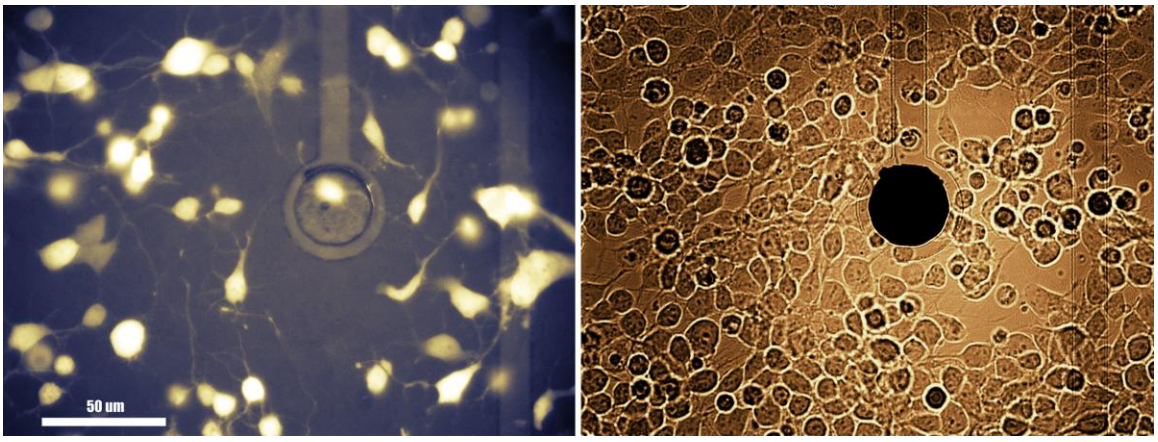

Figure 1.2: Density of dissociated cultures on MEAs. Each electrode has at least 5-10 cells in its close vicinity. The panel on the right shows an image of all the cells around an electrode. The panel on the left shows the same image with a portion of the neurons expressing yellow-fluorescent protein (YFP). Picture obtained from Peter Passaro.

MEAs have been used to study the electrical activity of a variety of tissue preparations for a plethora of applications. Cultured neuronal networks from various brain regions like the cortex [18, 23-26], hippocampus [24], retina [27, 28] and spinal

cord [29] have been studied extensively using this technology. These studies have led to valuable insights into the network correlates of learning and memory [30-32], mechanisms involved in visual perception [33-35], emergence and dynamics of spontaneous activity [23, 26, 36-40] and neural regeneration [41]. In addition, MEAs have also been used for drug screening by evaluating the action of various neurotoxins on the electrical activity of the network [42, 43]. Functional plastic changes in response to a local tetanic stimulation have been studied in much detail in dissociated cortical preparations on MEAs [30, 31, 37, 44]. Jimbo *et al.* (1999) concluded that potentiation or depression of activity in neuronal networks, caused by simultaneous tetanic stimulation at two electrodes, was not neuron-specific but pathway-specific. Marom's group has claimed to induce learning in dissociated cortical neurons [32]. They report that networks can be made to respond reliably to test stimuli by repetitively stimulating the network with a slow tetanus (0.3-1Hz). Ruaro *et al.* (2005) demonstrated that the network could 'learn' to differentiate complex patterns by tetanization at different corners of the MEA. But the results from these studies, demonstrating plastic changes in neuronal networks, are controversial since we and others have not been able to successfully replicate these results [45, 46]. In addition, these studies used very few stimuli, only one or two at a time and slow rates, to study functional changes.

We, in the Potter group, propose that in order to understand and harness the capacity of the network, it is necessary to increase the bandwidth of possible inputs and outputs in the network. The cortex *in vivo*, receives a continuous stream of information in the form of sensory input. To bring our isolated cultures closer to the *in vivo* cortex, we need to move towards a dynamical model capable of receiving and processing continual

inputs. MEAs, providing for simultaneous stimulation and recording from thousands of neurons, present the ideal technology to further this approach. Real-time tools developed by the Potter group, for recording and stimulating neuronal networks as well as analyzing high dimensional spike data, make it possible to study the dynamical properties of an ensemble of neurons. The present work builds on this unique set of tools and explores the rules of functional network-level plasticity using a continual flow of context stimuli serving to restore background sensory activity in cultured networks. Thus, using the cultured model system developed in this work, we can expect to study more naturalistic neural processing of sensory-like inputs, instead of using a sensory-deprived condition that was previously a necessary consequence of removing tissue from the brain.

1.2 Towards the embodiment of neural cultures

In order to study the brain, we should remind ourselves that the brain does not work in isolation, but produces relevant adaptive behavior in response to continuous feedback from its environment. Learning can be defined as a process by which experience results in a permanent change in behavior [47]. *In vitro* systems lack behavior as they are removed from the body of the animal. Hence, it is traditional to refer to the changes in network dynamics in cultured networks as plasticity, instead of as learning or memory. One of the primary goals of the Potter group is to design hybrid closed-loop systems (Hybrot, Figure 1.3) to re-embody these cultures by stimulating them, in biologically relevant time scales, based on their recent activity [48, 49] (Figure 1.3). Closed-loop brain–machine interfaces, like motor prostheses operated by brain control [50, 51], offer an unparalleled opportunity to investigate how plastic changes can be guided by modulating the input signals of the neurons based on the behaviors generated

by the output of the same neurons. Our lab has developed hardware and software systems that enable recording and stimulation from the same electrodes in real-time [19]. Thus, we have the unique capability of stimulating various sites in the network (sensory input) and simultaneously recording the output response of numerous neurons (motor output). These neuronal outputs can then be used to guide the behavior of a robot or a simulated animal [49] and the neuronal network can be stimulated as a function of hybrot behavior (Figure 1.3).

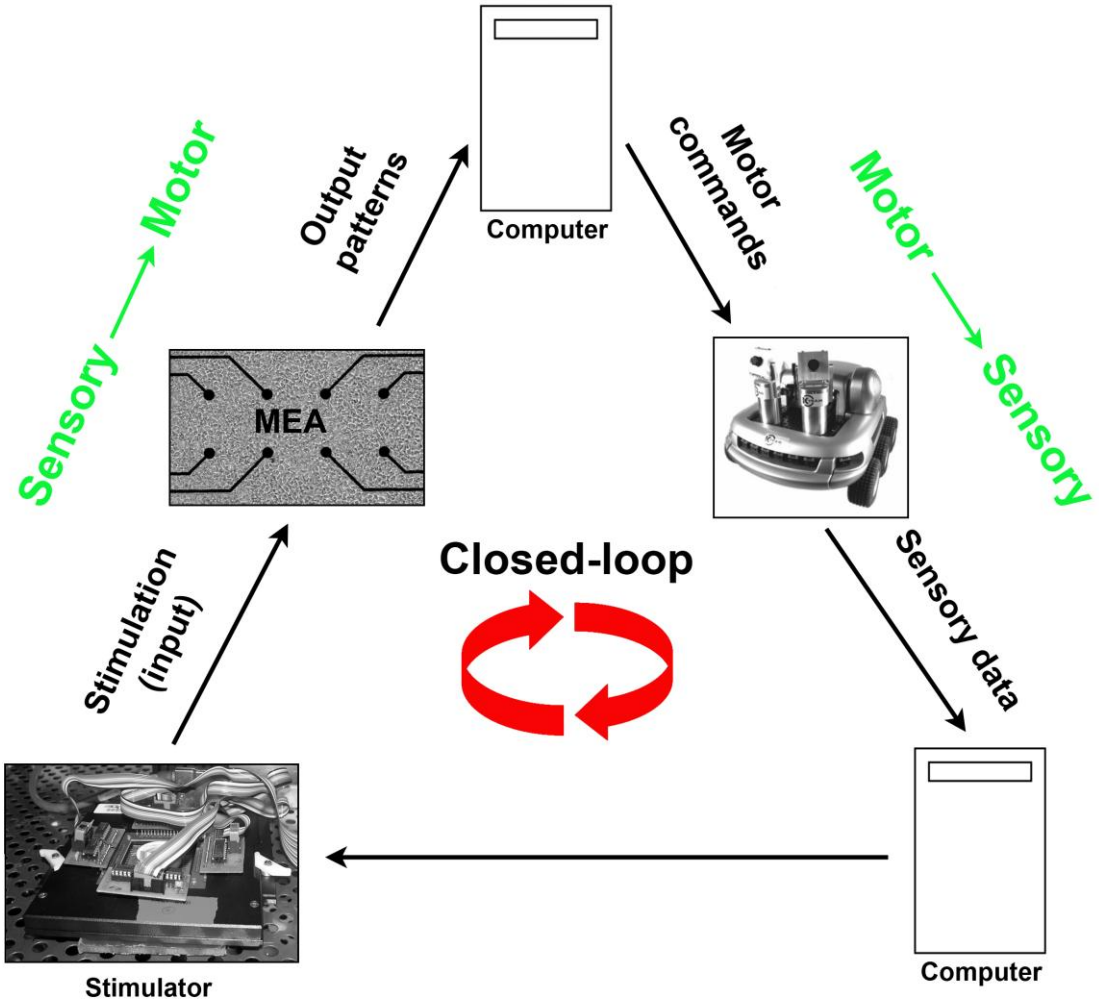

Figure 1.3: Schematic of the closed-loop embodied hybrot system for controlling robots. The output spiking patterns evoked by stimulating the neuronal network control the behavior of the robot. In turn, the behavior of the robot determines the stimulation pattern to be delivered to the culture, thus closing the loop. Figure created by author.

The first step in the design of closed-loop systems is to devise stimulation paradigms to induce plastic changes and analytical methods to detect these dynamic plastic changes. In the study of learning, there are two questions that can be asked: 1.What is the mechanism underlying the formation of associations? 2. What principles underlie the selection of some connections over others? In the following chapters of my dissertation, I will attempt to answer the first learning question by examining the changes in the stimulus-evoked responses or spontaneous intrinsic activity dynamics after tetanic stimuli, which are traditionally used to induce plastic changes in neuronal networks [52]. This work will provide the stimulus-response or the input-output (I/O) mappings, which could be used for future closed-loop studies, in order to tune the network to strengthen the 'appropriate' connections and weaken the 'inappropriate' ones. For example, in the concept of a reward, the 'appropriate' connections could be strengthened by repetitive stimulations that result in a desired output. By using the I/O mappings derived from this work to generate adaptive hybrot behavior in a closed-loop system, we can begin to answer the second part of the learning question stated above. We expect that the neuronal network will be able to drive its own stimulation or, via interaction with a simulated environment, would deliver pre-programmed stimulation patterns to impart structural or functional plasticity to the network.

1.3 Aims and Hypothesis

Since the hybrots would be controlled by network activity patterns, the first step in determining the I/O mappings was to study these patterns. Electrical activity in dissociated cultures is characterized by the presence of enduring spontaneous barrages of action potentials called bursts [23-25, 53-55]. Nearly every recordable electrode in the

MEA participates in these synchronized bursts. Hence, in contrast to information-carrying single cell bursts observed *in vivo* [56] , these culture-wide bursts are a result of activation of an ensemble of neurons. We hypothesized that these synchronized network-wide events, more like epileptic seizures [57], are likely to obscure subtle changes in synaptic weights involved in learning mechanisms [58, 59].

The first aim then, towards creating a suitable model to study learning and memory *in vitro*, was to suppress culture-wide bursting. Together with Daniel Wagenaar, I developed techniques to quiet spontaneous bursting activity [60]. Developing networks in the brain express a transient period of spontaneous bursting activity believed to be important for normal connectivity and development of neuronal circuits [61-65]. Such synchronized bursts characterize the early embryonic activity of neuronal circuits as diverse as the hippocampus, retina and spinal cord [66]. However, these correlated bursting patterns disappear within a week, due to heavy barrage of sensory input through the thalamocortical connections. Together with Steve and Daniel, I hypothesized that dissociated cortical networks developed persistent spontaneous bursting due to deafferentation [67]. The lack of external input, due to deafferentation, could lead to highly recurrent excitatory connections within the network [7, 67]. One can imagine that in such a highly excitable network, a single spike could trigger a huge barrage of activity (burst). Preventing spontaneous bursting using pharmacological agents, like excitatory channel blockers, could interfere with the plasticity mechanisms we aimed to study. Instead, we found that substituting electrical pulses for sensory input, by sprinkling them over multiple electrodes, could inhibit spontaneous bursting [60, 68]. This method allowed for the suppression of spontaneous bursting without compromising the ability of

the network to respond to additional stimuli. Thus, extra stimulation, like tetanus, could be superimposed on the background of burst-controlling stimulation, making this burst-controlled network feasible for the study of functional plasticity.

The next aim was to determine whether this burst-controlled model was more amenable for the study of use-dependent plasticity compared to the spontaneously bursting culture model. The amount of tetanus-induced plastic change was quantified on the background of different amounts of burst-controlling stimulation. A lower amount of spontaneous bursting did allow for easier induction and detection of functional changes caused by tetanus, by maintaining low variability in the stimulus-evoked responses. This suggests that uncontrolled changes during bursts might result in fluctuations in the efficacy of the synapses, making it difficult to discern induced plastic change from the intrinsic spontaneous changes in the activity of the network. This work is the first to experimentally demonstrate the effects of levels of ongoing activity on the efficacy of functional plastic changes in neuronal networks *in vitro*. Using these stimulus-response maps, which provide reliable ways to induce plastic changes, we can now begin to shape the activity dynamics of the neuronal network.

The rest of the dissertation is organized as follows -

Chapter 2, *Development and control of spontaneous bursting* lists the general properties of spontaneous bursting *in vitro* and details methods used to control spontaneous bursting using electrical stimulation. Correlated global bursting is one of the principal forms of activity spontaneously expressed by cultures prepared using tissue from the cortex, retina, hippocampus and spinal cord. The chapter details the typical properties of cortical *in vitro* synchronized bursts along with a review of the burst

literature. Various stimulation protocols used for the controlling bursts, including stimulation on multiple electrodes that resulted in perfect burst control, are also described.

Chapter 3, *Electrical burst control aids functional plasticity in cortical cultures* discusses the advantages of controlling bursts in the context of functional plasticity induced by tetanic stimulation. The effects of different levels of burst control on tetanus-induced changes were tested and the amount of functional change was inversely related to the amount of spontaneous bursting. This increased efficacy of inducing functional change was due to a simultaneous decrease in the intrinsic variability (drift) in the activity of the network. This work presents a new model to study functional plasticity in the context of naturalistic continuous stimuli, provided by electrical burst-control stimulation, as a means to restore background sensory input in dissociated networks.

Chapter 4, *Artificial sensory background alters GABA expression in cortical cultures* attempts to understand some of the cellular mechanisms involved in the electrical control of spontaneous bursting. Chronic suppression of spontaneous activity by TTX has been shown to decrease the proportion of GABAergic neurons in cortical cultures [69] suggesting that altered activity levels disrupt the balance between the excitatory and the inhibitory neurotransmission in the network. This chapter explores the activity-dependent nature of GABAergic neurotransmission and in particular discusses the potential role of GABAergic neurons in the onset of spontaneous bursting and long term burst suppression. The proportion of GABAergic neurons was low at the onset of spontaneous bursting in developing cultures. In addition, chronic burst suppression resulted in almost a two-fold increase in the proportion of GABAergic neurons compared

to spontaneously active sister cultures. These activity-dependent changes in expression of GABA are attributed to the homeostatic mechanisms maintaining the balance between excitatory and inhibitory influences in the network.

Chapter 5, *Plasticity of recurring spatiotemporal activity patterns in dissociated cortical networks*, describes the plasticity of intrinsic spontaneous activity patterns. Stable and repeating patterns found in the brain have been implied to represent memory substrates. Motivated by these studies, I explored the potential of bursts to encode information in spontaneously active cultures. Spontaneous bursts occurred in stable, spatiotemporally diverse, repeating patterns that were altered by tetanic stimulation. Thus, the presence of these properties in spontaneous bursts recommends their use as codes for information storage in intrinsically active neuronal networks.

Chapter 6, *Conclusion and Discussions*, enumerates the major conclusions of this body of work and discusses the potential applications of these results from open-loop experiments in the study of learning and behavior in embodied closed-loop hybrid systems. This chapter closes with a discussion of detailed ideas on the applying the I/O mappings (stimulus-response) obtained by this work in the real-time control of hybrot behavior.

After the main text, there are five appendices in alphabetical order. Appendix A, *Culturing methods*, details the methods used for culturing and maintaining dissociated cortical cultures on MEAs. Appendix B, *Electrical stimulation and recording*, describes the technical details of the electrical recording and stimulation set up used in this dissertation work. Appendix C, *Immunostaining techniques*, details the methods, reagents and techniques used for immunohistochemistry studies detailed in Chapter 4. Appendix

D, *Testing the stability of probe responses*, details the experiment protocol and results from a preliminary study that attempts to stabilize the responses to stimulation at a single electrode (probe), by controlling the activity before the probe, using another stimulus pulse delivered 100ms-2s before the probe. Appendix E, *Effects of long term electrical burst quieting* discusses the effects of chronic burst control stimulation on electrical activity and GABA expression in dissociated neuronal networks.

Portions of this dissertation have been published before. My work with Daniel Wagenaar, detailed in Chapter 3, was published in the Journal of Neuroscience. Details of this publication are included with the chapter. Chapter 5 was submitted to the Journal of Neuroscience and we have recently received the reviews, which were mostly positive. Chapter 4 has been submitted to the European Journal of Neuroscience and is currently being reviewed. Chapter 3 is based on a manuscript currently being modified for submission. The chapters have been previously presented in abstract or short paper forms at various conferences.

CHAPTER 2

DEVELOPMENT AND CONTROL OF SPONTANEOUS BURSTING

Population bursts of activity are a major component of spiking activity spontaneously expressed by dissociated cultured networks. Such synchronized global bursting has been observed in cultured networks prepared using tissue from the cortex [23-25, 37, 53-55, 70], hippocampus [61], spinal cord [29, 62, 63, 71] and retina [27, 33]. There is an idea that bursts are more reliable means to communicate information across a synapse than single spikes, because they increase the probability of transmitter release [56]. However, it is important not to confuse those single cell bursts lasting a few milliseconds with spontaneous bursting in dissociated cultures, which consist of correlated barrages of action potentials, on multiple neurons, lasting much longer (100ms-2s). Correlated network-wide bursting has been observed *in vivo* but only during a transient period of development [28, 64, 65], some stages of sleep [72] and pathological conditions like epilepsy [57].

We hypothesize that the persistence of bursting in dissociated cortical cultures, beyond the developmental phase, is caused by a lack of input from other brain areas due to deafferentation. To study this hypothesis, we grew small but dense monolayer cultures of cortical neurons and glia from rat embryos on multi-electrode arrays, and used electrical stimulation to substitute for afferents. We quantified the burstiness in spontaneous spiking activity and during several stimulation protocols. Although slow stimulation through individual electrodes increased burstiness as a result of burst entrainment, rapid stimulation reduced burstiness. Distributing stimuli across several

electrodes greatly enhanced burst control. We conclude that externally applied electrical stimulation can substitute for natural inputs to cortical neuronal ensembles in transforming burst-dominated activity to dispersed spiking, more reminiscent of the awake cortex *in vivo*. This non-pharmacological method of controlling bursts will be a critical tool for exploring the information processing capacities of neuronal ensembles *in vitro* and has potential applications for the treatment of epilepsy.

Portions of this chapter have been published in the Journal of Neuroscience[1].

2.1 Properties of spontaneous culture-wide bursts in dissociated cortical networks

Dissociated cortical cells are obtained by enzymatic and mechanical treatment on cortical tissue dissected from embryonic rats (Appendix A).

At the time of plating, after their extraction from the cortex, most cells are round and have no neurite extensions (Day1 in figure 2.1). But these dissociated cells extend neurites, to connect with each other, within hours of plating and soon form a dense interconnected network (Figure 2.2). Cultures are plated densely on the MEA resulting in a network ~50,000 cells covering the 1.5mm^2 electrode area (Figure 2.2). Each electrode can record the activity of 5-10 cells around the electrode as well as axons extending near the electrodes. In these mixed cultures of neurons and glia, neurite extensions can extend up to ~1mm across the array.

In spontaneously active cultures, uncorrelated spikes (action potentials) are observed from 4-5 days *in vitro* (DIV). However, within few days of the onset of spiking, in addition to such tonic firing, population bursts of activity are also observed.

[1] Wagenaar, D. A. Madhavan, R. Pine, J. and Potter, S. M. (2005) Controlling bursting in cortical cultures with closed-loop multi-electrode stimulation. *J. Neuroscience* 25: 680-688.

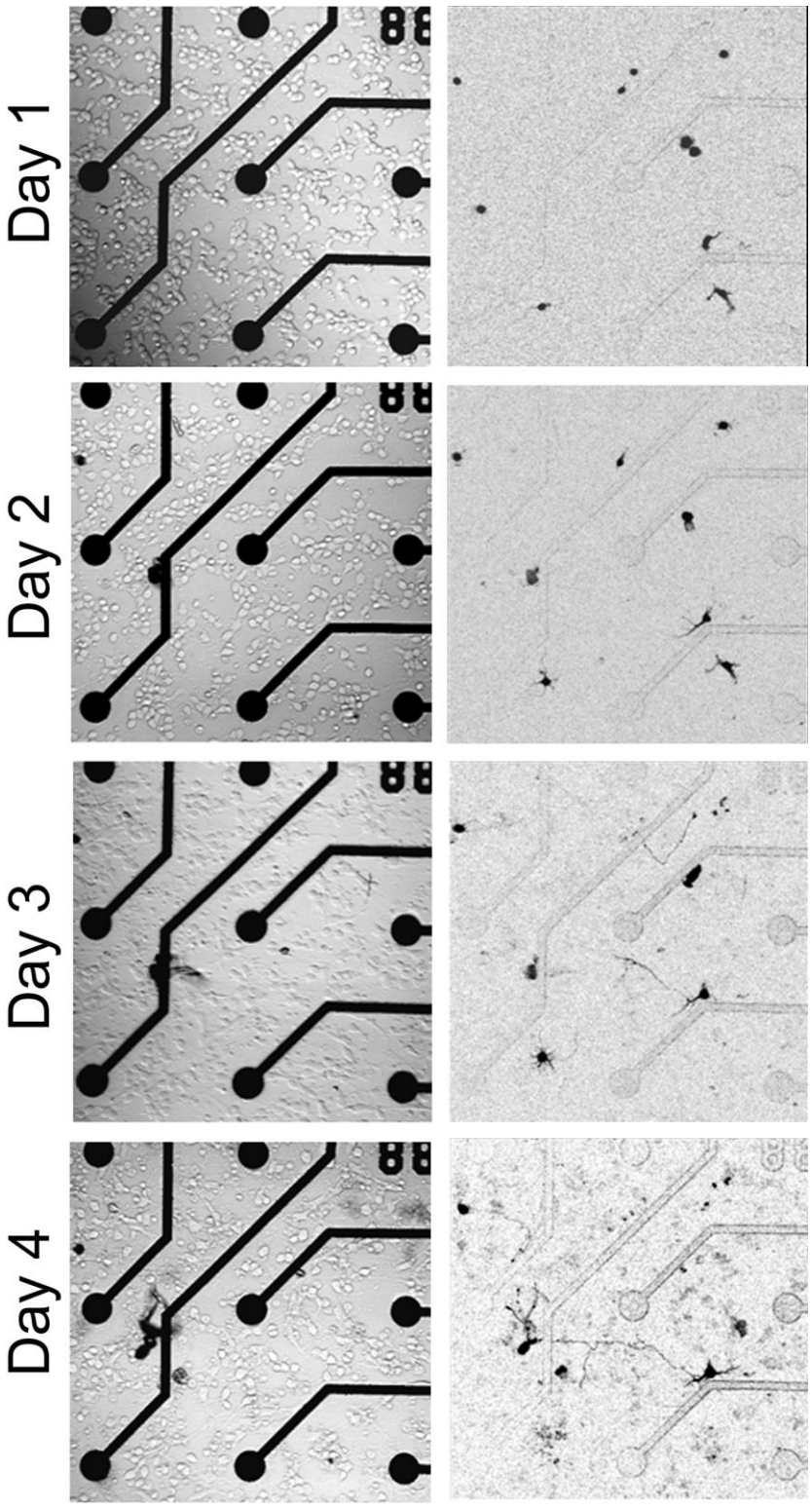

Figure 2.1: Development of embryonic cortical cultured networks. Phase contrast (top panels) and YFP labeled (bottom panels) images of developing neurons during the first 4 days *in vitro* are shown. Only ~5% of the neurons in the dish were YFP labeled. Images obtained from Mark Booth.

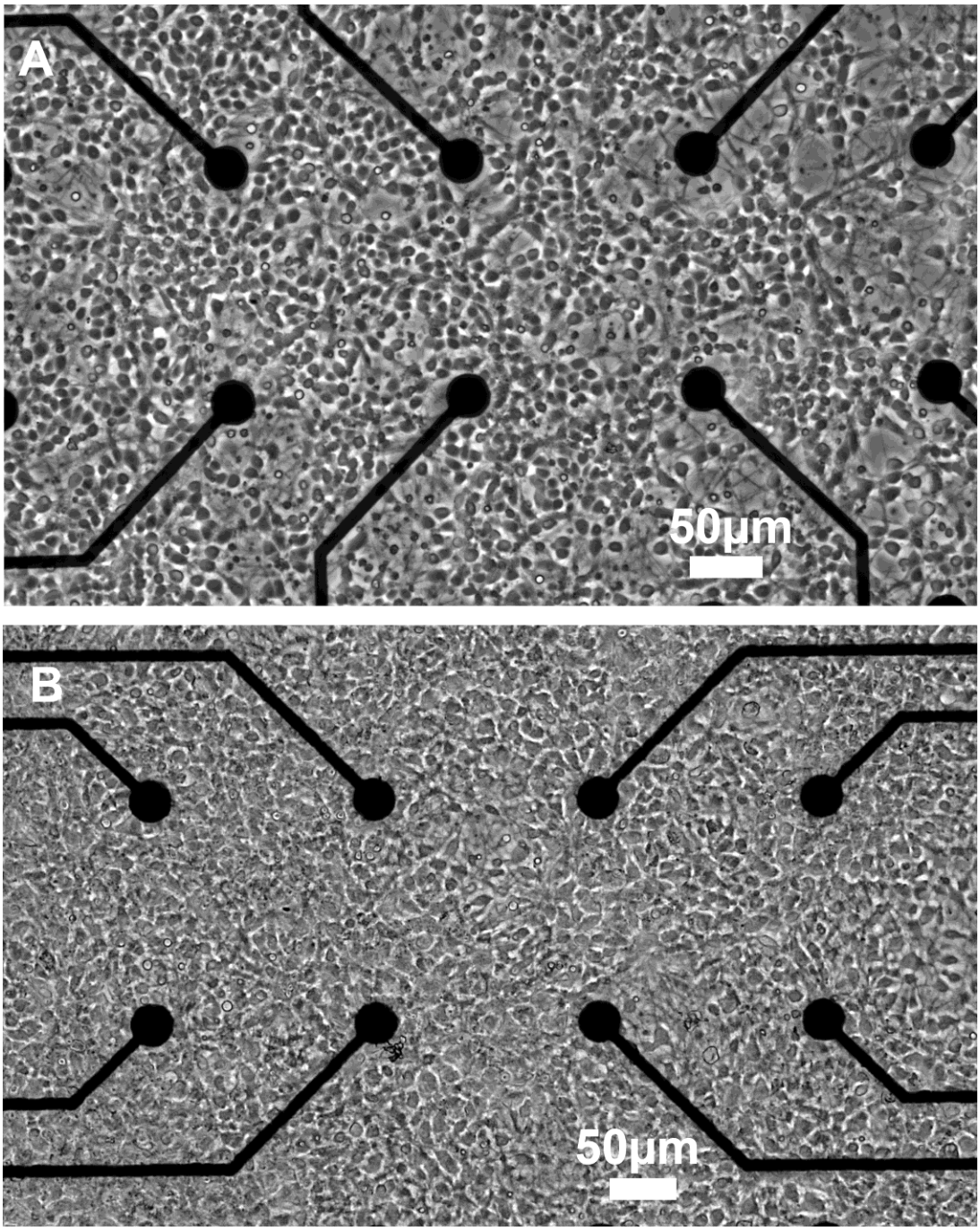

Figure 2.2: Development of dissociated culture in vitro. A. Culture at 4 DIV, onset of spiking **B.** Culture at 10 DIV, onset of spontaneous bursting. Images were taken by the author.

Spontaneous bursts are characterized by a synchronous increase in the firing rate (spikes per unit time) by a factor ≥10 on all the active electrodes. Such bursting is

observed from ~6-9 DIV and though the pattern of bursting changes over the course of a month, spontaneous bursting persists for the lifetime of the culture (Figure 2.3).

Bursts come in a wide range of shapes and sizes (Figure 2.3). They can be roughly categorized into four major types depending on the size (number of spikes within a burst), duration and shape. Big bursts consist of a sudden transient rise in firing rates over all the recordable electrodes (Figure 2.3A). In contrast, small bursts are shorter and consist of fewer spikes compared to big bursts (Figure 2.3A). Long-tailed bursts exhibit longer decay times compared to big bursts (Figure 2.3B). Some cultures express 'superbursts': stereotyped sequences of big bursts separated by periods of quiescence (Figure 2.3C). The frequencies of bursts as well as their sizes are variable between different platings and even between cultures from the same plating. Onset and type of bursting depends on the density of the culture [53]; denser cultures show an early onset of bursting and a higher incidence of big bursts, compared to sparse cultures (density at least an order of magnitude lower than dense cultures). In addition, cultures show large variations in burst types, from day to day. Typically, global big bursts are observed from around a week *in vitro*, after which the burstiness of the culture gradually increases and remains high for the rest of the lifetime of the culture.

Excitatory channel blockers can block spontaneous bursting. Excitatory channel blockers 2-amino-5-phosphonovalerate (APV, NMDA receptor antagonist), 6-cyano-7-nitroquinoxaline-2,3-dione (CNQX, non-NMDA glutamate receptor antagonist) and elevated Mg^{2+} (blocks NMDA receptor) reversibly block spontaneous bursting activity [24, 73] indicating that excitatory transmission is involved in the regulation of

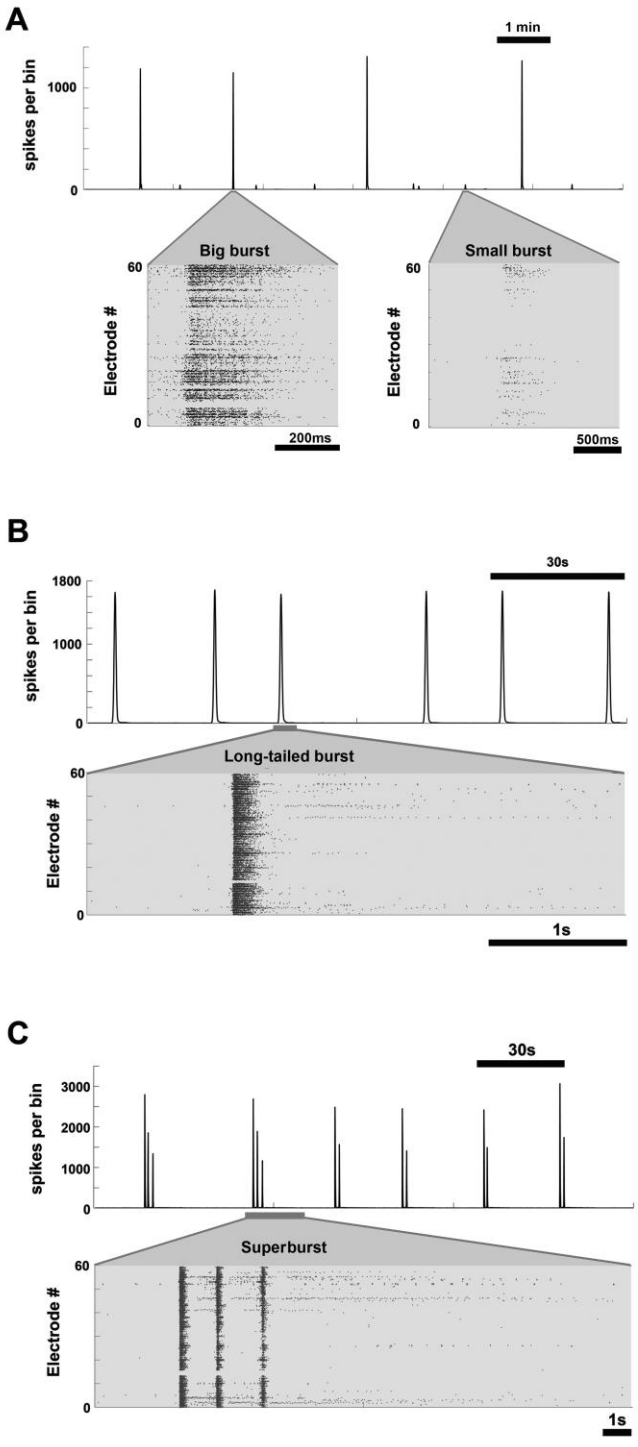

Figure 2.3: Taxonomy of spontaneous bursting observed during the first month in vitro. Array-wide firing rates (spikes in 50ms time bins) are shown with the insets showing raster plots of electrode firing rates. **A.** Chaotic bursting. Insets below show example spike raster plots for a big global burst and a small local burst. Recordings taken at 17 DIV. **B.** Long tailed bursting. Insets below show example spike raster plots for a long-tailed burst. Recordings taken at 28 DIV. **C.** Superbursts. Insets below show example spike raster plots for a superburst. Recordings taken at 26 DIV. Figure was prepared by the author.

spontaneous bursting in cortical networks. However, excitatory channel blockers, in addition to reducing the amount of spontaneous bursts, also reduce the overall firing rate of the network [73]. The effect of other common pharmacological agents on network activity has also been tested. Tetrodotoxin (TTX, sodium channel blocker) abolishes all electric activity in cortical networks [69] while picrotoxin, a GABAergic (inhibitory) synapse blocker, disinhibits network activity [24, 74].

Spontaneous bursting is predominantly a network phenomenon resulting from the interactions of large numbers of cells within the network. Eytan and Marom (2006) observed a set of neurons that reliably increased their firing rates tens of milliseconds before the peak of a burst and hence could be used to predict an upcoming network burst. Maeda *et al.* (1998) showed that the origin of spontaneous bursts varies with each burst; there is no 'pacemaker' cell that drives the network to burst. In a 1.5 hour recording of spontaneous (non-stimulated) activity, the likelihood of any given neuron, recorded on an electrode on the MEA initiating a burst, varied (Figure 2.4).

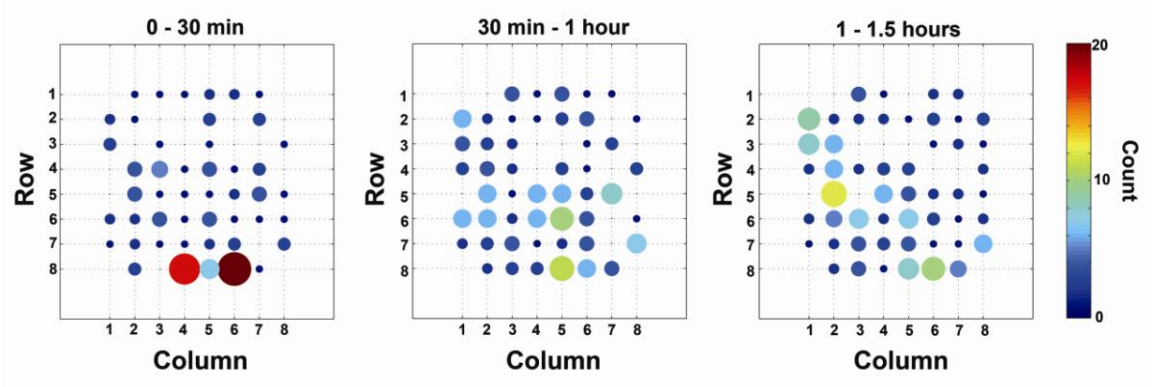

Figure 2.4 Burst initiation site. There is no one preferred site of initiation for a spontaneous burst. The number of times (count) any neuron near an electrode initiated a burst in 30 minute segments of a 1.5 hour of spontaneous recording, is shown. Since the initiation site of a burst changes over 1.5 hours, there could be no pacemaker neuron in the culture that drives spontaneous bursting. The color and size of the circles represents the number of times any electrode initiated a burst in the 30 minute of recording.

Opitz *et al.* (2002) showed that spontaneous bursting was followed by a period of network depression lasting seconds. They found a positive-correlation between burst duration and the preceding interval between bursts, suggesting that burst duration was modulated by parameters recovering from synaptic depression after the previous burst [26]. This also suggests the existence of a 'burst refractory period', which controls how soon after the occurrence of a burst, a new burst could be initiated.

Development of spontaneous synchronous activity is directly correlated to the development of synapses [75, 76] and has been thought to be important for the normal development of cortical cultures [69, 77]. Muramoto *et al.* (1993) showed that the frequency of synchronous Ca^{2+} oscillations increased with the development of synapses in cultured cortical neurons. This increase in synchronous activity was highly correlated to the number of synapses formed in the culture. Also, the functional blockade of synchronous activity using TTX, retarded the growth and maturation of synaptic connections and prevented the normal period of synapse elimination at 4 weeks *in vitro* [77] indicating that spontaneous, possibly synchronous, activity was necessary for network maturation. Chronic silencing of developing neocortical cultures using TTX has been shown to result in cell death [36] and corresponding increases in the ratio of excitatory to inhibitory synaptic activity [69]. In particular, the suppression of spiking activity was found to be accompanied by a decrease in GABA neurotransmission suggesting the role of GABA in maintaining synchronous activity in these networks [69, 78]. The role of GABA in spontaneous bursting has been addressed in more detail in Chapter 4 of this dissertation.

2.2 Persistence of spontaneous bursts represents a sensory-deprived state of the network

Most studies of dissociated networks on MEAs consider spontaneous bursts as useful outputs since they are the most dominant pattern of activity. Other laboratories have used spontaneous bursts to quantify the effects of neurotoxins [42] and in the study of functional plasticity in response to tetanic stimulation [37]. Unlike *in vitro* cultured networks, such global synchronized bursting is not present in the adult, awake, embodied brain. *In vivo*, synchronous activity has been observed during defined periods of early CNS development (for review see [79]) . This early form of activity is required for the structural and functional maturation in the developing nervous system. Waves of synchronous activity traveling through the retina have been implicated in the refinement of retinal projections to the lateral geniculate nucleus [80]. But, these synchronous waves disappear on the opening of the eye (visual experience). Since dissociated cultures lack (sensory) input due to deafferentation from the brain, the persistence of spontaneous bursting in cortical cultures can be a sign that these cultures are arrested in development [24, 81].

Homeostatic mechanisms regulate synaptic strengths in a network to maintain the firing rates within limits, to prevent hyper or hypo excitability [7]. Hence, it is possible that the lack of continuous structured input in dissociated cultures results in the development of stronger excitatory connections within the network. This increased sensitivity of the network to excitatory inputs would tend to result in even a small input triggering an intense barrage of action potentials or a global burst. Latham *et al.* (2000) showed that bursting occurs when there are few intrinsically active cells in a network.

We hypothesized that substituting for lack of afferent input by continuous electrical stimulation, could have the same effect as elevated tonic firing rates (caused by intrinsically firing cells) in reducing the amount of spontaneous bursting in dissociated cultures. Thus, electrical stimulation could represent thalamocortical inputs to the cortex in the brain, and serve to reduce the predominance of bursts and favor more locally differentiated neuronal activity.

2.3 Controlling spontaneous bursts through distributed electrical stimulation

Excitatory channel blockers can abolish spontaneous bursts, but this also reduces the overall firing rate of the network. In studies of network-level plasticity, these pharmacological methods of suppressing bursts might interfere with the learning. Since our long-term goal was to study functional plasticity in these networks, we wanted to devise methods that reduced the amount of spontaneous bursting without reducing the ability of the network to spike or respond to extra stimulation. This study was conducted along with Daniel Wagenaar and was published in the Journal of Neuroscience, 2005[1]. The parts of the study relevant to my dissertation have been discussed below.

2.3.1 Material and Methods

2.3.1.1 Cell culture

Neocortical cells were dissociated from the brains of embryonic day 18 rats and plated on MEAs. Timed-pregnant Wistar rats were killed by CO_2 inhalation according to protocols approved by the National Institutes of Health. Embryos were removed, chilled, and decapitated. The entire neocortex, excluding the hippocampus, was dissected under sterile conditions. Cortices were cut into 1 mm^3 cubes in Segal's medium [82] containing

(in mM): 5.8 MgCl2, 0.25 CaCl2, 1.6 HEPES, 90 Na2SO4, 30 K2SO4, 1 kynurenic acid, and 0.5 (APV), pH 7.3, using NaOH and 0.001% phenol red. After enzymatic digestion for 30 min by 2.5 U/ml papain (Roche 108014, Roche, Indianapolis, IN) in Segal's medium, cells were separated by six or nine trituration passes using a 1 ml pipette tip, in Neurobasal medium with B27 (Invitrogen, Carlsbad, CA), 0.5 mM Glutamax (Invitrogen), and 10% equine serum (Hyclone, Logan, UT). After every three passes, the cells already in suspension were transferred to a separate tube to reduce stress on them. Cells were centrifuged at 160x g onto 5% bovine serum albumin in PBS, resuspended by very gentle trituration, and passed through a 40µm cell strainer (Falcon, Bedford, MA) to remove large debris. 50,000 cells were plated in a 20µl drop of Neurobasal on MEAs precoated with polyethylene imine and laminin as described previously [22]. This led to a plating density of 2500 cells per square millimeter in a monolayer. After 1 hr of incubation, 1ml of Neurobasal was added to each culture dish. After 24 hr, the plating medium was replaced by a medium adapted from Jimbo *et al.* (1999): DMEM (Irvine Scientific, Santa Ana, CA) with 0.5 mM Glutamax and 10% equine serum, but no antibiotics or antimycotics. Cultures were maintained in an incubator with 5% CO_2 and 9% O_2 [83]. We replaced one-half of the medium every 5–7 d. Glial growth was not suppressed, because glia are essential to long-term culture health [84]. As a result, glia gradually formed a carpet over the neurons.

Our use of Teflon-sealed dishes [22] allowed us to maintain the incubator at 65% relative humidity, making it an electronics-friendly environment. Thus, we could perform all experiments inside the incubator, ensuring long-term stability of recording conditions. Experiments took place at 25–45DIV. At this age, >90% of electrodes recorded spikes.

Only cultures that fired at least three bursts in 10 min of pre-experimental screening were used.

2.3.1.2 Recording system

Electrical activity was recorded with a square array of 60 substrate-embedded titanium nitride electrodes, 30µm in diameter, with 200µm spacing (Multi Channel Systems, Reutlingen, Germany). After 1200x amplification, signals were sampled at 25 kHz using a Multi Channel Systems data acquisition card, controlled through our Meabench software [19] (available for free public download[2]). Meabench's digital filtering system for reducing stimulus artifacts [85] allowed us to detect action potentials as early as 2ms after stimulation (except on the electrode used for stimulation, which remained saturated by stimulation artifacts for 50–150 ms). Spikes were detected on-line by thresholding at 5x RMS noise and later validated based on the shapes of their waveforms.

2.3.1.3 Stimulation system

Stimuli were generated using our custom-made real-time 60 channel stimulator [86]. We used biphasic rectangular voltage pulses, positive phase first, because these were found to be the most effective stimulus at any given voltage [87]. We used stimulus pulse widths of 400µsec per phase and voltages between 100 and 900 mV. To prevent possible electrochemical damage to electrodes and nearby cells, higher voltages were not used. The stimulator was switched to high impedance output 100µsec after each pulse using the built-in switches of our stimulator.

[2] http://www.its.caltech.edu/~pinelab/wagenaar/meabench.html

2.3.1.4 Experimental protocols

Before experimenting on any MEA, we probed each electrode in the array with voltage pulses between 100 and 900 mV, in random order. For each electrode, we determined the voltage V* at which the response to multiple presentations of the same stimulus, was on average five times the spontaneous firing rate before the stimulation. Typically, 40–50 electrodes per dish were in sufficiently close contact with the culture to attain that level of response by voltages in the range tested. For each experimental series, we randomly selected either individual electrodes or groups of 2–25 electrodes from this pool.

We used the following two stimulation protocols. (1) "S" or single electrode stimulation: one electrode was stimulated repeatedly at its voltage V*. We used this protocol at 10 different frequencies between 0.05 and 50 stimuli per second (stim/sec). (2) "M" or multi-electrode stimulation: a group of 2–20 electrodes was stimulated cyclically at 2–20 stim/sec, such that each electrode received stimuli once per second, or 25 electrodes were stimulated cyclically at 50 stim/sec, each receiving 2 stim/sec. Each electrode was stimulated at its own previously determined V*.

Experimental runs lasted 5 min each and were randomly interleaved with each other and with control runs where spontaneous activity was recorded.

2.3.2 Results and Discussion

2.3.2.1 Single electrode stimulation

Responses to single electrode stimulation typically consisted of three phases: 1. An early phase (3-20ms post-stimulus) of precisely timed, typically non-synaptic responses with low jitter; 2. A late phase (20-50ms post-stimulus) of post-synaptic

responses; and 3. Bursts, evoked by low frequency (<1 Hz) but strong stimulation. Such bursts were time-locked to the stimulus pulse, usually in 50 - 200ms long but otherwise similar to spontaneous bursts. Example raster plots of early and late phase of stimulus responses are shown in figure 2.5. Each block shows the responses for an electrode. The electrodes are arranged in the geometry of the array with the colored block indicating the site of stimulation (Figure 2.5).

Figure 2.5: Responses to single electrode stimulation. Each grid (electrode) shows the raster plot of responses (50ms post-stimulus) to 20 presentations of the same stimulus. The electrodes are arranged in the geometry of the array and the colored grid indicates the position of the stimulation electrode. The gray line indicates the time of the stimulus. Figure created by the author.

Stimulation at a single electrode at low frequencies (0.1-0.5Hz, Protocol 'S') evoked bursts as previously observed by Maeda *et al.* (1998). On increasing the stimulus frequencies (1-5Hz), not all the stimuli evoked bursts and the burst rate started dropping

below spontaneous levels. On further increasing the frequency (10-50Hz), the reduction in number of bursts did not improve much and though the bursts are initially suppressed, they reappear after ~1 minute (Figure 2.6).

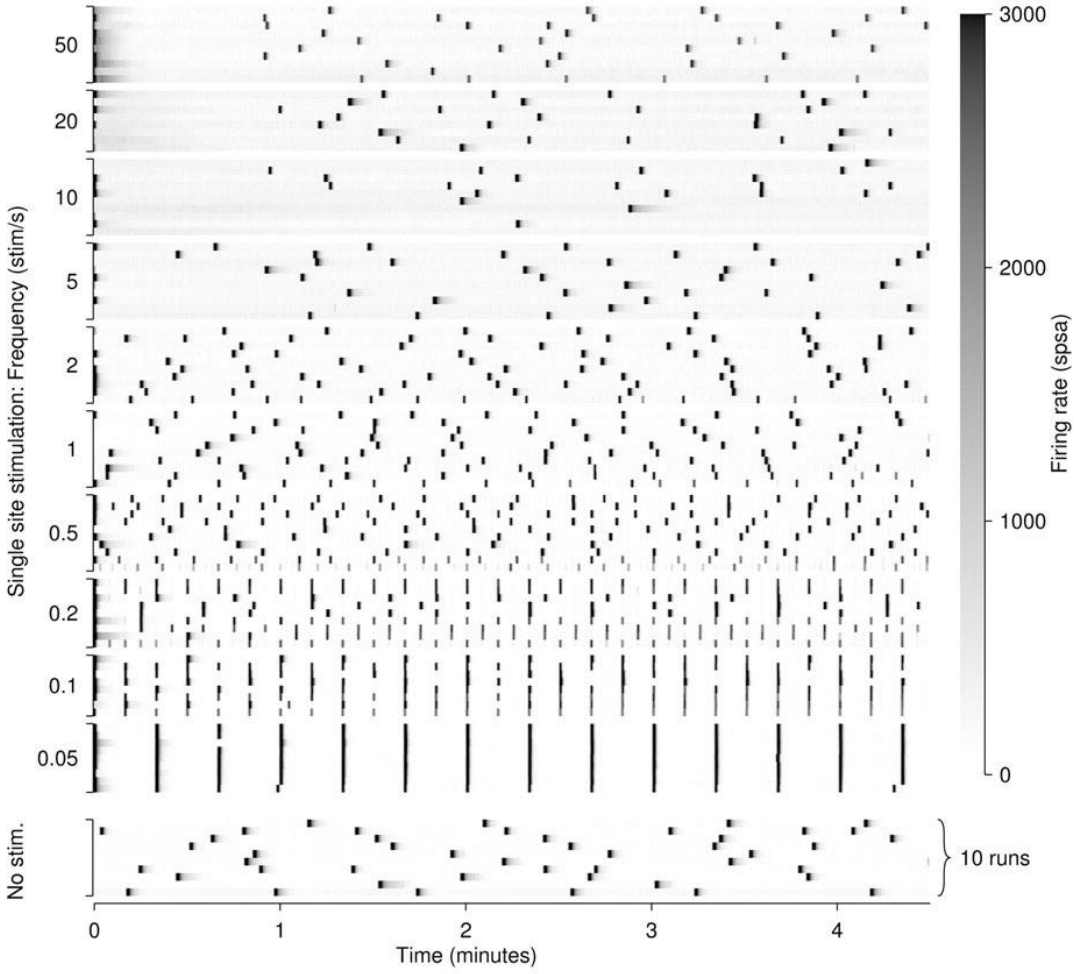

Figure 2.6: Burst distribution during single electrode stimulation and during spontaneous bursting. Each row shows the array-wide firing rate (spikes per second array-wide, spsa, scale on the right) as a function of time during one 5 minute experimental run. Since bursts are periods of high firing rates (high spsa), they appear on the graph as dark regions. In 10 examples of spontaneous activity (bottom panel, no stim), bursts occurred regularly at ~1 minute intervals. In 10 examples of stimulation at the rate of 0.05 stim/sec, the bursts were entrained to the stimulus. At higher frequencies between 1-5 stimulation/sec, the number of bursts begins to decrease, though some were still locked to the stimulus. At frequencies between 10-50 stimulation/sec, the bursts initially were suppressed, but they reappeared after ~1 minute. Data are from a culture at 39 DIV [60].

Additionally, we noticed that during high frequency (>5Hz) stimulation through a single electrode, the immediate evoked response rate (spikes within 20ms of the stimulus) decreased dramatically ~1 minute after the start of the stimulation run (Figure 2.7). This decreased efficacy in evoking early responses might be responsible for the lack of improvement of burst control at higher frequencies. The decay in the early responses might mean that the neurons around that electrode can no longer effectively influence the network.

In order to verify if this decrease in immediate responses was local to the electrode being stimulated, we stimulated a second electrode at a slower frequency [60]. It was found that the rapidly stimulated electrode did not affect the responses at the slowly stimulated electrode. Hence, this reduction of efficacy at the rapidly stimulated electrode was caused by a mechanism local to that electrode and not by a network-level fatiguing effect. In order to achieve successful burst quieting, we needed a stimulation protocol that had the burst quieting effect of rapid stimulation combined with the efficacy of slow stimulation.

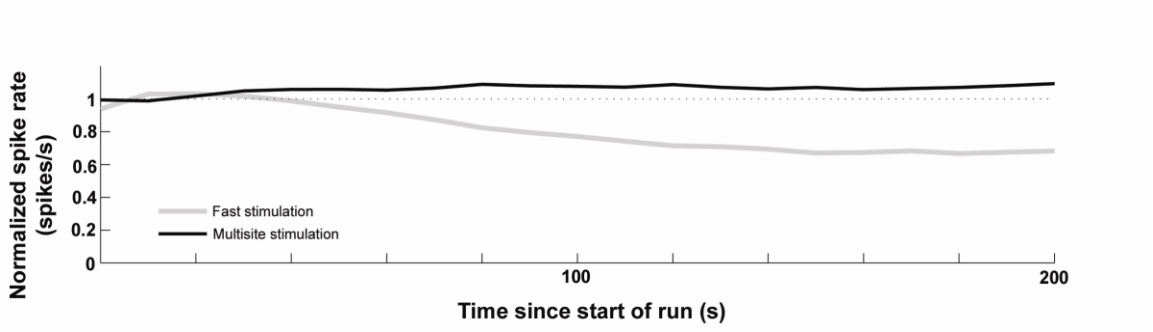

Figure 2.7: Early responses (0-20ms) decay in single electrode fast (10Hz) stimulation. Distributed stimulation over 10 electrodes at an aggregate rate of 10Hz did not suffer from this loss of efficacy of early responses.

2.3.2.2 Burst control by distributed electrical stimulation

We proceeded to test whether better burst control could be achieved by distributing the stimulation across several electrodes, in such a way that though the network is stimulated at a high frequency, each electrode gets stimulated at a low frequency (Protocol M, Methods). We found that this distributed stimulation protocol prevented the loss in the efficacy of early responses (Figure 2.7).

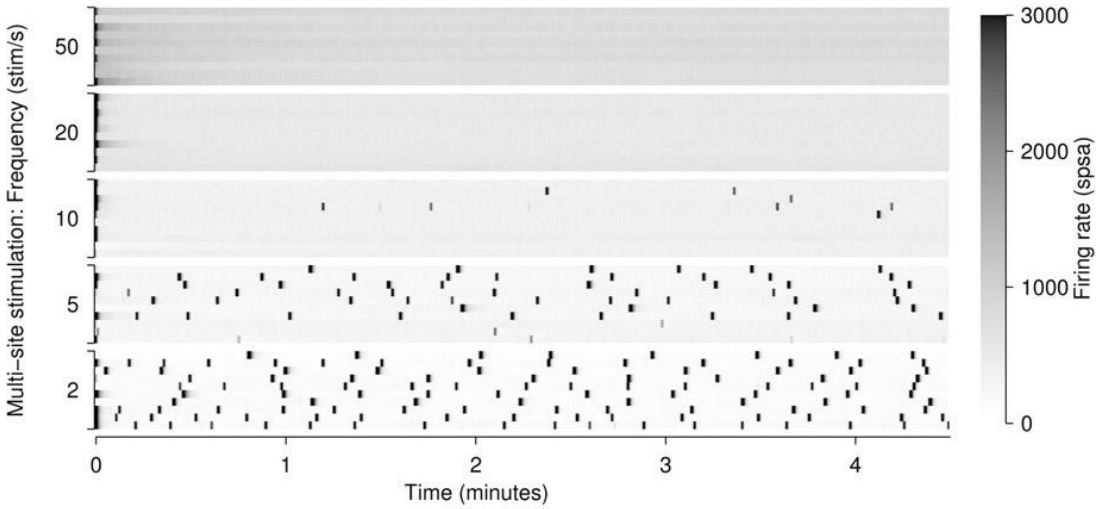

Figure 2.8: Multi-electrode stimulation quiets spontaneous bursts. A group of 2-20 electrodes was stimulated cyclically at 2-20 stimulation/sec, such that each electrode received stimuli once per second, or 25 electrodes were stimulated cyclically at 50 stimulation/sec, each receiving 2 stimulation/sec. Perfect burst control was obtained at frequencies above 10 stimulation/sec aggregate. The tonic firing rate increased (the background is more grey) as the stimulation frequency was increased [60].

At frequencies higher than 10 stim/sec, this protocol greatly improved burst reduction (Figure 2.8). Distributing stimuli across ≥20 electrodes proved highly effective in suppressing spontaneous bursting, but perfect burst suppression with this protocol was achieved at rates of 50 stimulation/sec distributed across 25 electrodes. At this frequency, all the spontaneous bursts were completely suppressed, independent of the choice of

electrodes. Effective burst suppression at lower frequencies required a careful selection of electrodes for stimulation.

Additionally, the tonic firing rate (background grey shading, Figure 2.8) increased as the distributed stimulation frequency was increased. Latham *et al.* (2000) showed that networks with a large fraction of intrinsically active neurons have a reduced tendency to burst. We extend their finding by demonstrating that increasing the tonic activity above spontaneous levels by high frequency electrical stimulation also reduces or suppresses spontaneous bursting. In all the tested cultures, the network adapted rapidly to the change in stimulation protocol, and spontaneous bursting resumed seconds after the stimulation was stopped (Figure 2.9).

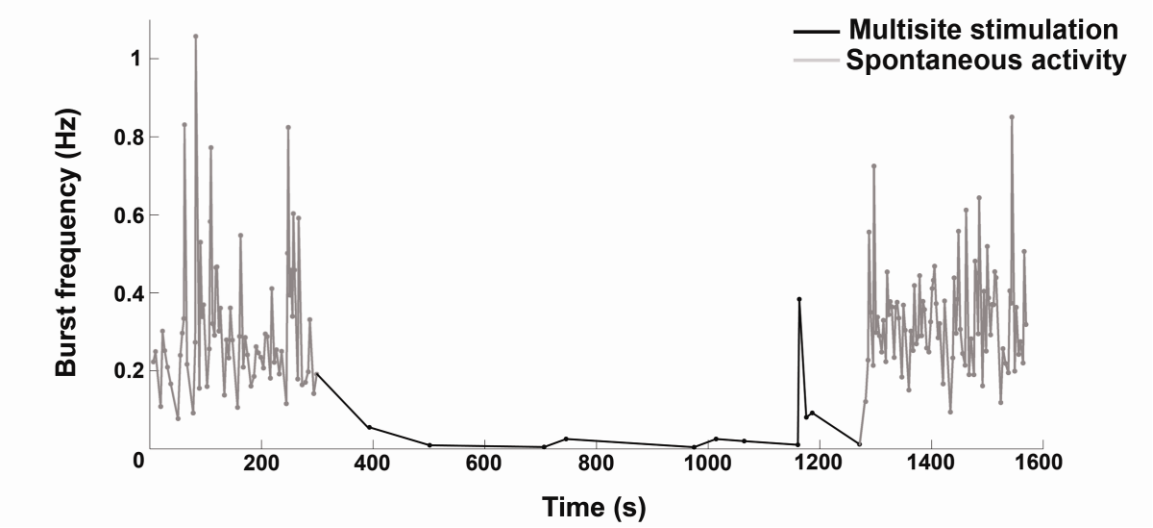

Figure 2.9: Spontaneous bursting was suppressed by multi-site stimulation and bursting resumed soon after the stimulation was stopped. The spontaneous burst frequency during periods of no stimulation (spontaneous activity) is show in gray and during multi-site stimulation is shown in black. Data from multi-site stimulation, consisting of 10Hz aggregate stimulation on 10 electrodes, on one representative culture.

Using electrical stimulation to control bursts has many advantages over pharmacological means such as elevated Mg^{2+}. Unlike pharmacological manipulations,

bursting resumed as soon as the stimulation was stopped (Figure 2.9) and the network was responsive to additional stimuli. Moreover, the culture adapted rapidly to change in stimulation (Figure 2.10), indicating that we could control the amount of spontaneous bursting in the network at will.

Thus, continuously applying distributed electrical stimulation is compatible with studies of long term network-level plasticity in dissociated cortical networks. Additional stimulation like tetanus or probes could be superimposed on the background of such continuous distributed stimulation. This model of a cultured neuronal network receiving continuous flow of sensory information would mimic more natural modes of activation. Spontaneous bursting has been shown to destabilize synaptic weights in a model network of a thousand integrate and fire neurons [59]. We suggest that burst suppression would lead to more stable connections and render the network amenable to tetanus-induced changes. Hence, burst control could make these cultures more suitable for the study of use-dependent plasticity and information processing related to learning and memory [19], as shown in Chapter 3.

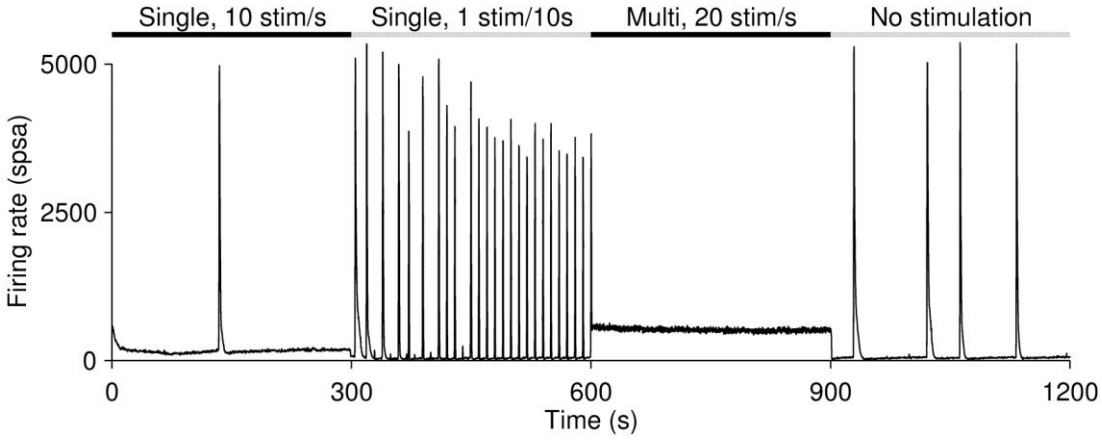

Figure 2.10: When switching between different stimulation protocols, the activity and bursting pattern readjusted rapidly to follow the stimulation [60].

2.3.2.3 Applications of burst quieting to control epileptic seizures

Since distributed stimulation was effective in controlling global bursting *in vitro* it would be interesting to test whether such stimulation would be effective *in vivo* in the control of epileptic seizures. Epileptic seizures in the human brain, though originating from different causes, are characterized by ensemble bursts extending over large areas of the cortex. The use of distributed stimulation instead of focal electrical stimulation [88-90] at the seizure foci might be more attractive for various reasons. First, by distributing the stimulus load over more electrodes, the amplitude of stimulation at a single electrode can be reduced. This could result in reduced damage to the tissue [91]. Second, since this technique uses multiple electrodes, the efficacy of the stimulation might hardly be affected by incorrect placement or loss of any single electrode. This *in vitro* study could direct new methods for control of seizures and other aberrant forms of global activity in the brain.

CHAPTER 3

ELECTRICAL CONTROL OF BURSTING AIDS FUNCTIONAL PLASTICITY IN CORTICAL CULTURES

Networks cultured *in vitro*, having been severed from the intact brain, lack the rich spatiotemporal sensory input the brain receives continuously. Substituting electrical stimulation for this missing input suppressed global synchronized bursts in dissociated cortical cultures and allowed for more tonic activity reminiscent of the adult awake brain. Synchronized bursting patterns dominate the spiking activity in dissociated cortical cultures, with most of the detected spikes occurring within bursts. We hypothesized that these culture-wide barrages of activity might overwhelm the effects of external plasticity-inducing electrical stimulation and that a burst-free state would be more amenable for studies of long term plasticity in dissociated cortical cultures. Tetanic stimulation was applied on the background of different amounts of burst controlling stimulation and the magnitude of tetanus-induced change was compared to the levels of bursting. Low levels bursting allowed significant tetanus-induced change, while high levels of bursting made it difficult to distinguish between induced change and ongoing variability in the neural responses. Furthermore, experiments with low levels of bursting showed a higher efficacy of inducing functional plasticity and the induced changes were maintained for at least 2 hours after tetanic stimulation. Hence, we recommend controlling bursting with artificial sensory input as a more realistic model for studying the network correlates of synaptic plasticity *in vitro*. By providing a link between aberrant patterns of synchronized

activity and the information processing capacities of neuronal ensembles, this study may be provide useful clues for treating learning disorders in juvenile epilepsy.

3.1 Introduction

Dissociated cortical cultures provide an accessible and controllable model of the brain while preserving the essential molecular and structural properties of the individual neurons in the cortex [20, 21]. Such cultured neuronal networks can be grown on multi-electrode arrays (MEAs), which provide a two-way interface with the cells through electrical recording and stimulation of neuronal activity [4, 6]. Complex spatiotemporal patterns of stimulation can be delivered continuously and rich dynamic network-level activity patterns can be followed over months [19] making this an attractive model for the study of long term functional changes in neuronal ensembles. Since we have complete control of the inputs to the neuronal network, this set up is ideal to explore the effects of diverse stimulation patterns on the network dynamics.

One of the major disadvantages of *in vitro* models is that they lack the rich spatiotemporal sensory inputs that the brain continuously receives. Multi-electrode stimulation protocols provide artificial sensory background to dissociated cortical networks [60] and make their activity patterns more like those recorded *in vivo* by eliminating synchronous population bursts, while preserving the ability of the network to fire action potentials. We propose that cultured networks receiving continuous multisite stimulation might be more suitable than isolated networks for the study of learning and long term plasticity *in vitro*.

Waves of activity observed in the developing retina sculpt neuronal connectivity [27, 28]. But, as the mature retina becomes visually responsive, these waves disappear,

since their continued presence could interfere with transmission of information [35]. Unlike developing networks *in vivo*, dissociated cortical networks retain synchronous bursting for their lifetime [24, 53, 54]. Modeled neuronal networks have shown that spontaneous bursts, characterized by transient increases in the population firing rates by a factor ≥10, destabilize synaptic weights [59]. Functional changes induced by tetanic stimulation delivered to dissociated cortical networks were comparable to ongoing spontaneous changes in spiking activity except when spontaneous bursts were suppressed using elevated magnesium [45]. Long term potentiation in hippocampal slices can be disrupted by electroencelographic seizure-like activity patterns [92, 93], possibly providing explanations for seizure-induced amnesia [94, 95] . Hence, we hypothesized that uncontrolled barrages of spiking activity act as a potential forgetting mechanism by possibly erasing the effects of subtle synaptic changes induced by external stimuli. By controlling the amounts of spontaneous bursting at will, by adjusting the frequency of distributed electrical stimulation [60], we can systematically test the effects of varying levels of ongoing activity on long term plastic changes.

The goal of this study was to investigate the effects of ongoing spontaneous activity on the ability to induce functional plasticity in neuronal networks. Functional plastic changes induced by tetanic stimulation were studied on a background of different levels of burst-controlling stimulation and the magnitudes of detected changes were compared to the levels of ongoing activity. Long term functional changes, lasting for at least 2 hours, were induced by the tetanus and the amount of tetanus-induced change was inversely proportional to the amount of non-stimulus locked bursting, thus demonstrating a direct link between levels of ongoing activity and long term plastic changes.

3.2 Materials and Methods

3.2.1 Cell culture

Dissociated cultures of neurons and glia, obtained from the cortex of embryonic day 18 Sasco Sprague-dawley rats, were cultured on MEAs using techniques described elsewhere [22]. Briefly, after enzymatic digestion using papain (Roche scientific, Indianapolis, IN) and mechanical dissociation using a 1mL pipette, the cells were strained and centrifuged (on to 5% bovine-serum albumin) to get rid of large debris. The dissociated cells were counted and plated on MEAs pre-coated with polyethylene imine (Sigma, St. Louis, MO) and 20µL drop of laminin (Invitrogen, Carlsbad, CA). 50,000 cells (neurons and glia) in a 20µL drop were plated on to the laminin and the cells were incubated 24 hours in the plating medium (Neurobasal (Invitrogen), 10% horse serum (Hyclone, Logan, UT), 2mL B27 (Invitrogen) and 100µL glutamax (Invitrogen)). The next day the entire medium was replaced with the feeding medium adapted from Jimbo *et al.* (1998) consisting of Dulbecco's modified eagle's medium (Irvine Scientific, Santa Ana, CA), 10% horse serum, 1mL sodium pyruvate (Sigma) and 100µL glutamax. The MEAs were sealed with a special Teflon membrane that allows for gas but not water exchange, eliminating the use of antibiotics in the feeding medium. The cultures were maintained in an incubator controlled at 5% CO2, 9% O2 and 65% humidity. This reduced humidity provides for an electronics-friendly environment, allowing us to perform all our electrophysiology inside the incubator. Since culture density has been shown to affect the rate of bursting [53], all the cultures used for this study were of the same density. Only cultures that exhibited robust spiking on >45 electrodes were chosen for experiments. The choice of cultures was not based on their spontaneous (un-

stimulated) burst rates. Cultures used for the present study were between the ages of 21 and 35 days *in vitro*.

3.2.2 Electrical recording and stimulation system

The multi-electrode arrays, MEAs, (Multichannel systems, Reutlingen, Germany) consist of 60 substrate embedded titanium nitride electrodes, 30µm in diameter, with 200µm spacing between the electrodes. The signals were recorded at 25kHz/channel using our custom-made real-time Meabench software, which also allows for online spike detection [19]. MeaBench's real time artifact suppression filter [85], allow us to record spikes as early as 2ms after stimulation (except on the electrode being stimulated). In order to stimulate 60 electrodes, we used our custom-made 60-channel stimulator [86]. Typical stimulus pulses were biphasic rectangular voltage pulses (<1V to prevent electrochemical damage to electrodes and nearby cells), positive phase first, because they were found to be most effective in evoking a response [87].

3.2.3 Experimental protocol

3.2.3.1. Choice of electrodes

Before each experiment, we probed each electrode 10 times with a 600mV stimulus pulse in random order; inter-stimulus interval was 1 second. The stimulation electrodes that evoked an array-wide response greater than the spontaneous firing rate were identified. Typically, 40-50 electrodes had sufficient contact with the cells to attain that level of response when stimulated with the fixed voltage pulse. For each of the identified stimulation electrodes, we calculated the mean array-wide spike rate, 200ms post-stimulus, over all 10 presentations of the stimulus. Six stimulus electrodes that

evoked the highest mean post-stimulus responses were identified. Probe and tetanus electrodes were chosen from this electrode pool. 20-25 other quieting electrodes were chosen from the remaining pool of identified stimulus electrodes.

3.2.3.2 Single electrode stimulation experiments

1-2 electrodes were stimulated in sequence, 1000 times each, with an inter-stimulus interval of 1-5 seconds. The stimulus pulses were of a fixed amplitude of 600mV. This experiment was repeated on three cultures, with 2-4 stimulation electrodes per culture.

3.2.3.3 Tetanus experiments

Several electrodes were probed [37] on a background of burst controlling stimulation to test for effects of the level of spontaneous bursting on post-stimulus responses after tetanic stimulation. A probe is a single stimulation at one electrode. Tetanic stimulation was used as a means to potentially induce plastic changes in the network. Experiments were performed on seven cultures from three different platings. Each culture was tested twice with different amounts of burst controlling stimulation.

3.2.3.4 Electrical burst control

Multi-site electrical burst control was used in the experiments to disrupt the level of spontaneous bursting in the culture [60]. While low frequency (0.5 - 2Hz) stimulation entrains bursts, 20Hz aggregate stimulation frequency showed imperfect burst-control and perfect burst control was obtained at 50Hz aggregate stimulation frequency [60]. To obtain varied levels of spontaneous bursting activity, a group of 20 or 25 electrodes were stimulated cyclically at 0Hz (no quieting stimulation), an aggregate of 20Hz (1

stimulation/sec) or an aggregate 50 Hz (2 stimuli/second) to disrupt the amount of spontaneous bursting in the culture (Figure 3.1). The electrodes for burst quieting were chosen arbitrarily from a pool of electrodes identified by initial probing (see *Choice of electrodes*). The quieting electrodes were stimulated with voltages between 200-400mV.

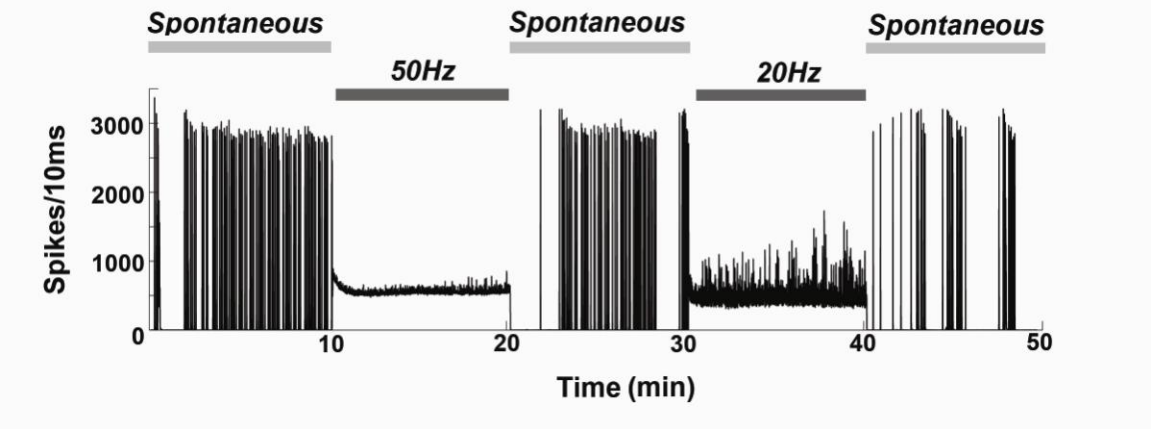

Figure 3.1: Multi-site electrical stimulation could reversibly control the amount of spontaneous bursting in the culture. Array-wide spike rate (number of spikes/10ms bin) of 10 minutes periods of spontaneous activity separated by 10 minutes of burst controlling stimulation are shown for a representative culture. Multi-site stimulation on 20 or 25 electrodes at an aggregate frequency of 20 or 50Hz was used to control the amount of bursting. While 20Hz distributed stimulation allowed some bursting, perfect burst control was observed on using 50Hz stimulation distributed on 25 electrodes. Spontaneous bursting resumed soon after the stimulation was stopped, though the pattern of bursting was changed.

3.2.3.5 Details of probe sequence

Test pulses of fixed amplitude (600mV or 800mV) were delivered to 4-6 chosen probe electrodes. The probe pulses were applied every 1-3 seconds such that each probe electrode was stimulated every 4-18 seconds. The burst controlling sequence was suspended for 50ms before and 200ms after a probe stimulus, so that responses to probes could be measured without interference from background burst control stimulation. Each probe electrode was stimulated 1000 times before and after the tetanus sequence.

3.2.3.6 Details of tetanic stimulation

Two of the probe electrodes were used as tetanus electrodes. Tetanus consisted of a train of stimuli delivered to two electrodes with an inter-stimulus interval of 10ms. Each train consisted of 20 such pairs at pair interval of 100ms. Tetanus sequence consisted of 150 such trains at 6 second intervals [45]. The tetanus train lasted for 15 minutes. The tetanus was longer than other studies to ensure network changes. During tetanization, burst control stimulation was suspended.

3.2.4 Analysis

3.2.4.1 Variability in post-stimulus responses

The spiking activity that occurred within 1 second before each stimulus (single electrode stimulation experiments) was binned into ten 100ms segments. The array-wide firing rates within each bin were measured and the burstiness factor (BF) was calculated using these 10 values (see *Burst detection*). The array-wide firing rate within 100ms post-stimulus was also measured (spikes per 10 ms). Thus, two values were calculated for each probe: one value for BF and one value (firing rate) for post-stimulus responses.

A thousand BF values calculated from 1000 probes were binned into 100 bins from 0 to 1. Responses (firing rates) from the stimuli that had BF values in the same bin were grouped together and the mean and standard deviation of the post-stimulus firing rates in each group was calculated. The significance of the correlation between BF and variance of post-stimulus responses was determined by the Spearman rank correlation test. Unlike other tests for correlation, this test does not require the assumption that the

relationship between the variables be linear. Instead, it just assesses how well an arbitrary monotonic function can describe the relationship between two variables.

3.2.4.2 Center of activity trajectory

To capture the dynamics of spatiotemporal patterns of responses to probe stimulation we used a novel measure of network response, Center of activity trajectory [59]. Intuitively, it is the spatially weighed average of temporally binned responses evoked by probe stimulation. Previous studies of *in vitro* use-dependent plasticity have used population firing rates as the measure to detect plastic changes [31, 44, 45]. There is an idea that neuronal activity levels can homeostatically regulate the properties of neural circuits to maintain firing rates within certain boundaries [7]. In view of this idea that firing rates are unstable, we used a novel measure, CAT, which incorporates both spatial and temporal dynamics of the network activity. CAT has been shown to be a more sensitive-measure of functional changes in multi-dimensional spiking data (Chao *et al.* (2007), *submitted*)

Evoked responses within 200ms of each probe stimulus were used to calculate the CAT. CAT has been described in detail elsewhere [59]. Briefly, firing rate histograms (FRH) were calculated for each recording electrode E_j in response to stimulation at probe electrode P_i, $FRH_{E_j}^{P_i}$ as the average number of spikes that occurred in 1ms moving time window with a time step of 100μs over trials. The FRH for each bin on each recording electrode was weighted by the physical location of the recording electrode in the 8 X 8 dimensional physical space of the MEA [59]. The X and Y component of the CAT vector

were appended together to create a CAT vector for responses evoked by each probe electrode.

3.2.4.3 Statistics

The probe periods were divided into four parts of equal duration to calculate statistics: *Pre1*, *Pre2*, *Post1* and *Post2*. The time interval between *Pre1* and *Pre2* (*i1*) and between *Pre2* and *Post1* was of the same duration as the tetanus. The 15-minute interval between *Pre2* and *Post1* was the tetanization. For each of the probes within an experiment the mean distance between the CAT vectors in *Pre2* to the centroid of CAT vectors in *Pre1* (Δ_{i1}) was compared to the mean distance of CAT vectors in *Pre1* to their own centroid (σ_{pre1}). The ratio of Δ_{i1} and σ_{pre1} was used to estimate the *intrinsic drift* in the responses between periods *Pre1* and *Pre2* before the tetanus (no drift if this ratio is 1).

$$Intrinsic\ drift = \frac{\Delta_{i1}}{\sigma_{pre1}}$$

A similar measure was used to calculate the *induced change* in responses between periods *Pre2* and *Post1* (tetanus-induced functional change). For each of the probes within an experiment the mean distance between the CAT vectors in *Post1* to the centroid of the CAT vectors in *Pre2* (Δ_{tet}) was compared to the mean distance of CAT vectors in Pre2 to their own centroid (σ_{pre2}). The ratio of Δ_{tet} and σ_{pre2} was used to estimate the *induced change* in the responses between periods *Pre2* and *Post1*.

$$Induced\ change = \frac{\Delta_{tet}}{\sigma_{pre2}}$$

The significance of the tetanus-induced changed was calculated by comparing the average values of *induced change* and *intrinsic drift* over all probes within an experiment using Wilcoxon's rank test for equal medians.

3.2.4.4 Burst detection

Burst detection methods have been described in detail previously [53]. Briefly, a burst on a single electrode (sub-burst) consisted of at least 5 spikes within 100ms separated from other bursts by at least 250ms. Sub-bursts overlapping in time were grouped together to form a single culture-wide burst. For each burst, the onset times and the offset times of the burst were defined. The onset of the burst was defined as the first time before the peak of the burst when the array-wide spike rate within the burst was 20% of the peak firing rate. The offset of a burst was defined to be the last time after the peak of the burst, that the spike rate within the burst was 20% of the peak firing rate. Single electrode stimulated at low frequencies (0.5-2Hz) can evoke bursts that are time-locked to the stimulus pulse. To tell apart non-stimulus locked bursts and stimulus-locked 'evoked' bursts, we classified any burst with an onset within 10ms of the stimulus to be an evoked burst. Other bursts were classified as non-stimulus locked bursts, referred in the further text simply as 'bursts'. Spontaneous bursts were bursts identified during periods of no stimulation.

In the single electrode stimulation experiments, we did not differentiate between non-stimulus locked and evoked bursts but instead quantified the burstiness of the culture. In the single electrode stimulation experiments, the burstiness factor for 1s of spiking activity that occurred before the stimulus was calculated as follows. The total numbers of spikes across all electrodes in 100ms bins were counted. Burstiness factor

(BF) was defined as the normalized fraction of the total number of spikes accounted for by the 15% of the bins with the highest count. BF close to 1 indicates a bursty culture while BF of 0 indicates no bursting. This measure was adapted from burstiness index described by Wagenaar et al. (2005), but with shorter time bins of 100ms instead of 1s.

3.3 Results

3.3.1 Spontaneous bursting can be controlled by multisite electrical stimulation

Spontaneous culture-wide bursting in cortical cultures, first observed at 5-8 days *in vitro* [23, 24, 38, 53] is a dominant pattern of activity for the lifetime of the culture. This global form of activity bears closer resemblance to synchronous waves of activity present during development [27], than single cell information-carrying bursts [56]. Spontaneous bursting can be abolished by using excitatory channel blockers [18, 24, 38] but this also reduces the overall firing rate of the culture. As described in Chapter 2, distributed electrical stimulation, unlike pharmacological interventions, reduced bursting without reducing the ability of the culture to respond to other electrical stimuli [60]. The amount of burst control could be varied by the varying the aggregate stimulation rate [60]. Stimulating the culture at an aggregate of 50Hz distributed over 25 electrodes resulted in the total suppression of bursting activity, while stimulating the same culture at a slower rate of 20Hz, distributed over 20 electrodes, resulted in ineffective burst control (Figure 3.1). Moreover, spontaneous bursting resumed shortly after the cessation of the stimulation (Figure 3.1) showing that bursts could be reversibly controlled by distributed stimulation. To obtain different levels of burst control in the *Tetanus experiments*, the cultures were stimulated at 0, 20 or 50Hz aggregate on 20-25 electrodes (see Materials and methods).

3.3.2 Burstiness of the network before the stimulation affects the variability of post-stimulus responses

Prior to testing the effects of controlling spontaneous bursting on functional plasticity, we determined whether the burstiness of the culture had any effects on the responses to single electrode electrical stimulation (see Materials and methods, *Single electrode stimulation*). The firing rates across the 100ms post-stimulus (post-probe) were compared to the burstiness of the culture in the 1 second period before the probe (Figure 3.2). The standard deviation of post-stimulus responses was low if the activity prior to the probe had fewer spontaneous bursts (burstiness factor, BF<0.2), and proportionally increased with the increase in BF. Low standard deviation of the post-stimulus firing rates was observed in trials with BF<0.2 pre-stimulus (dispersed spiking patterns, right panel, Figure 3.2). In contrast, trials with BF>0.2 pre-stimulus (higher incidence of spontaneous bursts), showed high standard deviation in the corresponding post-stimulus firing rate (right panels, Figure 3.2). The correlation coefficient between BF and the variability in the post-stimulus responses was 0.72 (tested for three cultures, 2-4 stimulus electrodes per culture, p-value<1e-4, Spearman's test for correlation).

Responses evoked by single-electrode 'probe' stimulation are used to test for functional plasticity induced by a strong tetanus train in dissociated cultures [30, 31]. The above results demonstrate that network activity dominated by spontaneous bursts increase the variability of probe-evoked responses (Figure 3.2), leading to an unstable baseline of responses for measuring tetanus-induced plastic changes. Thus, methods that reduce spontaneous bursting could help in maintaining stable post-stimulus responses and provide a steady baseline to detect functional plasticity.

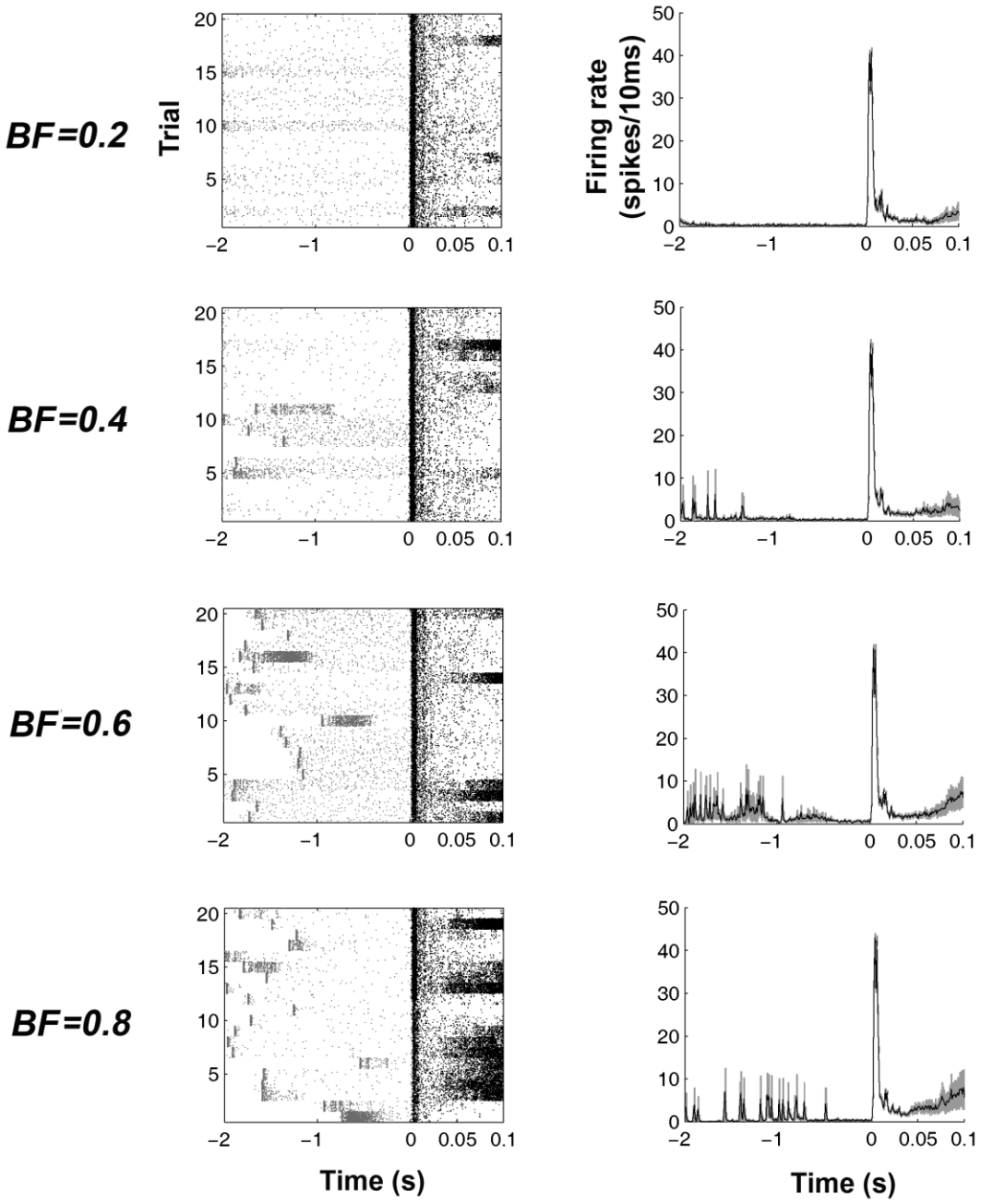

Figure 3.2: Variance in the post-stimulus responses was proportional to the amount of spontaneous bursting before the stimulus. The array-wide firing rates (right panels) and corresponding example raster plots (left panels) for different values of burstiness factor (BF) are shown. The mean and standard deviation of the array-wide firing rates (number of spikes/10ms) of activity 1 second before and 100ms after the stimulus for all 9 stimulation electrodes are shown in the right panels. Low amounts of spontaneous bursting before the stimulus (BF<0.2) allowed for more stable post-stimulus responses, compared to increased amount of spontaneous bursting before the stimulus (BF>0.2) that resulted in a larger variance in post-stimulus responses. .

3.3.3 Efficient burst control resulted in larger amounts of detected functional plasticity

To test for functional plasticity we stimulated the cultures with a strong tetanus on a background of varying amounts of burst control (see Materials and methods, *Tetanus experiments*).

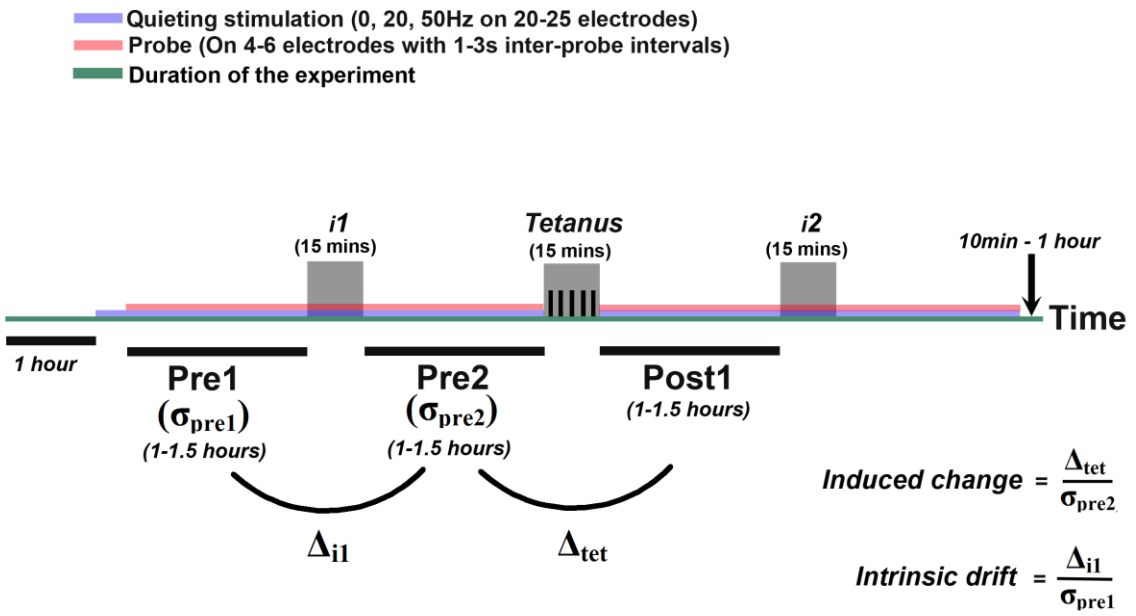

Figure 3.3: Time line of tetanus experiments explaining various terms used in the present study. Spontaneous activity was recorded for an hour before the beginning of each experiment. Quieting stimulation consisted of 20-25 electrodes stimulated cyclically at an aggregate of 0, 20 or 50Hz to allow for different amounts of spontaneous bursting. Superimposed on this quieting stimulation, 4-6 other electrodes (probes) were stimulated sequentially, 1000 times, with an inter-stimulus interval of 1-3 seconds. Tetanus consisted of 150 trains of 20 pulses pairs at 10Hz (inter-pulse interval of 10ms, inter-train interval of 6 seconds) applied on two of the probe electrodes. The tetanus lasted 15 minutes. The probe periods were divided into four parts of equal duration to calculate statistics: *Pre1*, *Pre2*, *Post1* and *Post2*. The time interval between *Pre1* and *Pre2* (i1) and between *Post1* and *Post2* (i2) was set to match the length of the tetanus. The 15-minute interval between *Pre2* and *Post1* was the tetanus period. For each of the probes within an experiment the mean distance between the CAT vectors in *Pre2* to the centroid of CAT vectors in *Pre1* (Δ_{i1}) was compared to the mean distance of CAT vectors in *Pre1* to their own centroid (σ_{pre1}). The ratio of Δ_{i1} and σ_{pre1} was used to estimate the *intrinsic drift* in the responses between periods *Pre1* and *Pre2* before the tetanus (no change if this ratio is 1). A similar measure was used to calculate the change in responses between periods *Pre2* and *Post1*. For each of the probes within an experiment the mean distance between the CAT vectors in *Post1* to the centroid of the CAT vectors in *Pre2* (Δ_{tet}) was compared to the mean distance of CAT vectors in Pre2 to their own centroid (σ_{pre2}). The ratio of Δ_{tet} and σ_{pre2} was used to estimate the *induced change* in the responses. The significance of the tetanus-induced changed was calculated by comparing the average values of *induced change* and *intrinsic drift* for all probes within an experiment using Wilcoxon's rank sum test for equal medians.

Since dissociated cortical cultures were found to be resistant to change [45], we used an unusually long tetanic train lasting 15min to ensure an effect. Varied levels of non-stimulus evoked bursting were achieved by stimulating 20-25 electrodes at the rates of 0, 20 or 50 stimuli/sec (see Materials and Methods, *Electrical burst control*). Probes were superimposed on the background of burst controlling stimulation and 200ms of post-probe responses were used to quantify the network dynamics using the center of activity trajectory (CAT, [59], see Materials and methods). The changes across the tetanus were compared to the average non-stimulus evoked burst rate (bursts/min) during the periods *Pre1* and *Pre2* before the tetanus and *Post1* after the tetanus (Figure 3.3).

Experiments with lower spontaneous burst rates (<1 burst/min) showed higher amounts of *induced change* compared to experiments with burst rates >1 burst/min (Figure 3.4A). An *induced change* value of 1 would indicate that the amount of change across the tetanus (between *Pre2* and *Post1*) was equal to the amount of intrinsic drift in *Pre2* before the tetanus, meaning that the tetanus did not cause a change in the evoked response. The *induced change* for experiments with low efficacy of burst control (spontaneous burst rate >1 burst/min) was close to 1, indicating that there was little significant detectable change caused by the tetanus in these experiments.

To summarize the results, the experiments were classified into two categories based on their mean burst rates; spontaneous burst rates <1 burst/min, labeled less-bursty and spontaneous burst rates >1 burst/min, labeled more-bursty. On average, the amount of *induced change* in the less-bursty experiments was significantly more than in the more-bursty experiments (Figure 3.4B, $p<1e-3$, Wilcoxon's rank sum test).

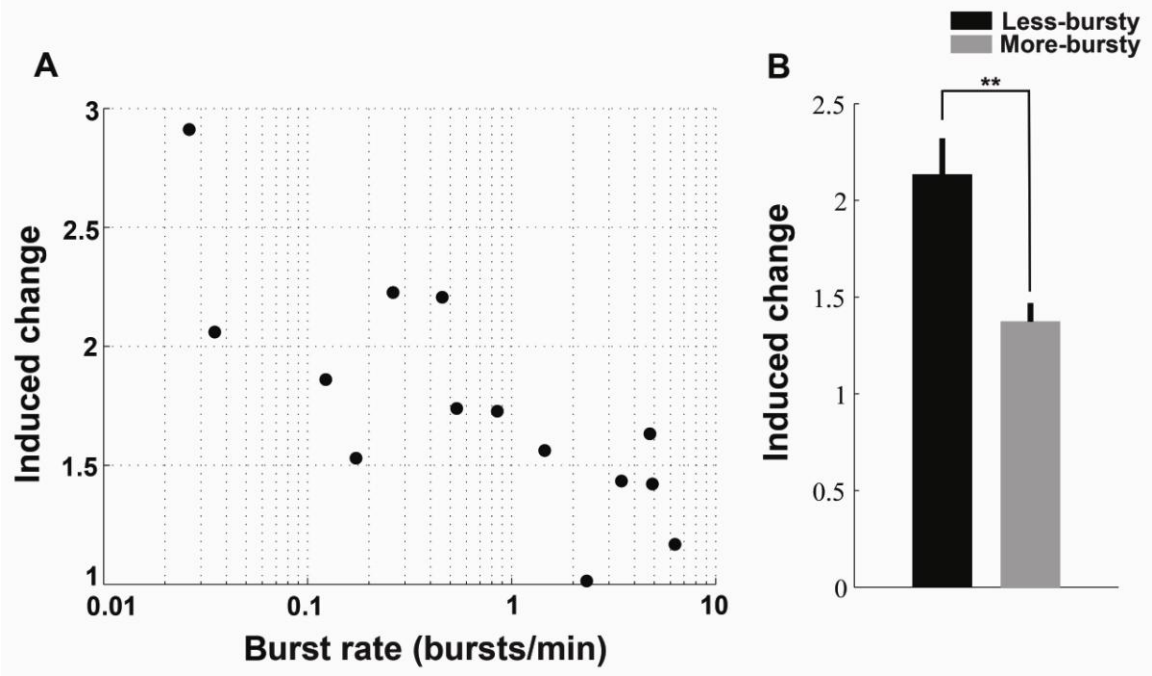

Figure 3.4: Lower amounts of bursts enhanced tetanus-induced change. A. Low rates of bursting increased the efficacy of detecting *induced change*. Correlation coefficient is -0.78, p-value<5e-3, Spearman rank correlation test. Each dot represents the average *induced change* for all the probes within one experiment and the graph shows data obtained from N=14 experiments, consisting of 4-6 probe electrodes each. **B.** On average *induced change* in the less-bursty experiments was significantly more than in the more-bursty experiments (p<1e-3, Wilcoxon's sign rank test). Error bars represent SEM. (** = p<1e-3).

3.3.4 Burst control reduced spontaneous drift in the probe responses

To investigate the lack of detectable *induced changes* in experiments with higher incidence of bursts, we compared the amount of *intrinsic drift* between periods *Pre1* and *Pre2* before the tetanus (see Materials and methods). An increase in burst rates resulted in decreased disparity between the *induced change* and the *intrinsic drift* (Figure 3.5A). A comparable value of the *induced change* and the *intrinsic drift* implies that indeed as inferred from figure 3.2, the increased variability in evoked responses before tetanus (drift) renders it difficult to detect tetanus-induced changes. On average, more-bursty experiments exhibited significantly higher amounts of drift than less-bursty experiments (Figure 3.5B, p<1e-2, Wilcoxon's rank sum test).

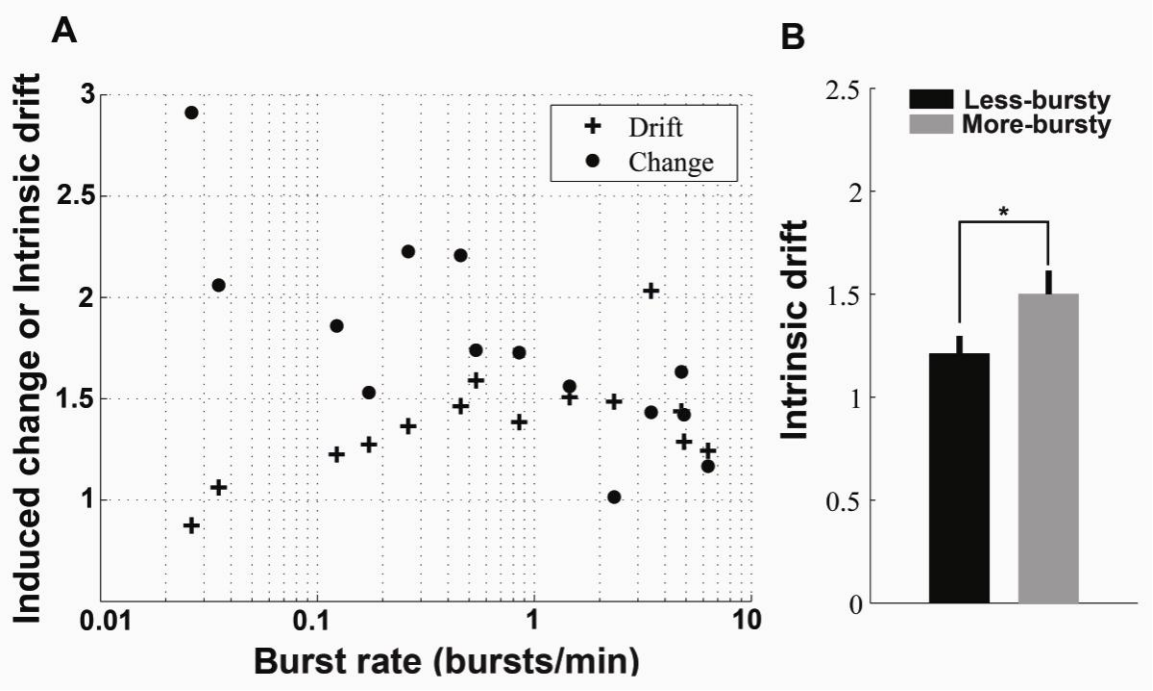

Figure 3.5: Increased rate of bursting was accompanied by increased intrinsic drift in probe responses, making it difficult to tell apart tetanus-induced induced change and intrinsic drift. A. The difference between *induced change*s (.) and *intrinsic drift* (+) was low in the experiments with high rates of bursting (>1 burst/min). Each point represents the average for all the probes in an experiment and the results from N=14 experiments, consisting of 4-6 probe electrodes each are shown. **B.** On average *intrinsic drift* in the more-bursty experiments was significantly more than in the less-bursty experiments (p<1e-2, Wilcoxon's sign rank test). Error bars represent SEM. (*=p<1e-2)

Correspondingly on testing for the significance of the difference in the magnitude of *induced change* and *intrinsic drift* using a one-tailed t-test, the rate of spontaneous bursting was found to be directly related to the p-value (correlation coefficient = 0.77). Hence, low levels of bursting provided increased ability to detect functional changes.

3.3.5 Control of spontaneous bursting made cultures more amenable for the induction of functional plasticity

To track the changes in probe responses over time, the changes in the CAT of probe responses (respective Δ/σ) were calculated with reference to the period *Pre1* at the start of the experiment (Figure 3.6A, B).

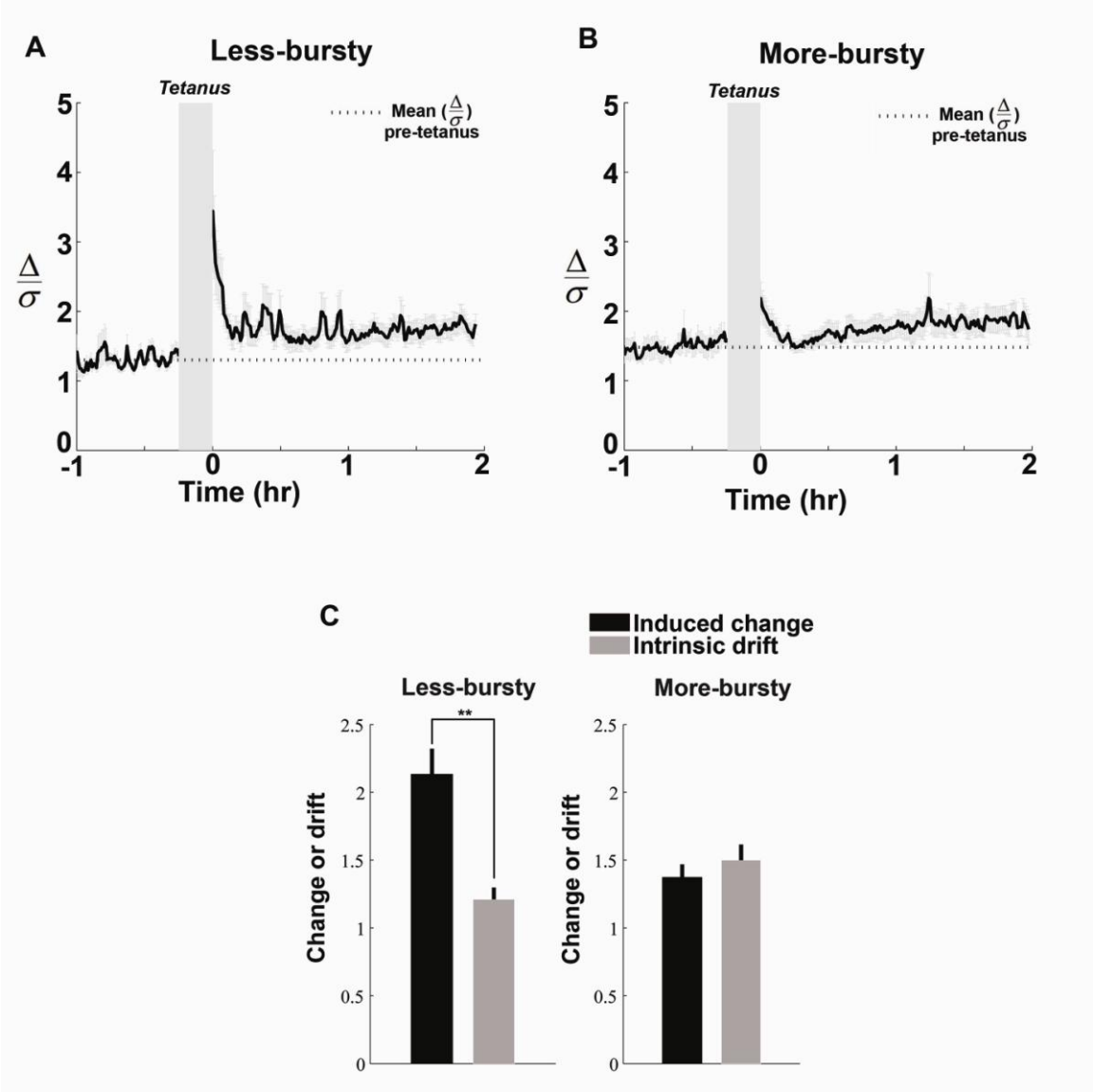

Figure 3.6: Less-bursty experiments exhibited more tetanus-induced changes that persisted for at least 2 hours compared to the more-bursty experiments. The average amount of change over time (Δ/σ) was determined as the distance between the CAT vectors in *Pre2* and the period after tetanus, normalized by the distance between CAT vectors in *Pre1* (using a time window of 20 probes (time step = 5 probes)). The average values for Δ/σ was calculated for all the probes in the less-bursty (A) and more-bursty (B) experiments. **A.** The average amount of *induced change* was significantly higher than the *intrinsic drift* before the tetanus in the less-bursty experiments. The significance of the change ($p<1e-3$, rank sum test) in the less-bursty experiments lasted for at least 2 hours after the tetanus. **B.** In the more-bursty experiments, though there was a transient short term change immediately after the tetanus, the changes retuned to pre-tetanus levels with ~15mins. The dotted lines indicate the mean pre-tetanus levels. The gray bar indicates the period of tetanization. **C.** On average, the *induced change* in the less-bursty experiments was significantly more than the *intrinsic drift* ($p<1e-3$). In contrast, the change and drift values were comparable in the more-bursty experiments. Error bars represent SEM. (** - $p<1e-3$)

On comparing the amounts of intrinsic and induced changes, not only did the less-bursty experiments exhibit higher amounts of tetanus-induced changes compared to the more-bursty experiments, but the change also lasted for the duration of the recording (at least 2 hours, Figure 3.6A, B). On average the amount of tetanus-induced change in less-bursty experiments was far greater than the intrinsic variability in probe responses (Figure 3.6C, $p<1e-3$, Wilcoxon's rank sum test). In contrast, the average *induced changes* were statistically difficult to discern from average *intrinsic drift* values in the more-bursty experiments (Figure 3.6C, $p = 0.5$, Wilcoxon's rank sum test).

Furthermore, for less-bursty experiments, the tetanus-induced changes did not return to pre-tetanus levels for the entire recording period indicating that burst-control did not just increase our ability to detect but also to induce long term, stable plastic changes that persist for at least 2 hours after the tetanus (Figure 3.6A). In the more-bursty experiments, though there was a small short-term change immediately following the tetanus, the response drifted considerably over the 2 hour period after the tetanus (Figure 3.6B).

Tetanus-induced plasticity has been difficult to demonstrate in dissociated cortical networks [45, 46]. Though burst-control allowed for higher efficacy to detect plastic changes, this does not directly imply that it provided improved ability to induce functional changes in cortical networks. To answer this, we compared the variability in the probe responses in the last 10mins of period *Post1* (Figure 7). Since the variability of probe responses was comparable for the lower and higher rates of bursting, the high magnitude of *induced change* in the less-bursty experiments was due to fewer bursts (efficient burst control) rather than low variability in probe responses.

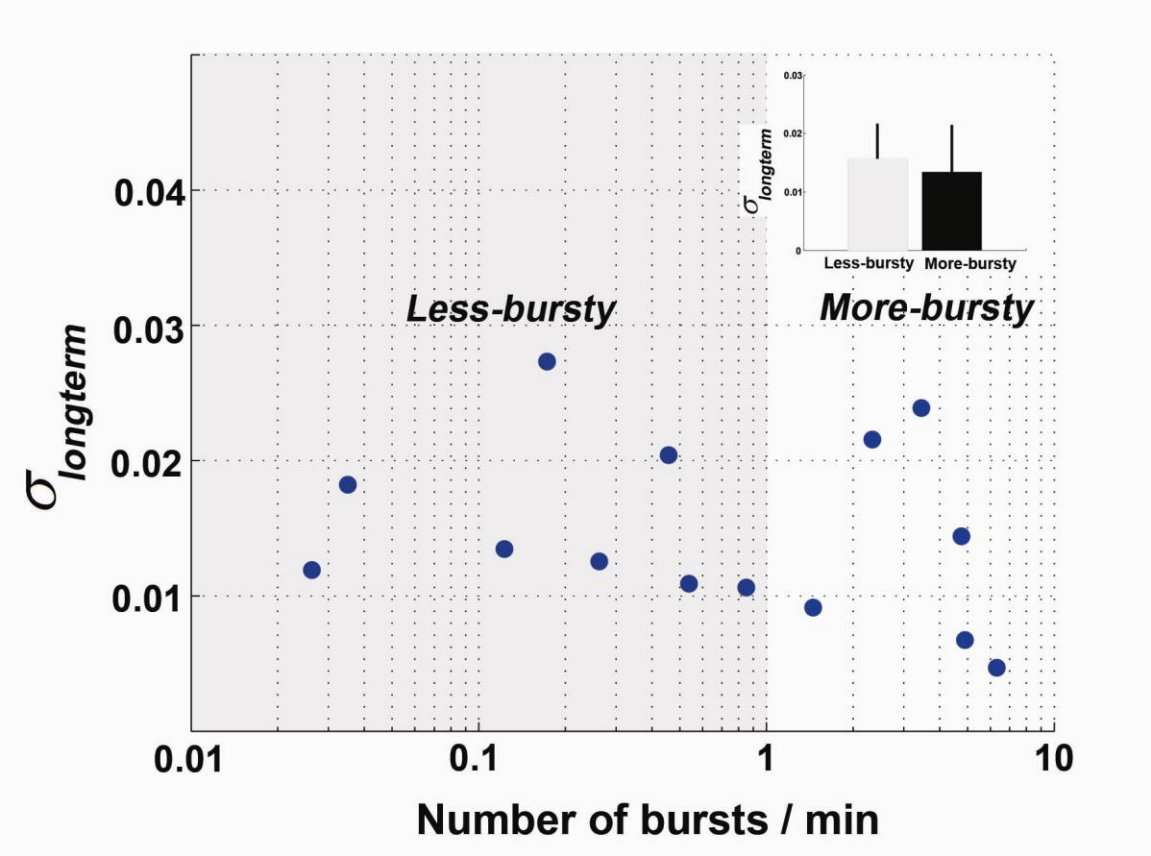

Figure 3.7: Long term post-tetanus variability of low and more bursty experiments was comparable. The variability of probe responses in the last 10mins of *Post1* was compared to the spontaneous burst rate. The inset shows the summary statistics for the graph.

3.3.6 Visualization of tetanus-induced changes using center of activity trajectories

To demonstrate the change in the spatiotemporal dynamics of tetanus-induced changes in the less and more-bursty experiments, the average center of activity (CA) trajectories for the periods *Pre1*, *Pre2* and *Post1* were plotted (Figure 3.8). The shape of the CA trajectories changed across the tetanus for at least 4 out of 6 probes in the less-bursty experiment, indicating that the tetanus altered the spatiotemporal flow of activity in the network (Figure 3.8A). In addition, even if the shapes of the CA trajectories varied between *Pre1* and *Pre2*, the change across the tetanus (between *Pre2* and *Post1*) was clearly more (Figure 3.8A). An ineffective burst controlling background stimulation

applied on the same culture resulted in a more-bursty regime and the average CA trajectories for the more-bursty experiment are shown in figure 3.8B.

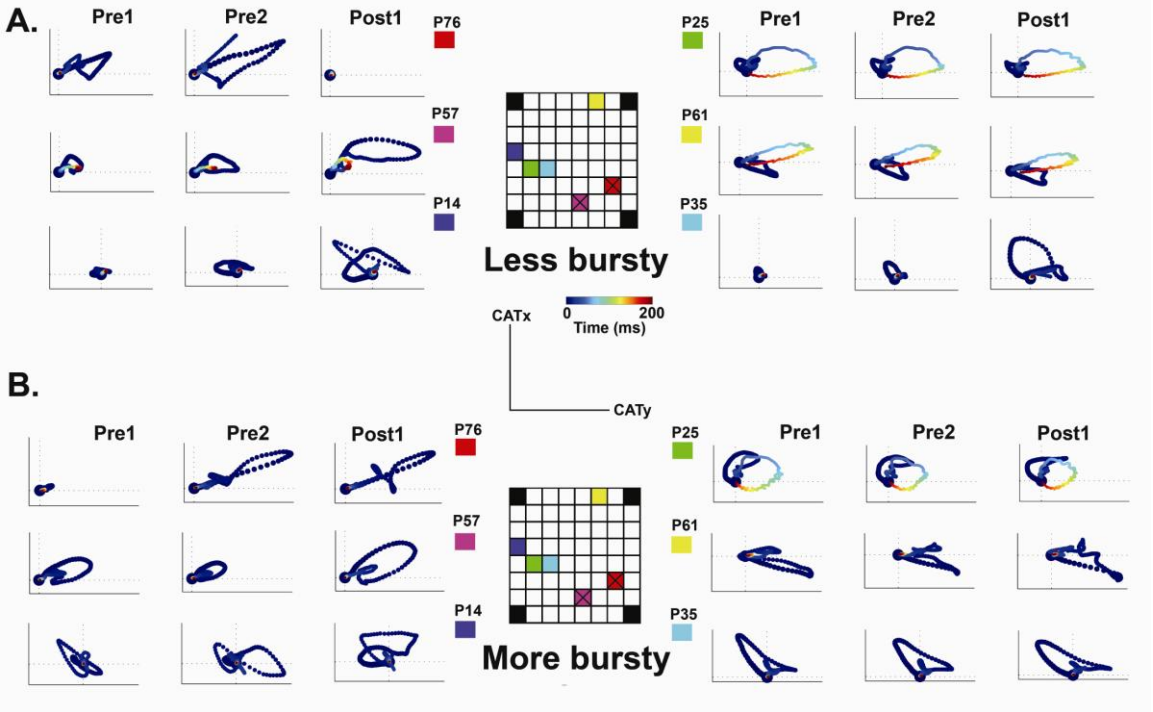

Figure 3.8: CA trajectories for Pre1, Pre2 and Post1 periods for a representative less-bursty and more-bursty experiment on the same culture. The location of the probe electrodes are shown on the MEA grid with colors representing the different probe electrodes. The crossed colored grids indicate position of the pair of tetanus electrodes. The color scale on the CA trajectories represents time of 0-200ms post-stimulus. A. CA trajectories for 6 probe electrodes for a representative less-bursty experiment. The CAT drifted between *Pre1* and *Pre2* periods but the *induced change* from *Pre2* and *Post1* (across the tetanus) was more than the *intrinsic drift* for most probe electrodes. B. CA trajectories for 6 probe electrodes for a representative more-bursty experiment. The *intrinsic drift* in CAT between *Pre1* and *Pre2* periods was comparable to the *induced change* between *Pre2* and *Post1* for most probe electrodes.

The spontaneous burst rate (burst rate in one hour spontaneous recording prior to the experimental period, Figure 3.3) in the seven cultures used for the *Tetanus experiments* ranged from a minimum of 0.38 bursts/min to a maximum of 27.45 bursts/min (Average of 11.56 ± 2.67 bursts/min in N=7 cultures used in the *Tetanus experiments*, Mean ± SEM). There was no significant correlation between the mean

spontaneous burst rate prior to the experiment and the amount of *induced change* (p=0.6, Spearman test for correlation) or *intrinsic drift* (p=0.7, Spearman test for correlation) in the network response.

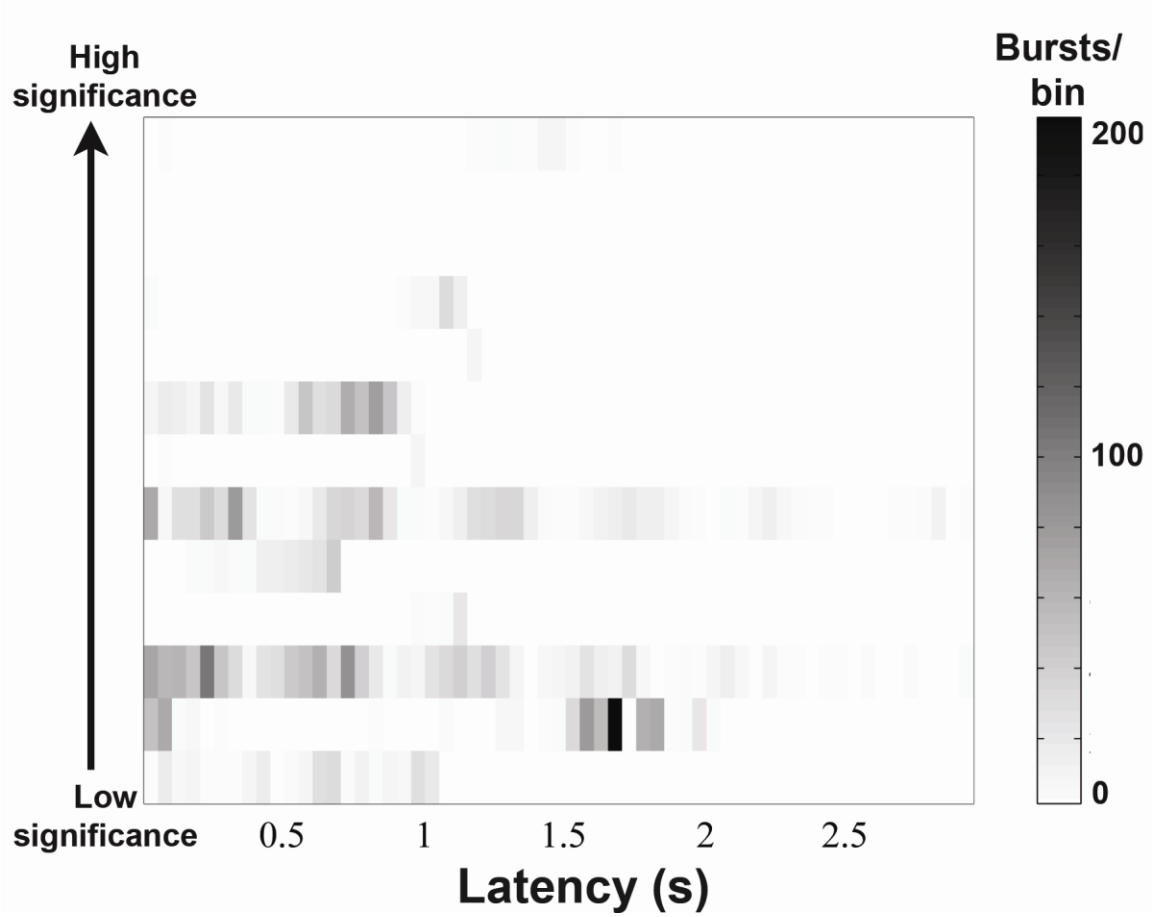

Figure 3.9: Relation between the onset of spontaneous bursts and significance of the induced change across the tetanus. Each row shows one experiment with the number of bursts in a 50ms bin (coded by gray scale on the right) as a function of the latency between the onset of a burst and time of the following probe pulse. The y-axis was sorted by the significance between the change across the tetanus and the drift in the period before the tetanus (latency). There was no clear relationship between the latency (from the onset of the burst to the time of the probe pulse) and significance of the induced changes. The experiments with high significance of *induced change* showed low levels of spontaneous bursting. This indicates that it did not matter when before the stimulus the spontaneous burst occurred but whether it occurred at all.

Hence, the amount of change or drift depended on the presence of bursts (or the degree of burst control) during the period of testing rather than the innate tendency of the culture to burst. Moreover, no clear correlation was observed between the latencies of

onsets of spontaneous bursts before the stimulus and the significance of the *induced change* (Figure 3.9). This suggests that the ability to induce plastic changes was based not so much on when a burst occurred, but on whether it occurred at all.

3.4 Discussion

Functional plasticity has been demonstrated in dissociated cortical networks on MEAs [30-32, 37, 44] but the results are controversial, since other experiments on dissociated cultures using similar protocols failed to induce significant plasticity [45, 46]. Jimbo *et al.* (1999) demonstrated pathway-specific potentiation and depression of network activity induced by tetanus by suppressing bursts using elevated levels of extracellular Mg^{2+}. We preferred non-pharmacological methods to suppress bursting, as their methods might interfere directly with plasticity mechanisms by blocking the activation of NMDA receptors. Other studies of functional plasticity in dissociated cultures have used a lower density of cells [30, 32], that exhibit lower spontaneous burst rates compared to high density cultures [53]. We used cell densities an order of magnitude higher than the above mentioned studies, to achieve densities more representative of the brain [96]. The present study of functional plasticity in dense, electrically burst-quieted cultures is the first to demonstrate experimentally the effect of burst-levels on the ability to induce network-level plastic changes in dissociated cultures, without biasing the results on the choice of cultures based on their spontaneous burst rates.

Bursts have been known to effect tetanus-induced plasticity and network state. Maeda *et al.* (1998) found that evoking bursts was necessary for inducing functional

plasticity and spontaneous bursting changed the synaptic weights in a model network of integrate-and-fire neurons [59]. We found that the efficacy of inducing plastic changes in dissociated cortical networks was directly related to the amount of bursting during the testing period, with lower burst rates allowing for higher magnitudes of tetanus-induced changes (Figure 3.4). Furthermore, tetanic stimulation resulted in stable changes that persist for up to 2 hours in the experiments with a high efficacy of burst control. Thus, the control of bursting was necessary for induction of long term stable plastic changes in dissociated cortical networks.

3.4.1 Why is spontaneous bursting bad for plasticity in cortical cultures in vitro?

Synchronized bursting in dissociated cortical cultures is predominantly a network phenomenon resulting from large amounts of positive feedback between excitatory cells in the network [74]. Accordingly, excitatory channel blockers could abolish spontaneous bursting. Correlated activity during barrages of action potentials occurring within spontaneous bursts could activate NMDA channels, leading to unpredictable changes in network synaptic weights. These uncontrolled fluctuations in synaptic efficacy could effectively reset the subtle changes caused by external stimulation, like tetanus, used to induce activity-dependent modifications in the network. Additionally, redistribution of synaptic weights could result in more variability of responses to multiple presentations of the same stimulus (Figure 3.2).

The variability of stimulus-evoked responses could be a reflection of oscillating neuronal excitability caused by irregular synchronized bursting. Immediately after a burst, there is a transient depletion of available neurotransmitter vesicles [26]. Stimulations presented during this period would exhibit a proportional reduction in the

number of evoked spikes resulting in increased fluctuations in the evoked response. *In vivo*, on a trial-by-trial basis, sensory-evoked cortical responses are extremely variable. Such trial-to-trial variability was found to be the highest under medium levels of anesthesia, during which the cortical rhythms exhibited rhythmic population bursts [97]. Anesthetic induced burst events dynamically modulated the shape, amplitude and latency of evoked responses. We extend these findings by demonstrating that the variability of evoked responses could interfere with plasticity mechanisms, by clouding the induced changes.

3.4.2 Epilepsy and learning

Since global synchronized activity interferes with plasticity *in vitro*, it would be interesting to determine whether it would have similar effects in the brain. Recurrent seizures have been shown to cause cognitive impairments in children [98-100]. Swann (2004) hypothesized that seizures in the immature brain trigger neuroprotective homeostatic processes, which could diminish glutamatergic transmission to prevent continuation of seizures. Since NMDA mediates synaptic plasticity, reduction in NMDA receptor mediated synaptic transmission might also reduce the ability of neuronal circuits to form and store memories [101]. In immature rats, recurrent seizures caused learning deficiencies in parallel with changes in excitatory receptor distributions [98]. If abolishing bursts *in vitro* affects the ability of the circuit to express plastic changes, an understanding of the mechanisms of spontaneous burst control might provide clues for the treatment of learning disorders observed in juvenile epilepsy. An important disadvantage of animal models is that they provide difficult or reduced accessibility to the networks being studied; detailed imaging and electrophysiology of neural circuits in

vivo usually requires immobilization and/or anesthetization [11, 12]. This *in vitro* culture system might be an attractive model of the brain by allowing for the detailed study of long term molecular as well as network level effects of aberrant activity patterns on functional plasticity, without the need for anesthetics.

Thus, this *in vitro* study of functional plasticity provides new methods that could be potentially used *in vivo*, with two-way electrode arrays, to investigate brain function as well as neurological disorders like epilepsy. One major drawback for traditional *in vitro* neural models is that they lack the sensory inputs that neural systems in the brain receive continuously. The study of the plasticity of network spatiotemporal dynamics, with continuous input (sensory) and continuous output (behavior) might be a more realistic model of the brain, than isolated culture models which receive intermittent input during periods of observation [19].

CHAPTER 4

ARTIFICIAL SENSORY BACKGROUND STIMULATION INDUCES ALTERED GABA EXPRESSION IN CORTICAL CULTURES[3]

GABA, the major inhibitory neurotransmitter in adult mammalian cortex, plays a crucial role in cortical development. We studied the activity-dependent changes in the proportion of GABAergic neurons in developing dissociated cortical cultures by tracking the levels of electrical spiking activity and GABAergic neurons in spontaneously active dissociated cortical cultures for a month. Immunocytochemical studies showed a significant early decrease in the percent of GABAergic neurons from 5.6% at 7 DIV to 2.5% at 10 days *in vitro* (DIV). This period corresponded to the time when spontaneous bursting was first observed in developing cultures. However, the GABA percents started to increase after 2 weeks *in vitro*, reaching 12% at 21 DIV. Spontaneous bursting in dissociated cultures can be disrupted by electrical stimulation distributed over multiple sites in the network [60]. Cultures in which spontaneous bursts were suppressed for two days showed almost a two-fold increase in the percent GABAergic neurons compared to spontaneously bursting cultures at the same age. This increased proportion of GABAergic neurons, after the onset of bursting and electrical burst quieting, suggests that activity-dependent modulation of inhibitory neurotransmitter levels could be involved in the regulation of spontaneous bursting. These homeostatic mechanisms may have been triggered to counteract the increased activity in the network during bursting or electrical burst-quieting stimulation. This study of development and control of network-level

[3] Submitted to the European Journal of Neuroscience, in review

synchronized activity could contribute to the understanding of brain disorders with aberrant synchronous activity, like epilepsy.

4.1 Introduction

Spontaneous synchronized bursts, occurring in perinatal animals, act as a means to wire the cortex [28, 64, 65] but they are replaced by heterogeneous activity in the adult awake cortex, presumably due to heavy sensory input. In contrast, dissociated cortical cultures *in vitro* continue to exhibit robust spontaneous culture-wide bursting for their lifetime [22]. Thus, the persistence of spontaneous bursts of activity in dissociated cultures suggests that they may be trapped in a developmental phase due to the lack of sensory input caused by deafferentation [24, 81]. Sprinkling electrical stimulation over multiple electrodes, as a substitute for sensory input in dissociated cortical cultures, abolished spontaneous bursting and allowed for dispersed firing patterns reminiscent of the adult awake brain [60].

GABAergic systems are involved in the modulation of neuronal excitability in the immature nervous system [64, 102-105]. GABA has been shown to modulate spontaneous bursting in the developing retina [106, 107] and GABA-receptor mediated activity was necessary to stop propagation of spontaneous retinal waves [108]. Motivated by these studies, we investigated the potential role of GABAergic neurons in the spontaneous emergence and electrical stimulation induced suppression of spontaneous bursting in dissociated cortical cultures. The profile of the development of excitatory and inhibitory levels in dissociated cortical cultures has been previously documented [96, 109], but this developmental profile has not been compared to the levels of spontaneously

occurring spiking activity. Our main goal was to investigate the correlations between the proportion of inhibitory and amounts of spiking activity in cortical cultures *in vitro*.

Dissociated cortical cultures have been used as experimental models for the study of ensemble network activity for decades [2, 20, 21, 28, 52, 54, 110]. Cortical networks cultured on multi-electrode arrays (MEAs) [4, 6] provide a unique system that allows for both stimulation and recording of network dynamics for months [19] while simultaneously providing the accessibility to continuously explore their molecular as well as cellular properties. Latham *et al.* (2000) showed that networks with a large fraction of intrinsically firing neurons have reduced tendency to burst. Electrical stimulation increased the tonic activity above spontaneous levels, resulting in the suppression spontaneous bursting [60]. Since chronic blockade of activity using TTX decreased the ratio of inhibitory neurons [69], we hypothesized that the chronic increase of firing activity, during electrical burst-controlling stimulation, may result in a corresponding increase in the inhibitory proportion. To investigate this hypothesis, we followed the spontaneous electrical activity of dissociated cortical cultures over a month and tested them for immunoreactivity to GABA. Furthermore, we tested the effects of chronic electrical burst-quieting on GABAergic expression, compared to that in spontaneously bursting cultures.

4.2 Materials and Methods

4.2.1 Cell culture

Cortical cells (both neurons and glia), were obtained from E18 rat cortical tissue and plated on multi-electrode arrays and glass-bottom petri-dishes (http://www.glass-bottom-dishes.com) using methods described elsewhere [22, 60]. Briefly, timed-pregnant

Sasco Sprague-Dawley rats were euthanized using isoflurane according to NIH-approved protocols. Embryos were removed and euthanized by chilling and decapitation. The entire neocortex, excluding the hippocampus, was dissected in Hanks Balanced Salt solution (HBSS, Invitrogen, Carlsbad, CA) under sterile conditions. After enzymatic digestion using papain (Roche Scientific, Indianapolis, IN), cells were mechanically dissociated by 2-3 passes through a 1mL pipette tip, in Neurobasal medium (Invitrogen) with B27 (Invitrogen), 0.5mM Glutamax (Invitrogen) and 10% horse serum (Hyclone, Logan, UT). To remove debris, cells were passed through a 40μm cell strainer (Falcon) and centrifuged at 150x*g* onto 5% bovine serum albumin (BSA) in phosphate buffered saline (PBS). The pellet of cells was resuspended and 50,000 cells were plated in a 10μL drop of Neurobasal on pre-coated arrays. MEAs and glass-bottom dishes were pre-coated with polyethylene imine (PEI, Sigma, St. Louis, MO) and a 20μL drop of laminin (Invitrogen). This resulted in a plating density of ~3000 cells/mm^2 on the day of plating. All cultures used in this study were plated with same volume of cell suspension at the same cell suspension density (cells/μL), since the culture density affects the types and amount of activity expressed [53]. After 30 minutes of incubation, 1mL of Neurobasal medium was added to each culture dish. After 24 hours, the Neurobasal medium was replaced by feeding medium adapted from Jimbo *et al.* 1998 (Dulbecco's modified Eagle's medium (DMEM, Irvine scientific, Santa Ana, CA), 10% horse serum, 0.5mM glutamax and 1% sodium pyruvate (Sigma)). Cultures were maintained in an incubator at 35°C, 65% RH, 5% CO2, and 9% O2. Twice a week, half of the culture medium was exchanged with fresh feeding medium. Cultures were maintained in dishes sealed with gas-permeable teflon membrane [22] that allowed for exchange of O_2 and CO_2, but was

impermeable to water. This greatly reduced the risk of infection and hence no antibiotics or antimycotics were added to the media. The use of teflon-sealed dishes allows for the maintenance of the incubator at 65% humidity, making it an electronics-friendly environment. All electrical recordings were performed inside the incubator, ensuring long term stability of our recordings. The glass bottom dishes were used as negative controls for staining (see *Immunostaining methods*). The MEAs are insulated with silicon nitride that is oxidized into silicon dioxide, the main component of glass, on exposure to air. Hence, the substrate was similar on the MEAs and the glass-bottom petri dishes. The growth of the cultures was the same on both the substrates (verified by visual inspection).

4.2.2 Immunostaining

Cultures were fixed with 4% paraformaldehyde in PBS (Invitrogen) at room temperature for 30 min. After treatment with 0.1% Triton X-100 in PBS for 20 min, they were incubated in 4% goat serum for 1.5 hr and then in the primary antibodies anti-GABA (anti-gamma aminobutyric acid, rabbit, 1:200, AB131 (Chemicon, Temecula, CA) and anti-MAP2 (anti-microtubule associated protein 2, mouse, 1:200, MAB378 (Chemicon)) overnight at 4°C. After washes, cells were incubated with secondary antibodies (Alexa Fluor 594 goat anti-rabbit, 1:500 and Alexa Flour 488 goat anti-mouse, 1:200 (Molecular probes, Eugene, OR)) for 1.5 hours at room temperature. Cell nuclei were stained using Hoechst staining (Molecular probes). Negative controls for staining were conducted with the same procedure without the primary antibodies.

4.2.3 Experimental protocols

4.2.3.1 Spontaneous experiments

We cultured three batches of 25-30 sister cultures; 10-15 cultures on MEAs and 15 cultures on petri dishes. We followed the spontaneous electrical activity of the MEA cultures over a month and fixed and stained both MEA cultures as well as cultures on petri dishes, to investigate the levels of transmitter expressions at different ages. Three cultures out of this batch were fixed at various ages *in vitro* over a month. Two cultures (one on an MEA and another on a petri dish) were stained with antibodies against GABA, MAP2 and nucleic acid stain Hoechst and the third culture was a negative control for the staining (no primary antibody, only secondary antibody added). Spontaneous electrical activity was recorded every day for 30 minutes for each MEA culture. The spontaneous spike rate (number of spikes per second) and the burst rate (number of bursts per minute) were calculated for each recording session. Cultures on petri dishes were not tested for electrical activity but showed comparable structural development and density to cultures on MEAs (verified by visual inspection).

4.2.3.2 Quieted experiments

Two sister cultures were stained on the first day of the experiment to serve as the 'baseline'. Two other sister cultures were chronically burst-quieted by multi-site electrical background stimulation for 2 days ('quieted'), while two sister cultures were allowed to express spontaneous bursts in parallel to serve as a 'control'. Multi-site electrical stimulation consisted of sequential stimulation of 59 electrodes on the MEA at an aggregate of 59Hz (Inter-stimulus interval of 17ms). This stimulation protocol suppressed spontaneous bursting for the duration of the stimulation. The stimulus pulses

were biphasic, positive-phase first with a stimulus voltage of 300-400mV and pulse duration of 400μs in each phase [87]. After 2 days of treatment, the burst-quieted cultures and control cultures were stained for anti-MAP2 and anti-GABA immunoreactivity. The experiment was repeated on six batches of six sister cultures at 12-21 DIV.

4.2.4 Imaging methods

For all experiments, five regions (the center and the four corners of the culture) were imaged for each fixed culture using a Zeiss axioscop2 upright fluorescence microscope (Carl Zeiss Inc., Thornwood, NY) using a 40X water immersion objective lens (Zeiss Achroplan 40X / 0,80 W, ∞/0). The density of cells in our culture was ~3000 cells/mm^2, which is an order of magnitude higher than most other studies in dissociated cortical networks [30, 111]. This high packing density of neurons made it difficult to tell apart individual neurons using automated image processing software. Thus, the numbers of MAP2-positive and GABA-positive cell somata were counted manually for each image by two people independently. The percent of GABA-positive neurons for a frame was calculated as the ratio of the number of GABA-positive cells to the number of MAP2-positive neurons in the frame. Fluorescence images were captured using an Olympus microfire digital camera (Olympus America Inc., Center Valley, PA). The light source for the scope was a 100W halogen lamp. Images were acquired using a FITC filter cube for Alexa Flour 488, Texas red cube for Alexa Flour 594 and DAPI cube for the Hoechst. The three dyes were also imaged simultaneously using a triple cube (FITC/Texas red/DAPI). The images were overlaid using Adobe Photoshop CS (Adobe systems Inc., San Jose, CA). Mature cultures have a thickness of ~15-20μm and we quantified the number of MAP2 and GABA positive neurons on one focal plane for each

culture. To verify that these numbers were representative, cultures at 10 and 12 DIV were imaged through the thickness of the culture. The cultures were ~15µm thick and 15 images were obtained with a step size of 1µm. The numbers of MAP2 and GABA positive cells were counted. The ratio of GABAergic neurons did not change considerably in the different sections through the thickness of the culture.

4.2.5 Electrical stimulation and recording

Electrical signals were recorded through an 8X8 array with 59 recordable silicon nitride electrodes (Multichannel systems, Reutlingen, Germany). The electrodes are 30µm in diameter and are spaced 200µm apart. After 1200x amplification, signals were sampled at 25 kHz using the MCCard (Multichannel Systems data acquisition card). Data acquisition, spike detection, artifact suppression [85] and visualization were controlled using our open-source MeaBench software which allows for detecting spikes as early as 2 ms after stimulation [19]. Spikes were detected online by thresholding at 5x RMS noise. Stimulus pulses were delivered using our custom built 60-channel stimulator [86]. Biphasic rectangular pulses (300-400mV, 400µs), positive phase first were used, since these were found to be most effective at eliciting a response [87].

4.2.6 Analysis

Array-wide spike detection rate (ASDR) was calculated as the number of spikes that were detected on all 59 recordable electrodes in 1 second. To obtain higher temporal resolution, in some cases ASDR was calculated using 50ms time bins instead of 1s (indicated in the text). Culture-wide bursts were identified by a burst detector algorithm described elsewhere [112]. Briefly, any 100ms window with more than 5 spikes on one electrode was considered a part of a burstlet. Each burstlet had to be at least 250ms apart

from another burstlet. Global bursts were identified as burstlets on several electrodes that overlapped in time. Burst rate was defined as the number of bursts that occur per minute of recording. For each recorded culture, for each day, the mean spike rate and mean burst rate were calculated for each of the 30-minute recording sessions.

4.2.7 Application of bicuculline methiodide (BMI)

A stock solution of 400µM of BMI in the feeding medium was prepared and adjusted to pH 7.4. During bath application of BMI, double the required concentration (2X) was prepared. 0.5mL of media was carefully removed from the top of the MEA culture dish and 0.5mL of the 2X BMI was added. This resulted in a final concentration of 50µM BMI in the culture dish. After 2 hours of exposure to BMI, the entire medium in the MEA dish replaced with the feeding medium, after washing the cultures twice with the feeding medium to ensure the complete removal of BMI.

4.3 Results

4.3.1 Development of spontaneous bursting in dissociated cultures

Spontaneous spiking was observed from 3-5 DIV and bursts appeared at 5-7 DIV, but at this time the bursts were few and far apart. Typical development of spontaneous activity in a dissociated cortical culture is shown in figure 4.1. Spontaneous irregular bursts were replaced by robust bursting at regular intervals by 2 weeks *in vitro* (Figure 4.1). Though the pattern of bursting changed over the course of 3 weeks *in vitro* [53], bursts were prevalent throughout the recording period of a month (Figure 4.1).

The onset of spontaneous bursts and their development has been shown to be dependent on the plating density of the cultures. High-density cultures showed earlier

incidence of culture-wide spontaneous bursting compared to sparsely plated cultures [53]. The culture plating densities in this study were ~3000 cells/mm^2, which represents the fast-developing dense cultures. The density of neurons in our cultures was ~2000 MAP2+ neurons/mm^2 a day after the cell plating.

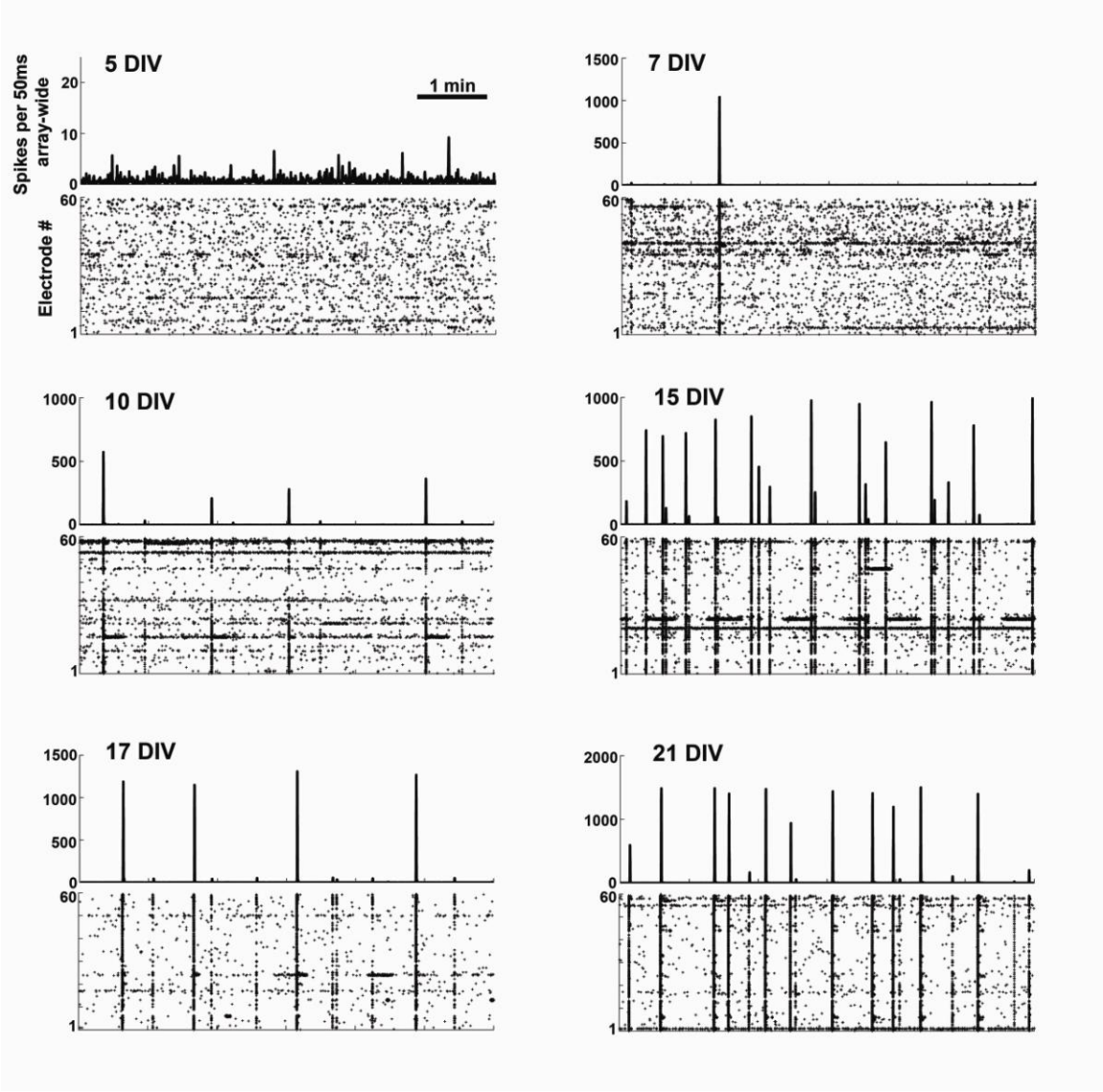

Figure 4.1: Development of spontaneous spiking and bursting for a representative culture during the first 3 weeks in vitro. Each plot shows a firing rate histogram (ASDR per 50ms) and raster plot of spiking activity on 59 electrodes for 5 minutes of spontaneous recording. Spontaneous spiking started at 5 DIV and spontaneous bursts were expressed after 7 DIV. Spontaneous bursts persisted for the life of the culture though the pattern of firing changed over the course of 3 weeks. Note that the vertical scales are different for each panel to provide clarity.

4.3.2 Effect of bicuculline methiodide (GABA antagonist) on spontaneous bursting

In the immature brain, GABAergic synapses are excitatory because of higher concentration of intracellular Cl^- leading to a positive reversal potential [102]. In mature circuits, GABA is inhibitory due to the expression of a chloride transporter, which alters the reversal potential of GABA to a negative value. To test the influence of GABAergic synapses in dissociated cortical cultures, we exposed 2-3 week old cultures to 50µM bicuculline methiodide (BMI), a $GABA_A$-receptor antagonist, for 2 hours.

The spontaneous burst rate before and during application of BMI for 2 hours was compared (Figure 4.2A, B). Acute bath application of 50µM BMI caused a significant decrease in the rate of spontaneous bursting (Figure 4.2C, $p<1e-4$, rank sum test). This decreased burst rate was accompanied by a significant increase in the number of spikes within bursts (Figure 4.2D, $p<1e-4$, rank sum test) and the inter-burst interval (Figure 4.2E, $p<1e-4$, rank sum test) compared to spontaneous activity before addition of BMI. Such increased intensity of spontaneous bursts after exposure to GABA antagonists picrotoxin [24, 42] and BMI [24, 111] has been reported in other studies using similar preparations. This increase in activity levels after exposure to BMI indicates that GABA was inhibitory in dissociated cultures at 2-3 weeks *in vitro*.

4.3.3 Activity-dependent change in the number of GABA-positive neurons in spontaneously active cultures

In order to investigate the relationship between electrical activity and inhibitory transmitter levels in dissociated cultures, we followed the activity of three batches of sister cultures for a month.

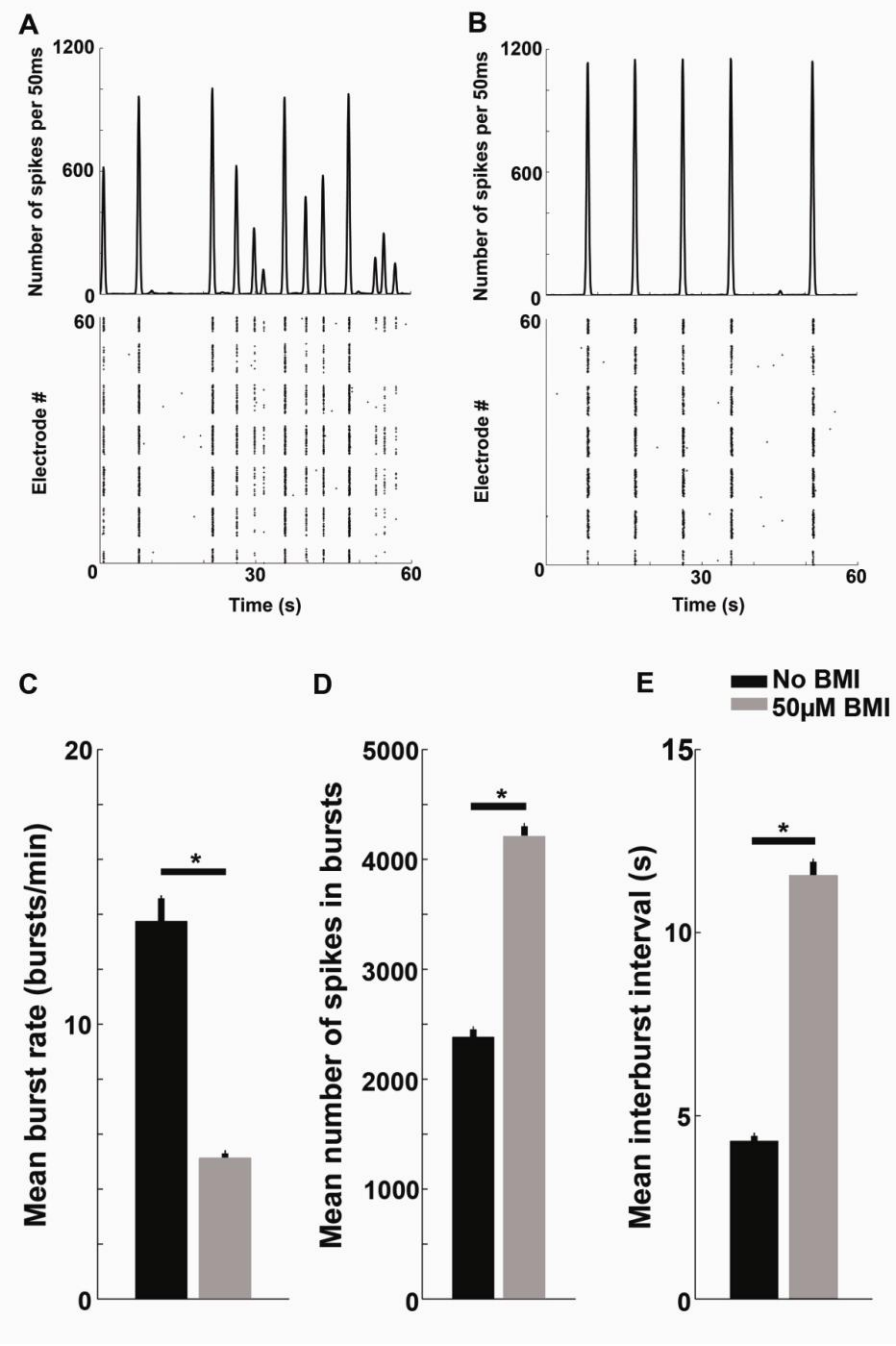

Figure 4.2: Acute exposure to 50 µM BMI for 2 hours increased the intensity of bursting and the inter-burst intervals. A. One minute of spontaneous activity before exposure to BMI. The top panel shows the firing rate (ASDR per 50ms time bin) and the bottom panel shows the raster plot over all 59 channels on the MEA. **B.** Culture exposed to 50µM BMI for 2 hours. The firing rate within bursts (peaks in the histogram) was higher than spontaneous bursts in A. In addition, the interval between bursts was higher in cultures exposed to BMI than in non-treated controls in A. The figure shows a representative culture at 19 DIV. **C,D, E** show summary statistics comparing the burst rate, number of spikes within bursts and inter-burst intervals for spontaneous activity before (black) and during exposure to BMI (grey bars) for two cultures. Asterisk * - p<1e-4, rank sum test.

Since, GABA is the most common inhibitory neurotransmitter in the CNS, immunohistochemistry was used to identify the fraction of GABA-positive neurons (see Materials and Methods). We grow mixed cultures of neurons and glia, [22] since glial cells provide trophic support for the long-term survival of the neurons [82]. To distinguish neurons from other cells in the culture, the cells were labeled for anti-MAP2 (microtubule associated protein) immunoreactivity and the nuclei of all the cells were identified by Hoechst staining (Figure 4.3).

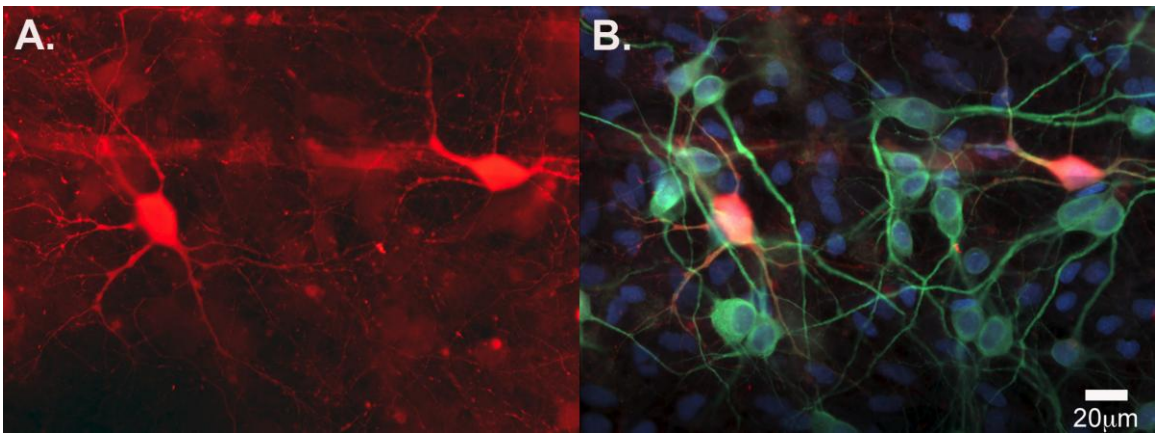

Figure 4.3: Fluorescence image of immunocytochemically stained neurons at 12 days in vitro. A. Anti-GABA immunoreactivity **B.** Anti-MAP2 (green) and anti-GABA (red) immunoreactivity. The cell nuclei were marked by Hoechst (blue). Scale bar, 20µm.

We distinguished two types of GABA-positive neurons based on soma size; large (20-25µm in diameter) and small (6-8µm in diameter) (Figure 4.4). The large GABAergic neurons were present from early days *in vitro*, whereas small ones appeared after a week *in vitro*. Large GABAergic neurons have been shown to be present 4 hours after plating, while the later born smaller ones were present only in the absence of mitotic

inhibition [113]. We observed both populations of GABAergic neurons since we used no mitotic inhibitors at any time.

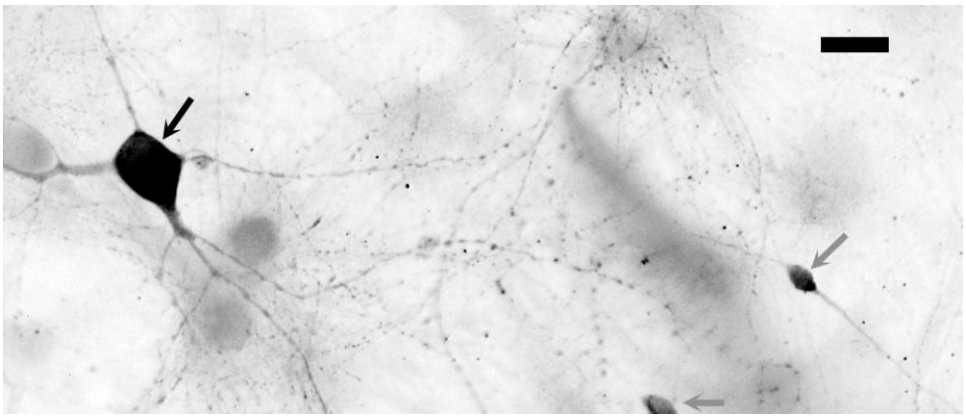

Figure 4.4: Morphologically distinct populations of GABAergic neurons, based on soma size, at 21 DIV. Small GABAergic neurons (indicated by grey arrows) were expressed after 1 week *in vitro*, while the large GABAergic neurons (indicated by the black arrow) were present since the first few hours after plating. Scale bar, 20µm

We counted the number of MAP2-positive cells (the number of neurons) and the number of GABA-positive cells (the number of GABAergic neurons) in each image and the mean percent GABAergic neurons was calculated over 5 such frames for each culture per day *in vitro* (Figure 4.5, the figure shows data from 40 cultures from 3 platings). The mean fraction of GABA-positive neurons in spontaneously active cultures decreased from 5.58 ± 0.4% at 7 DIV to 2.51 ± 0.6% (Mean ± SEM) at 10 DIV (Figure 4.5) but thereafter increased until the 3rd week *in vitro*. At 21 days *in vitro*, the GABA-positive fraction had increased to 12.21 ± 1.7%. However, after 3 weeks *in vitro*, the GABA levels dropped to 8.5 ± 2.5% at 30 DIV. There was a transient increase in the percent GABA levels at 13DIV (Figure 4.5), which might be related to the onset of 'superbursts' observed ~ 2 weeks *in vitro* [40, 53].

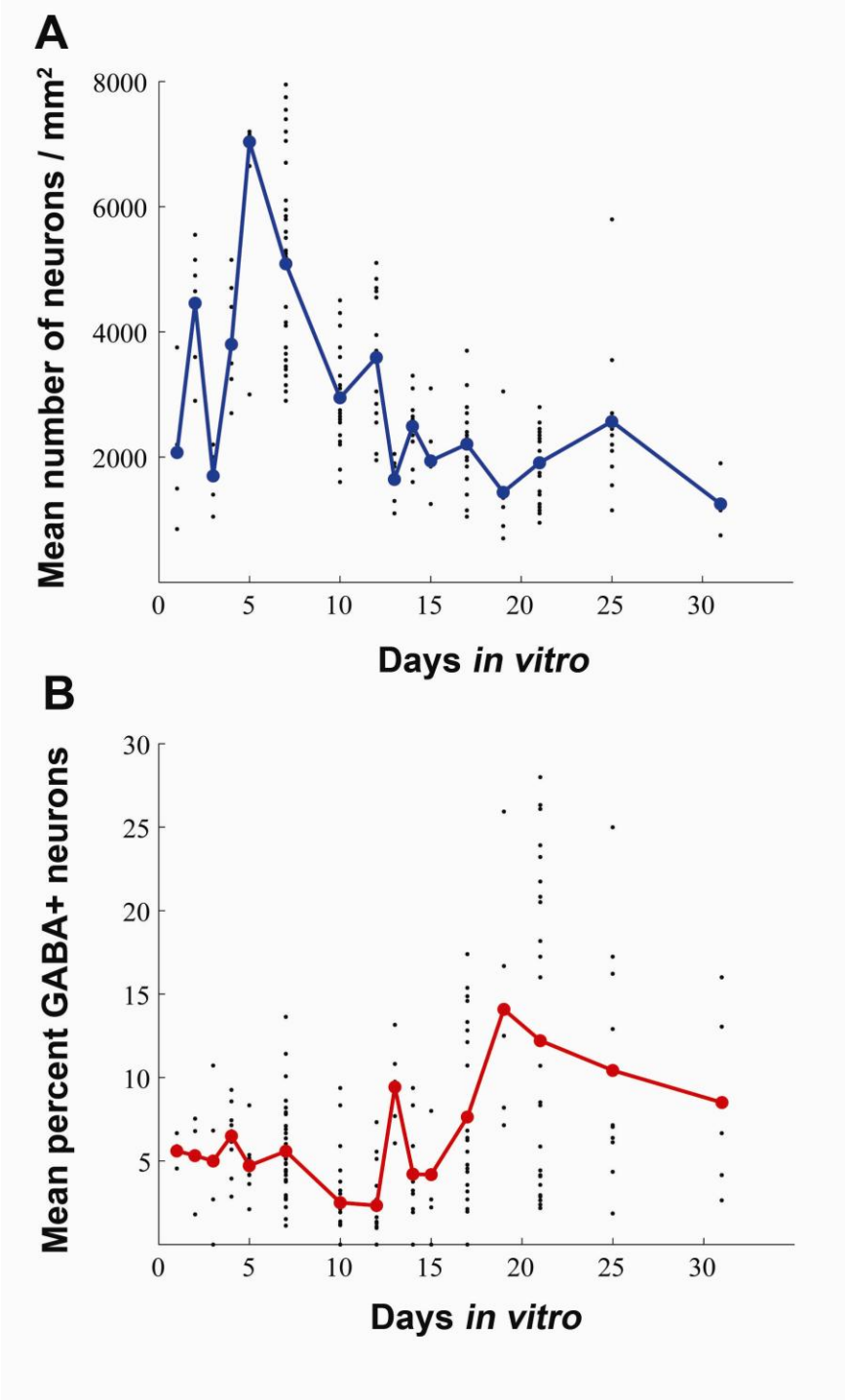

Figure 4.5: Profile of neuronal density and proportion of GABA-positive neurons over a month in vitro. A. The mean density of neurons (neurons/mm^2) increased during the first week *in vitro* and decreased during the 2nd week. The dots indicate the density of MAP2-positive cells for individual images for each culture stained that day. **B.** The mean percent of GABAergic neurons (red line) decreased at10 days *in vitro* and increased after 2 weeks *in vitro* (no electrical stimulation) in spontaneously active cultures. The dots indicate the percent GABAergic neurons for individual images for each culture imaged that day. The lines represent the mean of the all the images over all the dishes for each particular day. The graph shows data from 5 frames each from 40 cultures (three separate platings).

This variation of GABA levels during development in culture corresponds with other studies that have shown that GABA and GAD levels *in vitro* increased after 1 week *in vitro* and peaked around 2-3 weeks *in vitro* and then settled to a constant number at 4 weeks *in vitro* [109]. In parallel, the average density of all neurons peaked in the first week *in vitro* and then decreased after two weeks *in vitro* (Figure 4.5). De Lima *et al.* (1997) showed similar changes in neuronal densities and observed that this change profile was independent of the initial plating density. The plating densities in their study varied between 100-400 cells/mm^2 [114].

To determine whether the change in the percent GABAergic neurons was activity dependent we calculated the mean spike rate and mean burst rate of the cultures over a month *in vitro* (see Materials and Methods). Figure 4.6 shows that, on average (21 cultures on MEAs from three platings), the cultures exhibited spontaneous firing from 3 DIV (Figure 4.6A) and spontaneous bursts were observed from 5 DIV (Figure 4.6B). The percent GABAergic neurons decreased at 8-10 DIV, which corresponds to the period around the onset of spontaneous bursting (Figure 4.5, 4.6).

The spontaneous spiking activity changes considerably in the first 4 weeks *in vitro*, from tonic spiking to culture-wide bursting (Figure 4.1). To compare the levels of spontaneous activity and percent of GABA-positive neurons, we divided the first 4 weeks *in vitro* into 5 groups depending on their firing patterns and age *in vitro* (Figure 4.7):

(1) 0-3 DIV, the period before the onset of spiking.

(2) 4-7 DIV, the period of onset of spiking and global bursting.

(3) 8-14 DIV, 2nd week *in vitro*.

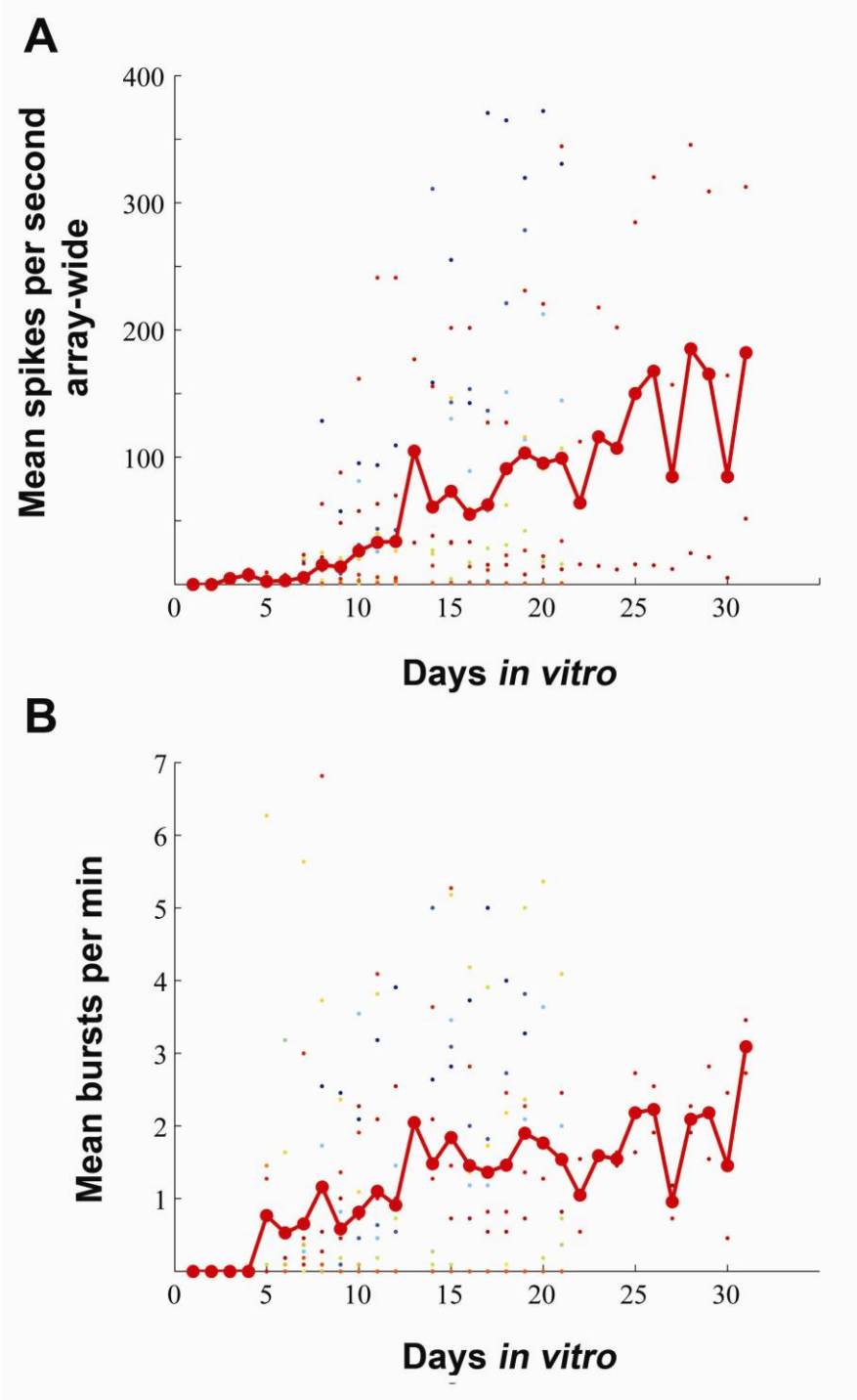

Figure 4.6: Development of the mean spike rate and burst rate for one month in culture. The colored dots indicate recordings from 21 cultures from three separate platings. The dots indicate the mean firing rate (ASDR per second) for each culture over 30 minutes. **A.** Cultures started spiking at ~3 DIV and the spike rate continuously increased during rest of the 31 day recording period. The mean spike rate (spikes per sec array-wide) includes all the spikes, both within and outside bursts, that occurred during the recording period. **B.** Spontaneous bursting was observed from ~5 DIV and the burst rate increased until 2 weeks *in vitro*, after which the burst rate was relatively constant.

(4) 15-21 DIV, the 3rd week *in vitro*.

(5) 22-28 DIV, 4th week *in vitro*.

The percent of GABAergic neurons significantly decreased at 8-14 DIV (Figure 4.7A, $p<5e-3$, rank sum test) along with a significant increase in the population firing rate (Figure 4.7B, $p<5e-3$, rank sum test) indicating a low proportion of GABAergic neurons during the onset of spontaneous firing and bursting. The percent GABAergic neurons increased significantly at 15-21 DIV (Figure 4,7A, $p<1e-4$, rank sum test), along with a significant increase in the population firing and bursting rates and did not change significantly up to the 4th week *in vitro* (Figure 4.7). We hypothesize that this increased GABAergic proportion after 2 weeks *in vitro* could be regulated by homeostatic mechanisms regulating network dynamics in response to increased activity attributed to the prominence of spontaneous bursting.

Other studies, quantifying the content and release of neurotransmitters in cortical dissociated cultures, have shown that chronic silencing of spontaneous activity by TTX (tetrodotoxin, which blocks voltage-gated sodium channels) resulted in a decrease of GABA content [69]. Moreover, synchronous activity has been suggested to play a role in the regulation of the proportion of GABAergic neurons in dissociated cortical cultures [36, 78]. Our results suggest a relation between number of GABA-positive neurons and the onset of spontaneous synchronous bursting (Figure 4.7).

Spontaneous bursts in dissociated cultures could be successfully suppressed by distributed electrical stimulation [60]. Since, there is evidence for the potential role of GABAergic neurons in the regulation of synchronous activity, we investigated whether

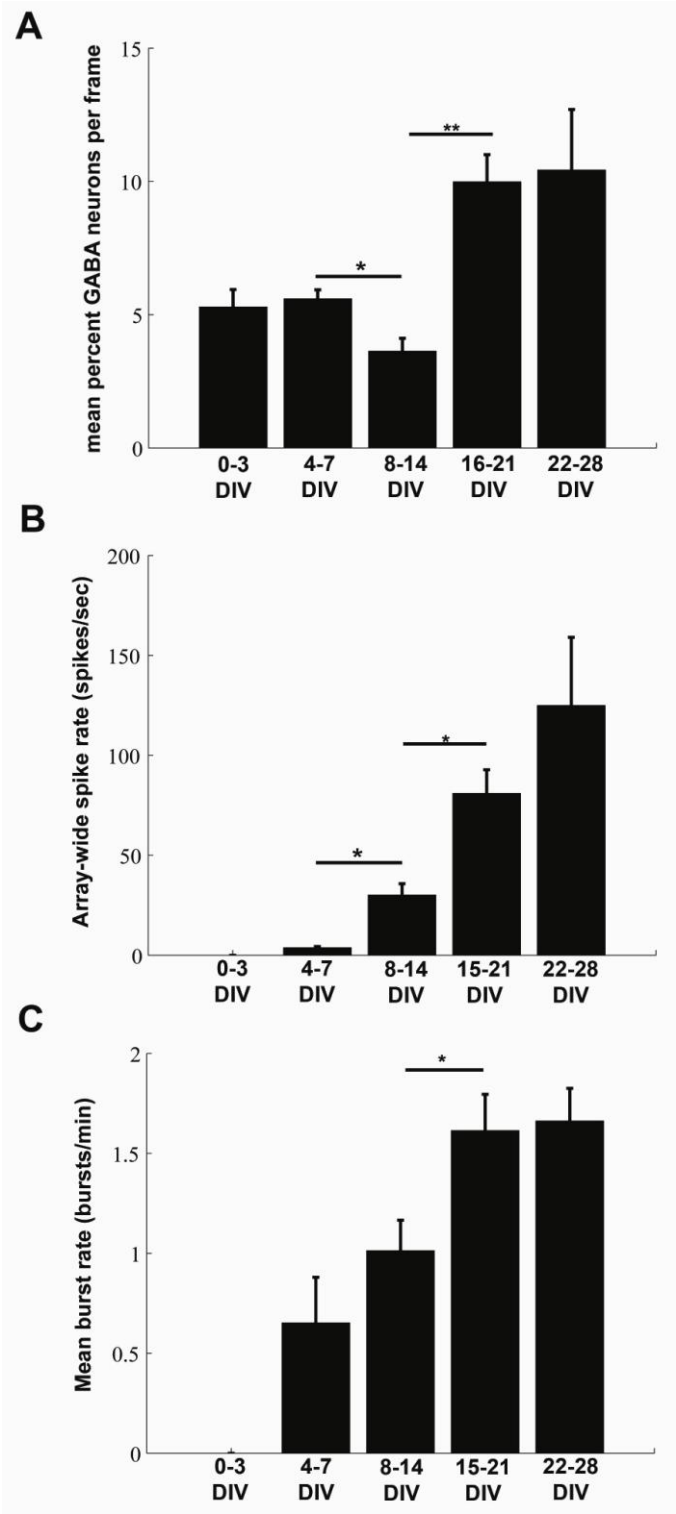

Figure 4.7: Proportion of GABAergic neurons and spontaneous activity levels for different age groups. A. The percent of GABAergic neurons decreased significantly at 8-14 DIV (period after the onset of spontaneous bursts) and increased after 2 weeks *in vitro*. **B.** ASDR increased significantly after the first week *in vitro*. **C.** Spontaneous burst rate increased significantly over the first 2 weeks *in vitro* after which it remained relatively constant.

long-term electrical quieting of spontaneous bursts involved similar changes in the fraction of inhibitory neurons.

4.3.4 Proportion of GABAergic neurons increased significantly in chronically burst-quieted cultures

Based on the observation that the proportion of GABAergic neurons was low at the onset of bursting and increased later, we proceeded to the test whether the percent of GABAergic neurons in chronically burst-quieted cultures was different from spontaneously active cultures (see Materials and methods). Six pairs of sister cultures (12 – 21 DIV) were either burst-quieted by multi-site electrical background stimulation for 2 days, or allowed to express spontaneous bursts (N=6 experiments, see Materials and methods). The electrical burst-quieting protocol (see Material and methods) resulted in the successful and complete suppression of all the spontaneous bursts for the duration of chronic burst-quieting. The burst-quieted cultures showed a significant increase in percent GABA neurons compared to the spontaneously active 'control' cultures of the same age ($p<1e-2$, t-test, N=6 experiments) (Figure 4.8). Representative images of anti-GABA staining for a control (non-stimulated sister culture) and a chronically burst-quieted culture are shown in Figure 4.9.

De Lima *et al.* (2004) showed that long-term blockade of glutamatergic activity in 2 week old cortical cultures resulted in the loss of a subpopulation of GABAergic neurons [115]. The average number of neurons in control cultures (at 12 – 21 DIV) was 1925 ± 155.5 neurons/mm^2 and quieted cultures was 1553 ± 169.3 neurons/mm^2 (Mean ± SEM calculated for each image, averaged over N=6 experiments). Since the total number of neurons in control and quieted cultures were not statistically different (p=0.1, t-test),

the increased fraction of GABA-positive neurons in quieted cultures (compared to control) is unlikely caused by cell death or neurogenesis (unless the number of new non-GABAergic neurons were equal to the number of dead GABAergic neurons).

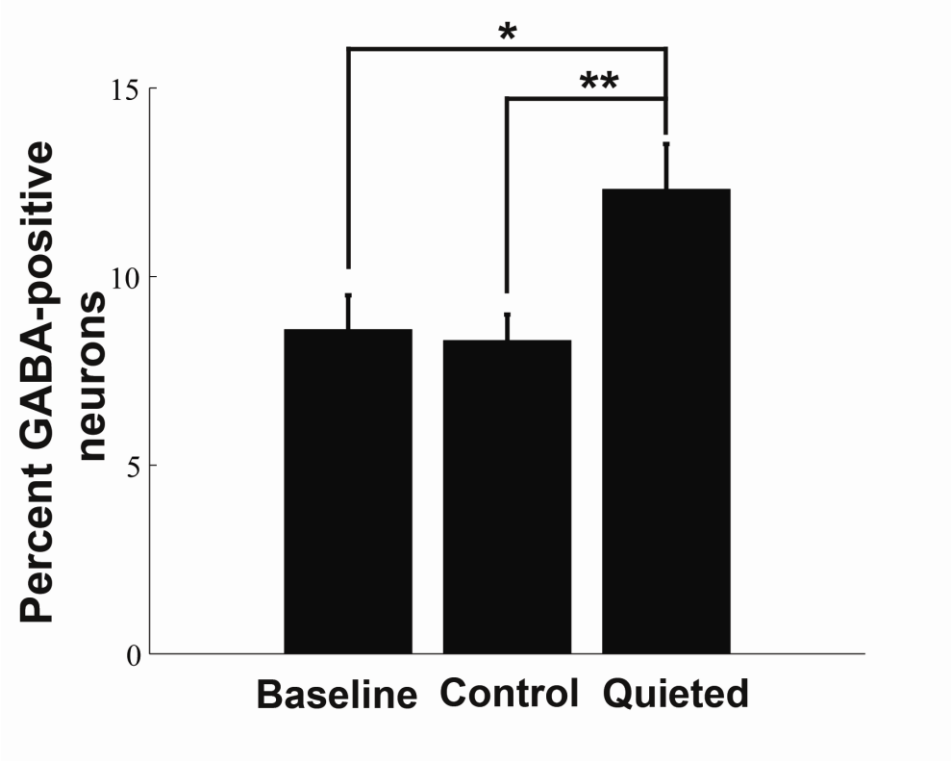

Figure 4.8: Chronic burst-quieting increased the percent of GABAergic neurons. Burst-quieted cultures showed significant increase in the percent of GABAergic neurons compared to 'baseline' cultures before the chronic quieting period ($p<5e-2$, t-test) and same-age spontaneously bursting 'control' cultures ($p<1e-2$, t-test). Average data over six experiments is shown in the figure. Asterisk *- $p<5e-2$, ** - $p<0.1e-2$

Altered activity levels affect the proportion of GABAergic neurons in dissociated cortical cultures [69, 111]. Correspondingly, to investigate if the increased proportion of GABAergic neurons was related to the activity levels during the electrical burst quieting, we quantified the average firing rate in electrically burst-quieted cultures. The mean firing rate during periods of electrical burst-quieting (2349 ± 0.15 ASDR, Mean ± SEM for an hour recording in a quieted experiment) was 50 times higher than during

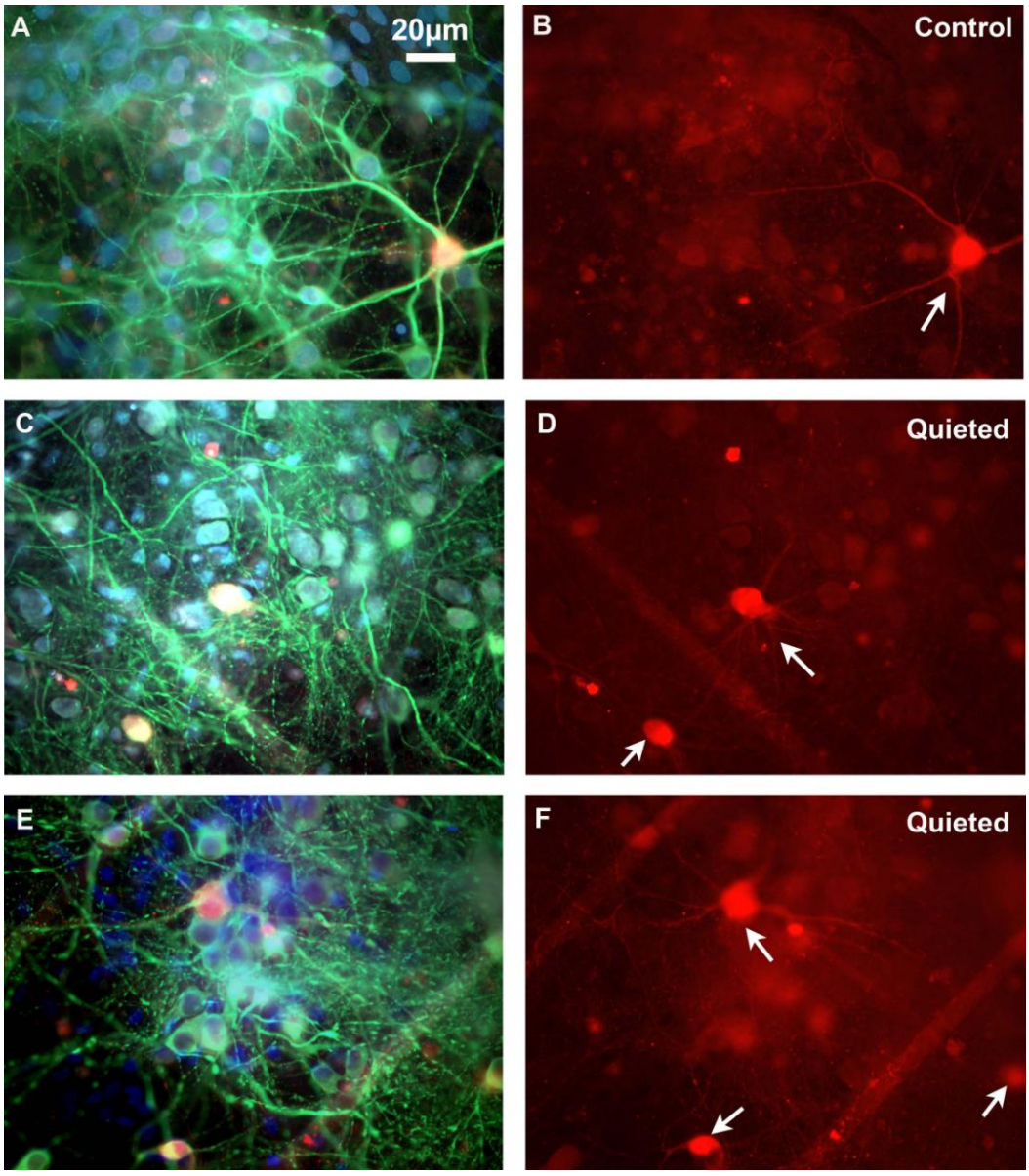

Figure 4.9: The fraction of GABAergic neurons increased in the chronically burst-quieted cultures, compared to spontaneously bursting sister cultures of the same age. Representative images of spontaneously active (A, control) and same age sister culture subjected to 2 days of electrical burst-quieting (B, C, quieted). The number of GABAergic neurons increased at least two-fold in the quieted culture (D, F) compared to the control culture (B). Panels A, C and E show the corresponding anti-MAP2 and anti-GABA immunoreactivity as the anti-GABA staining in panels B, D and F. Scale bar, 20µm.

spontaneous bursting (48.9 ± 0.16 spikes/second ASDR, Mean ± SEM, maximum firing rate was 2916 spikes/second ASDR, hour recording in the same culture before burst-quieting). Thus, the increased proportion of GABAergic neurons in response to increased spike activity seems to be directed by homeostasis of network excitability.

4.4 Discussion

Homeostatic mechanisms operate at all levels in the brain to maintain the balance between excitation and inhibition, to avoid pathological conditions. In this study, we investigated the role of activity-dependent homeostatic changes in neurotransmitter expression in the development and control of persistent spontaneous bursting in dissociated cultures. Global bursting observed in dissociated cortical cultures, characterized by drastic increases in overall firing rate, is thought to be mediated by recurrent excitatory connections in the networks [24]. We hypothesized that persistent spontaneous bursting in dissociated cortical networks *in vitro* was a result of lack of afferent input [24, 60]. Depriving cortical circuits of natural inputs results in the down-regulation of GABA, possibly to maintain appropriate levels of activity after deafferentation [116]. Correspondingly, we observed a low percent of GABA-positive neurons in the first week *in vitro*. This was followed by an increase in the percent of GABAergic neurons in the week after the onset of spontaneous bursting (Figure 4.7, 4.10). This suggests the presence of homeostatic modulation of inhibitory transmitter levels to balance the effects of increased excitation during spontaneous bursting.

GABAergic neuron levels vary in response to altered levels of activity in neuronal networks. Several studies *in vivo* have demonstrated decreased GABA immunoreactivity caused by chronic activity blockade [104, 117, 118]. Visual deprivation in monkeys

results in the reversible decrease of the number of GABA immunoreactive neurons in the deprived part of the cortex [104]. Benevento *et al.* (1995) showed a significant decrease in the density of GABAergic neurons in the visual cortex of dark-reared rats. Deafferentation, resulting in a disturbed balance of cortical activity, caused decreased expression of GAD67 (Glutamic acid decarboxylase, enzyme responsible for converting to glutamic acid to GABA) [118]. We conducted similar but opposite experiments to explore the role of GABAergic neurons in the artificial reafferentation of dissociated cortical cultures by background electrical stimulation.

Substituting background electrical stimulation for the lack of sensory input suppressed spontaneous bursting [60] and caused a significant increase in the percent of GABAergic neurons ($p<1e-2$, t-test), possibly a homeostatic response to increased activity of artificial reafferentation. In addition, the density of neurons (neurons/mm^2) was not statistically different in the chronically burst-quieted cultures and same age control cultures. This suggests that the changes in the fraction of GABA-positive neurons in the chronically burst-quieted cultures were not a result of neural cell death or neurogenesis, but instead involved modulation of GABA expression.

Altering Ca^{2+} spike activity spontaneously generated by embryonic spinal cord neurons *in vivo* changes the expression of neurotransmitters in a homeostatic manner, to maintain a balance between excitation and inhibition [119]. Our results suggest that the effects of electrical burst control for long periods involve activity-dependent changes in neurotransmitter expression, which increase the fraction of inhibitory neurons, resulting in fewer spontaneous bursts.

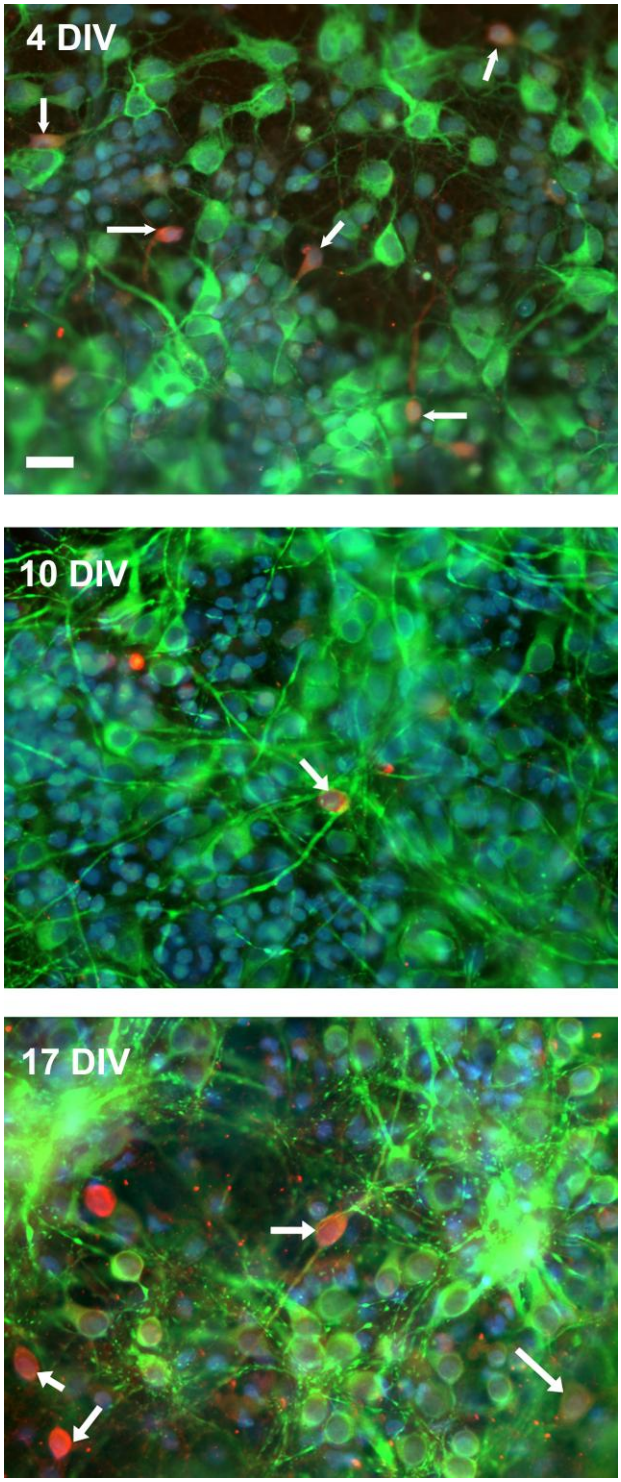

Figure 4.10: Development of proportion of GABAergic neurons before, during and after the onset of spontaneous bursting in vitro. The proportion of GABAergic neurons decreased at 10 DIV, which represents the onset of spontaneous bursting and then increased at 17 DIV. The arrows indicate some of the GABA-positive neurons in the field of view. Images are from cultures used in a representative spontaneous experiment. Scale bar, 20μm.

4.4.1 Dual role of GABA in the brain

GABA shifts from being excitatory to inhibitory during development because of a progressive reduction in intracellular Cl^- concentration. This results in the reversal potential of GABA becoming more negative and GABA exerting a hyperpolarizing effect on the post-synaptic neuron [102]. In the rat neocortex, activation of $GABA_A$ receptors produces membrane depolarization in the early part of the first postnatal week [120, 121] but GABA becomes inhibitory starting from the end of the first postnatal week [105].

In our dissociated cortical cultures, acute exposure (2 hours) to $GABA_A$ antagonist bicuculline methiodide (BMI) at 2-3 weeks *in vitro* resulted in the broadening of spontaneous bursts (Figure 2) due to an increase in the number of spikes within the burst [24, 26] indicating that GABA was inhibitory during this period. But, this broadening of bursts was accompanied with an increase in the period between bursts [122]. Opitz *et al.* (2002) found evidence for synaptic depression after a spontaneous burst, which may be caused by the depletion of available neurotransmitter vesicles after a barrage of activity. This indicates the presence of a *burst refractory period* that would set a limit on how soon a culture can spontaneously burst after the occurrence of a prior burst. Increased inter-burst intervals, observed after exposure to BMI, may be caused by an increase in the burst refractory period caused by increased intensity of firing during bursts.

4.4.2 Spontaneous bursts and functional plasticity

Memory impairment is a common consequence of seizures. Studies in rat epileptic models have shown that rats experiencing early-life seizures exhibited spatial learning deficits [123] caused by the decreased expression of NMDA receptors [124],

which are important for synaptic plasticity. Additionally, seizure activity regulates the expression of neurotransmitters homeostatically to suppress global activity. Mossy fibers normally generate excitatory glutamatergic postsynaptic potentials on hippocampal CA3 pyramidal cells, but generate inhibitory GABAergic postsynaptic potentials after kindled seizures [125].

Synchronized global bursting expressed by cultures *in vitro* can be likened to epileptic seizures [57]. In unstimulated cultures, bursting results when there are too few intrinsically bursting cells in the network [55]. Electrical stimulation suppresses spontaneous bursting by mimicking intrinsically bursting cells or background sensory input [60]. Some successful studies of network plasticity [30, 31] used elevated levels of Mg^{2+} to quiet the spontaneous bursts and demonstrated pathway-specific potentiation and depression in the neuronal network caused by high frequency tetanic stimulation [31]. Contrary to these and other studies investigating network-level plastic changes on MEAs, we observed no significant functional changes to tetanic stimulation in similar experiments but without pharmacological interventions [45], probably due to differences in the levels of spontaneous activity. Modeling studies indicate that spontaneous bursting resets synaptic weights in the network [59]. It is possible that global spontaneous bursts overwhelm responses to external stimulation like a tetanus [73, 126] and decrease the ability to induce plastic changes in the network. We suggest that synchronized seizure-like bursting activity *in vitro* could potentially create an imbalance of excitation and inhibition in dissociated cortical networks, analogous to the way epileptic seizures in young children cause more seizures and learning problems. We suggest dissociated

culture models, with bursting controlled by artificial reafferentation, to be more suitable for the study of learning and memory *in vitro*.

Artificial reafferentation allows *in vitro* cortical networks to better approximate the intact cortex in various ways. We found that multi-site stimulation produced GABA expression similar to the cortex *in vivo*. In chronic burst-quieting experiments, the average percent of GABAergic neurons in spontaneously active 'control' cultures was 7.6 ± 0.7% (N=6 cultures) which is significantly lower than the 15-20% of GABAergic neurons found in the cortex *in vivo* [96, 127, 128]. Low proportion of GABAergic neurons in dissociated, deafferented cultures were accompanied with aberrant activity patterns. In contrast, chronically burst-quieted cultures of the same age showed a higher percentage of GABAergic neurons (12.3 ± 1.2% from N=6 cultures) which was closer to GABAergic proportions *in vivo*. Furthermore, such a continuously stimulated cultured network better represents the *in vivo* cortex receiving continuous sensory input, compared to intermittently stimulated cultured networks. Closed-loop suppression of spontaneous bursting, by tuning stimulation voltage to precisely control of the amount of network activity [60], could be an important tool for achieving long term burst control in such a model network.

CHAPTER 5

PLASTICITY OF SPONTANEOUS RECURRING SPATIOTEMPORAL PATTERNS IN CORTICAL NETWORKS[4]

How do neurons encode and store information for long periods? Repeatable patterns of activity have been reported in various cortical structures and suggested to play a role in information processing and memory mechanisms. To study the potential role of repetitive patterns in memory mechanisms, we investigated patterns of spontaneous activity in dissociated cortical cultures *in vitro*. Spontaneous electrical activity was recorded from these networks cultured on a grid of 60 extracellular substrate-embedded electrodes (multi-electrode arrays, MEAs). These networks expressed spontaneous culture-wide bursting from ~1 week *in vitro*. During bursts, a large portion of the active electrodes showed elevated levels of firing. Spatiotemporal activity patterns within spontaneous bursts were clustered using a correlation-based clustering algorithm and the occurrences of these burst clusters were tracked over several hours. This analysis revealed spatiotemporally diverse bursts occurring in well-defined patterns, which remained stable for several hours. Activity evoked by a strong local tetanus resulted in a significant change in the occurrences of spontaneous bursts belonging to different clusters, indicating a change in the dynamical flow of information in the neuronal network. The diversity of spatiotemporal structure and long-term stability of spontaneous bursts together with their plastic nature strongly suggests that such repetitive network patterns could be used as codes for information transfer and storage in cortical networks.

[4] Submitted to the *Journal of Neuroscience*.

5.1 Introduction

Cortical structures produce repeatable spatiotemporal activity patterns, which could potentially be involved in cortical information processing and storage. Beggs and Plenz (2004) enumerated the requirements for recurring activity patterns to serve as substrates of memory. In order to represent information, the activity patterns should exhibit long-term stability over hours, possess millisecond temporal precision and should occur in diverse varieties [129]. They demonstrated that these properties were satisfied by recurring patterns of local field potentials (neuronal avalanches) observed in cortical slices *in vitro* [129].

Other laboratories have demonstrated the presence of recurring spontaneous patterns of action potentials in various brain structures. *In vivo* recordings from the rat hippocampus and macaque cortex revealed neural ensemble activity patterns which were repeated in a temporally compressed fashion during slow wave sleep [130, 131] possibly to consolidate the information acquired during active behavioral episodes [132, 133]. Repeating precisely-timed 'motifs' of Ca^{2+} signals and post-synaptic potentials have been reported in spontaneous activity in cortical networks both *in vivo* and *in vitro* [134, 135] suggesting these dynamic ensembles as substrates of information storage and flow in cortical networks. Stable spatiotemporal attractors in sequences of culture-wide bursts ('superbursts') have been found in dissociated cortical cultures indicating that dissociated networks can exhibit precise spatiotemporal activity patterns previously thought to require specific network structure [40].

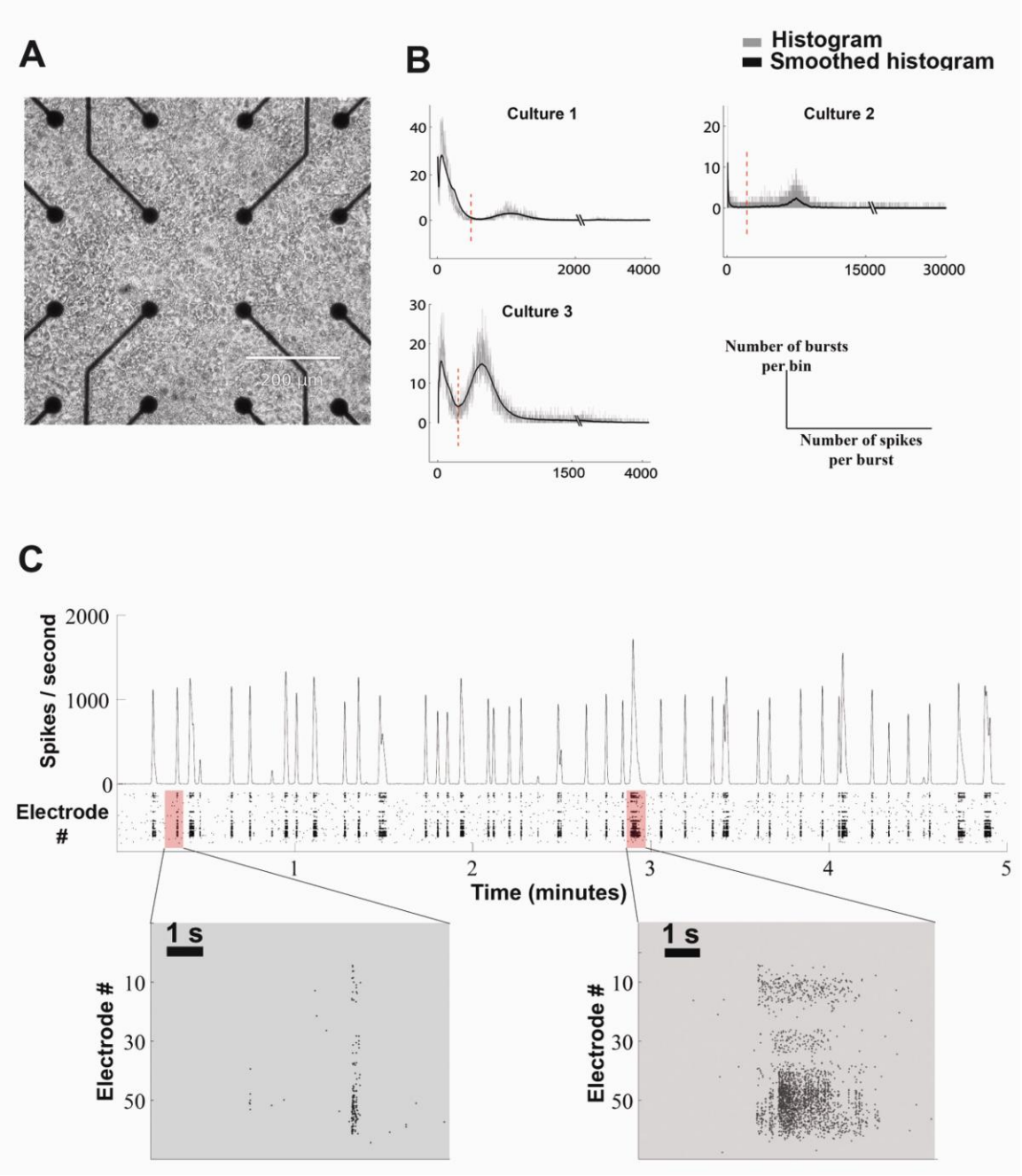

Figure 5.1: Multi-electrode recording of spontaneous activity in a dissociated cortical culture. **A**. Typical 3-week old culture on a Multi-electrode array (MEA). **B**. Bursts were of different sizes depending on the number of spikes in a burst. Bursts were classified into two categories: small and big bursts depending on a threshold number of spikes within a burst. Figure shows histogram of number of spikes in each burst from three cultures used for *Spontaneous experiments*. Red line indicates the threshold for each culture. Note that the axes are different for each culture. **C**. Spike raster plot and array-wide spike rate histograms of spontaneous activity for 5 minutes of spontaneous recording. The inset shows typical examples of bursts classified as 'big' and 'small' bursts. Recording was taken at 24 days-*in-vitro*.

Induction of synaptic plasticity is widely believed to be necessary for information storage [136]. Therefore, to investigate the role of spontaneous activity in memory mechanisms it is important to study its plasticity in addition to the properties described by Beggs and Plenz (2004). Dissociated cortical networks cultured on multi-electrode arrays (MEAs, Figure 5.1A) [4, 6] express spontaneous network wide bursting persisting for the lifetime of the culture [23-25, 36, 38, 53, 70, 137]. Such robust spontaneous activity in an isolated *in vitro* system provides a unique model to study and manipulate the network dynamics of intrinsic spontaneous activity, for long periods up to many months [22], through electrical recording and stimulation without the usual *in vivo* confounds of anesthesia and uncontrolled sensory input. Dissociated *in vitro* neural cultures have been used for decades as experimental models of the brain since they have been shown to preserve many electrical and morphological properties of cortical networks [18, 20, 24].

The goal of the present study was to investigate the spatiotemporal structure within repetitive spontaneous bursting [49] and their putative role in information storage in cultured cortical networks. We also examined whether spatiotemporal burst patterns could be altered by tetanic stimulation and quantified the amount of information carried by spatiotemporally diverse burst patterns.

5.2 Materials and Methods

5.2.1 Cell culture

Neocortical cells were dissociated from brains of E18 rats and plated on multi-electrode arrays (MEAs). Timed-pregnant Sasco Sprague-Dawley rats (Charles River) were euthanized with isoflurane according to NIH-approved protocols. Embryos were removed and euthanized by chilling and decapitation. The entire neocortex, excluding the

hippocampus, was dissected in Hanks Balanced Salt solution (HBSS, Invitrogen, Carlsbad, CA) under sterile conditions. After enzymatic digestion in 2.5U/mL Papain (Roche Scientific 108014, Indianapolis, IN) in Segal's medium [82] for 20 minutes, cells were mechanically dissociated by 6-9 passes through a 1mL pipette tip [22], in Neurobasal medium (Invitrogen) with B27 (Invitrogen), 0.5mM Glutamax (Invitrogen) and 10% horse serum (Hyclone, Logan, UT). Cells were passed through a 40μm cell strainer (Falcon, Bedford, MA) to remove large debris and then were centrifuged at 150x*g* onto 5% bovine serum albumin (BSA) in phosphate buffered saline (PBS). The pellet of cells was resuspended and 50,000 cells were plated in a 20μL drop of Neurobasal on pre-coated MEAs. MEAs were pre-coated with polyethylene imine (PEI, Sigma, St. Louis, MO) and laminin (Invitrogen) as previously described [22]. After 30 minutes of incubation, 1mL of Neurobasal media was added to each culture dish. After 24 hours, the Neurobasal medium was replaced by feeding medium adapted from Jimbo *et al.* [30] (Dulbecco's modified Eagle's medium (DMEM, Irvine scientific, Santa Ana, CA), 10% horse serum (Hyclone), 0.5mM glutamax (Invitrogen) and 1% sodium pyruvate (Sigma)). Cultures were maintained in an incubator at 35°C, 65% RH, 5% CO2, and 9% O2. The culture medium was exchanged with fresh feeding medium every 7 days. Cultures were maintained in dishes sealed with gas-permeable Teflon membrane [22] to prevent infection and evaporation. The use of Teflon-sealed dishes allows for the maintenance of the incubator at 65% humidity, making it an electronics-friendly environment. All experiments were performed inside the incubator, ensuring long-term stability of our recordings. All recordings were done on 2-4 week old cultures.

5.2.2 Recording system

Electrical signals were recorded through a square array of 59 titanium nitride electrodes (Multichannel systems, Reutlingen, Germany). The electrodes were 30µm in diameter and 200µm apart and referenced to a larger ground electrode. After 1200x amplification, signals were sampled at 25 kHz using Multichannel Systems data acquisition card (MCCard). Data acquisition, spike detection, artifact suppression [85] and visualization were controlled using our open-source MeaBench software [19] which allows for detecting spikes as early as 2 ms after stimulation [85]. Spikes were detected online by thresholding at 5x RMS noise.

5.2.3 Stimulation system

Stimulus pulses were delivered using our custom built 60-channel stimulator [86]. Biphasic voltage-controlled rectangular pulses (600-800mV, 400µs), positive phase first were used, since these were found to be most effective at eliciting neural responses [87].

5.2.4 Experiment Protocols

Two types of experiments were performed, Spontaneous (no stimulation) and Probe (low frequency stimulation applied at a single electrode).

5.2.4.1 Choice of electrodes

Each of the 59 recordable electrodes was stimulated 10 times with a 600mV, 400µs, biphasic stimulation pulse at 1 Hz. The electrodes that showed the highest responses in the first 200ms after stimulation were chosen as candidate electrodes. A random sample out of these candidate electrodes was chosen for delivering tetani and probes.

5.2.4.2 Spontaneous experiments

Spontaneous activity was recorded for 3 hours (Period *Pre*). Tetanization consisted of a train of stimuli at 20Hz, applied simultaneously on two electrodes lasting for 15 minutes. Another recording of spontaneous activity for 3 hours followed this treatment (Period *Post*). The tetanization was unusually long to increase the likelihood of inducing plasticity. This experiment was repeated 5 times on 4 cultures. One culture was tested twice with different tetanus electrodes pairs. The interval between these two experiments was 4 hours.

5.2.4.3 Probe experiments

A single stimulus pulse on an electrode is called a probe [37]. A block of probing consisted of a single electrode stimulated 5400 times with inter-probe interval of 2 seconds. Each block of probing lasted 3 hours (Period *Pre*). After the *Pre* period, tetanic stimulation was applied at two electrodes. Tetanization consisted of a train of stimuli at 20Hz, applied for 15 minutes simultaneously on two electrodes (one probe electrode and one other electrode). The tetanus was followed by another block of probing (Period *Post*). This experiment was repeated 5 times on 4 cultures.

5.2.5 Analysis

5.2.5.1 Burst detection

Network-wide bursts were identified by a burst detector algorithm described elsewhere [112]. Briefly, any 100ms window with more than 5 spikes on one electrode was considered a part of a burst. For *Spontaneous experiments* all the bursts were identified as spontaneous bursts. The frequency of probe stimulation was 0.5Hz and

bursts have been previously shown to be entrained to the stimulus pulse at this stimulation frequency [60]. We classified bursts from *Probe experiments* into two categories: non-time locked bursts and evoked bursts. An evoked burst was a burst whose onset was within 10 ms after the probe pulse. The onset of the burst was defined as the first time before the peak of the burst when the array-wide spike rate during a burst was 20% of peak firing rate during the burst (Figure 5.2A). Offset of the burst was defined as the last time after the peak of the burst when the array-wide firing rate was 20% of the peak firing rate during the burst (Figure 5.2A).

5.2.5.2 Burst Activity Matrix (BAM) for spontaneous and evoked bursts

Classification of bursts

Bursts (spontaneous and evoked bursts) were classified into two groups, "small" and "big", based on the number of spikes within each network-wide burst. For each experiment, a histogram of the number of spikes in every burst (time bin=100ms) in the experiment was generated (Figure 5.1B). There were two distinct peaks in this histogram. The threshold for classifying bursts was determined as the minimum point between the two peaks (Figure 5.1B). Bursts having a number of spikes below the threshold were considered "small" and bursts having a number of spikes above the threshold were considered "big". The length of the burst was defined as the time from the onset to the offset of the burst. The *Burst Activity Matrix* (BAM) for each burst was generated by counting the number of spikes within the length of the burst on each of the 60 electrodes using a 100 ms moving time bin (time step = 10 ms).

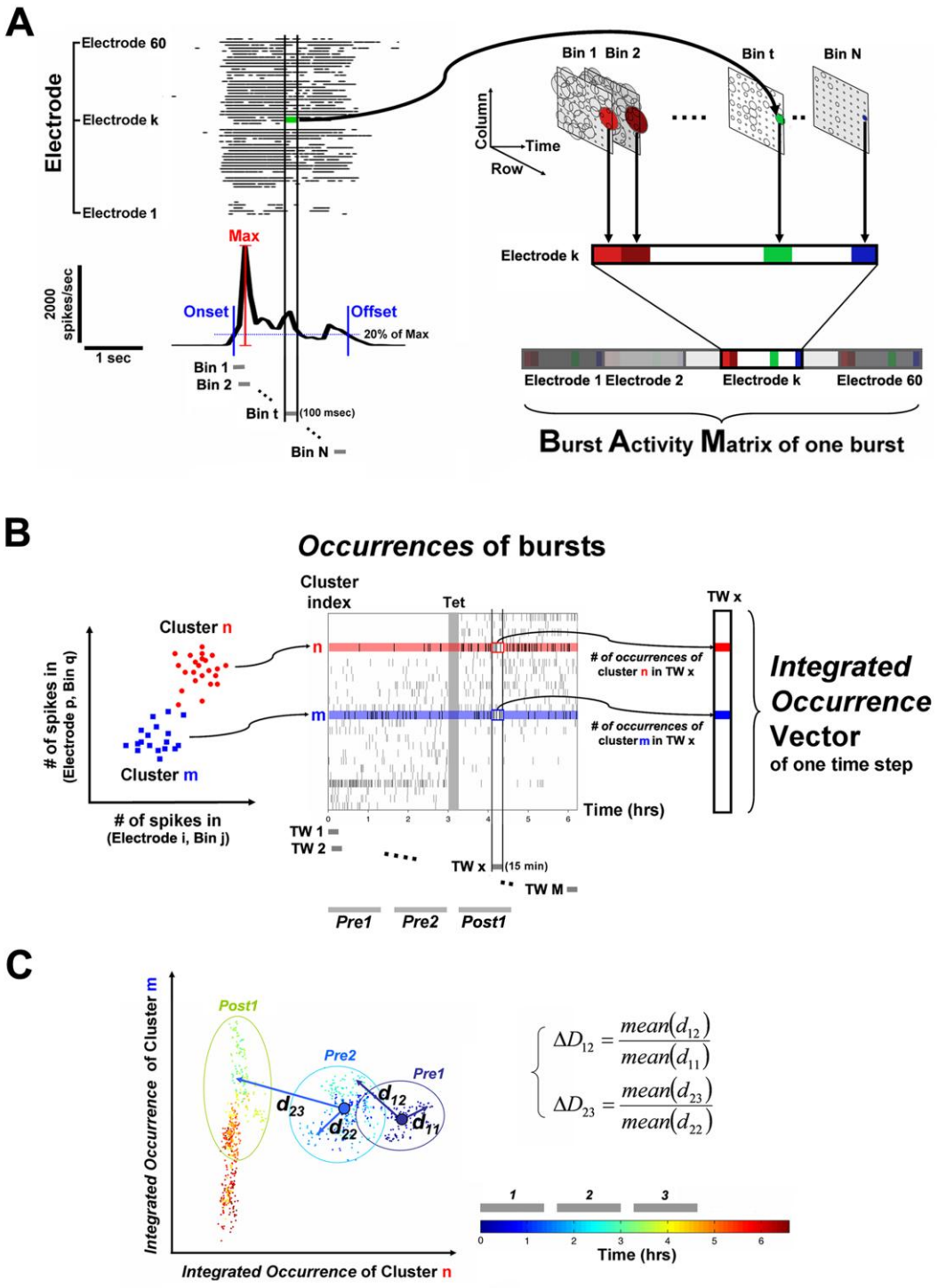

$$\begin{cases} \Delta D_{12} = \dfrac{mean(d_{12})}{mean(d_{11})} \\ \Delta D_{23} = \dfrac{mean(d_{23})}{mean(d_{22})} \end{cases}$$

Figure 5.2: Pictorial description of analysis of spatiotemporal patterns within spontaneous bursts and statistics on the change of distribution of burst patterns across the tetanus. **A.** Raster plot and corresponding histogram of spontaneous spiking activity on 60 electrodes. Small and big bursts were detected, the onset and offset times of bursting activity were calculated and the difference between the offset and onset times was determined as the length of the burst. The *Burst Activity Matrix* (BAM) for each burst was generated by counting number of spikes within the length of the burst on each of the 60

electrodes using a 100 ms moving time bin (time step = 10 ms). BAM vector for each burst is a 60 X N dimensional vector, where N= number of bins in the longest burst. The right panel shows example frames of BAM for different time bins for 60 electrodes (arranged in the original coordinates of the multi-electrode array). Size of the circle represents the number of spikes on that particular electrode for a particular time bin with the colored circle representing value at Electrode k. **B.** A 2-dimensional cross-section of a BAM vector plotted in 60 X N dimensional space is shown. BAMs of all bursts were compared against each other and clustered using a paired clustering algorithm (dendrogram, see Supplementary materials). *Occurrence* represents when a bursts within a specific BAM cluster happen (Figure 5.4). *Integrated Occurrence* was defined as the total number of *Occurrences* of bursts in a 15-minute time window moved by a time step of 30s. *Integrated Occurrences* were calculated across three periods of the same length equally spaced in time, *Pre1*, *Pre2* and *Post1*. Periods *Pre1* and *Pre2* were before the tetanus stimulation and period *Post1* was after the tetanus. **C.** A 2-dimensional cross-section of *Integrated Occurrences* of all BAM clusters (S X R dimensional vector, S= Number of BAM clusters, R = Number of 15 minute moving time-windows) is shown. Color bar represents the time elapsed during the experiment and each point represents the *Integrated Occurrence* of the BAM clusters. The centroid of *Integrated Occurrences* in periods *Pre1*, *Pre2* and *Post1* were calculated. The change across periods was calculated as the Euclidean distance of each point in a period from the centroid of the previous period (d_{12} and d_{23} in the figure) normalized by the Euclidean distance of each point in the previous period from its centroid (d_{11} and d_{22} in the figure). We measured two quantities: ΔD_{12} and ΔD_{23}. ΔD_{12} represents the change in the *Integrated Occurrence* of BAM clusters in the *Pre1* and *Pre2* periods (within the *Pre* period), and ΔD_{23} represents the change in the *Integrated Occurrence* of BAM clusters in the *Pre2* and *Post1* periods (across the tetanus). The significance of the change in *Integrated Occurrence* of bursts across the tetanus (ΔD_{23}) and within the *Pre* period (ΔD_{23}) was tested by Wilcoxon's Rank sum test.

All the BAM vectors were made to have the same number of elements, as in the longest burst, by padding the smaller vectors with zeros at the ends. The BAM for each burst is a 60xN dimensional vector where N= number of time bins in the longest burst (Figure 5.2A).

Clustering of BAMs

The method used for clustering the BAMs was adapted from Beggs and Plenz (2004) who used the algorithm to cluster local field potentials (LFPs) recorded from cortical slices. We investigated the presence of spatiotemporal structure within spontaneous bursts using the same clustering methods (Figure 5.3).

BAMs of all the bursts were compared against each other for correlation. A dendrogram (paired clustering algorithm) was used to sort the correlation matrix. This procedure grouped BAMs with high similarity values into families i.e. it groups pairs of

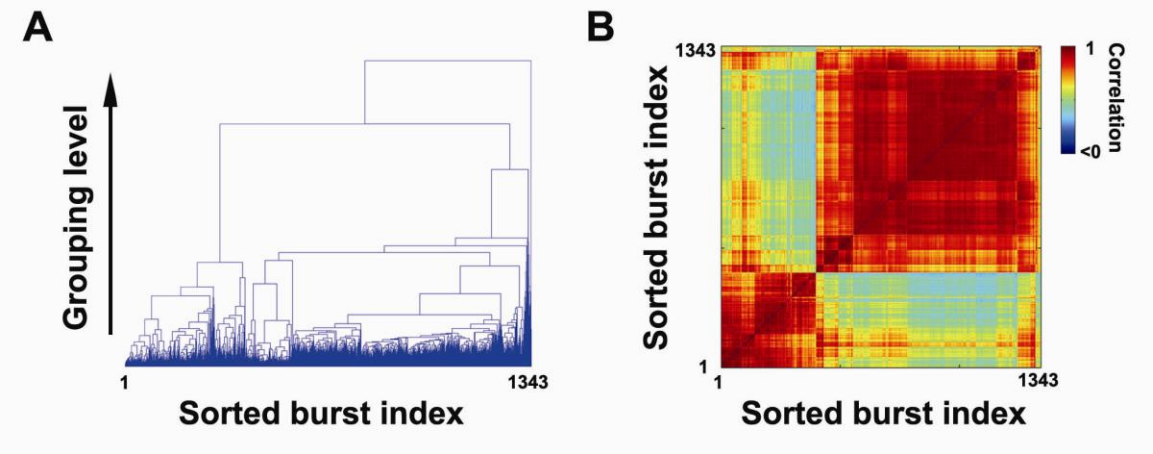

Figure 5.3: A. An example of a dendrogram showing different levels of the grouping process. All the individual BAMs are shown at the bottom in sorted order (BAMs that similar to each other were arranged together). At each level, the two most similar BAMs were grouped together, connected by a line. **B.** The corresponding sorted correlation matrix of BAMs. "Blocks" with high correlation values along the diagonal represent groups of bursts with similar BAMs. Data presented are from one representative *Spontaneous experiment*. The colorbar indicates the correlation values.

BAMs together in order of least distance in similarity space. A contrast function was calculated to determine optimal number of clusters [39]. The peak of the contrast function indicated the level at which the most distinct grouping of clusters occurred. *Occurrence* represents when the bursts in different BAM clusters happen (Figure 5.2B). *Integrated Occurrence* vector (Figure 5.2B) was created by counting the total number of *Occurrences* of each burst cluster in a 15-minute time window moved by a time step of 30s. This vector represents the distribution of burst types indicating the network's tendencies to express certain spatiotemporal activity patterns.

Statistics of Occurrence

The *Integrated Occurrences* were calculated for both the *Pre* (before the tetanus) and *Post* (after the tetanus) periods for all experiments. The *Pre* period was split into two parts *Pre1* and *Pre2*, separated by a sham period equal to the duration of the tetanus (15

minutes). The *Post* period was split into two parts *Post1* and *Post2*, separated by a sham period equal to the duration of the tetanus. The centroid of *Integrated Occurrences* in periods *Pre1*, *Pre2* and *Post1* were calculated (Figure 5.2C). The following quantity was calculated –

$$\Delta D_{ij} = \frac{mean(d_{ij})}{mean(d_{ii})}$$

where mean (d_{ii}) is the average Euclidian distance of each *Integrated Occurrence* in period *i* to the centroid of period *i*, and mean (d_{ij}) is the average Euclidian distance of each *Integrated Occurrence* in period *i* to the centroid of period *j* (Figure 5.2C). Therefore, ΔD_{ij} indicates the ratio of the change of *Integrated Occurrence* of BAM clusters from period *i* to period *j* over their drift within period *i*. ΔD_{ij} =1 indicates that there was no significant change from period *i* to period *j*.

For *Spontaneous experiments* and *Probe experiments*, we measured two quantities: ΔD_{12} and ΔD_{23}. ΔD_{12} represents the ΔD_{ij} of the *Pre1* and *Pre2* periods (within the *Pre* period), and ΔD_{23} represents the ΔD_{ij} of the *Pre2* and *Post1* periods (across the tetanus). This would allow us to detect whether the change in *Integrated Occurrence* of BAM clusters across the tetanus (ΔD_{23}) was more than their drift (ΔD_{12}) within the period *Pre* (Figure 5.2C). The significance of the change in *Integrated Occurrence* of bursts across the tetanus (ΔD_{23}) and within the *Pre* period (ΔD_{23}) was tested using Wilcoxon's Rank sum test.

Shuffling methods

The BAMs of spontaneous bursts were shuffled in various ways to determine whether their structure was more significant than expected by chance [129]. "Frame shuffling" randomly rearranged the sequence of time bins within each BAM. This method changes the temporal order while preserving the spatial information. "Electrode shuffling" randomly rearranged the electrodes within each BAM. This method changes the spatial order while preserving the temporal information. "Matched shuffling" randomly rearranged the activity on each electrode within each time bin within each BAM. This method changes both the temporal as well as spatial structure of the data. Unlike "frame shuffling" and "electrode shuffling", "matched shuffling" does not change the firing rate on each electrode. The mean correlation values between BAM clusters in the shuffled dataset were compared with the mean correlation values between BAM clusters in original non-shuffled dataset.

5.2.5.3 Quantifying Information carried by burst patterns

Modified information

The amount of new information learned due to the tetanus was defined as the number of new clusters that occurred in the *Post* period but never in the *Pre* period. The amount of information forgotten due to the tetanus was defined as the number of clusters that occurred in the *Pre* period but did not occur in the *Post* period. Both the amount of information forgotten or newly acquired represented modified information content in the network.

$$\text{Information}_{\text{modified}} = \frac{P(\text{Pre} \cup \text{Post}) - P(\text{Pre} \cap \text{Post})}{P(\text{Pre} \cup \text{Post})}$$

P (Post $\cap$ Pre) = Number of BAM clusters that occurred in the *Pre* and the *Post* periods

P (Pre $\cup$ Post) = Number of BAM clusters that occurred in the *Pre* or the *Post* periods

To reduce false positives, a threshold was set for the minimum number of occurrences of a BAM cluster. Only clusters that occurred at least 5 times in the 3-hour periods *Pre* and *Post* tetanus were included in the analysis.

Retained Information:

$$P(\text{Post} \mid \text{Pre}) = \frac{P(\text{Pre} \cap \text{Post})}{P(\text{Pre})}$$

P (Pre) = Number of BAM clusters that occurred in the *Pre* period

P (Post $\cap$ Pre) = Number of BAM clusters that occurred in the *Pre* and the *Post* periods

The equation represents the probability that a BAM cluster that occurred in the *Pre* period also occurred in the *Post* period. This conditional probability denotes the amount of information that was preserved across the tetanus between the *Pre* and *Post* periods. The clusters that were preserved across the tetanus were identified. To reduce false positives, a threshold was set for the minimum number of occurrences of a BAM cluster in the *Post* period. The number of *Occurrence*s of a cluster in the *Post* period

should be at least 50% of its number of *Occurrence*s in the *Pre* period for it to be included in this analysis. *Integrated Occurrence* for these clusters was calculated using a 30-minute moving time window with a time step of 10 minutes. The significance of the change of *Integrated Occurrence* of these clusters across tetanus was determined by Wilcoxon's rank sum test.

5.2.5.4 Burst initiation site

The burst initiation site is determined as the electrode that the first spike in the burst occurred on (burst onset, figure 2A). For each 15min time window (time step = 30s) during a *Spontaneous experiment*, the burst initiation probability (BIP) was calculated for every electrode. BIP vector was computed as the number of times the burst onset happened at an electrode normalized by the total number of bursts in the time window. This results in a 1X60 BIP vector for every time window (summation of these 60 values equals to 1). The same statistics (as used to evaluate the *Integrated occurrence* of BAM) was applied on BIP vectors to quantify the changes before and across the tetanization.

5.3 Results

5.3.1 General properties of spontaneous network-wide bursts in dissociated cultures

Synchronous spontaneous bursts separated by periods of quiescence are considered dominant patterns of activity in dissociated cortical cultures [23, 24, 53, 54, 70, 137]. These networks exhibit robust spiking activity from around 4-5 days *in vitro* (DIV) and spontaneous bursts are expressed from around 6-10 DIV [18, 53], depending on the density of the cultures [53]. Also, network-wide synchronized bursting can be

entrained to the electrical stimulus during slow (1Hz) focal electrical stimulation [23, 37, 60, 70].

Spontaneous bursting is a robust phenomenon, which persists throughout the lifetime of the culture. It can be blocked by glutamate receptor blockers [70, 137] but this also abolishes most of the spontaneous spiking activity in the network [18]. We have shown that network-wide bursts can be controlled or eliminated using distributed patterns of electrical stimulation [60] but they reappeared within seconds after the cessation of stimulation.

Bursts occur in different sizes and patterns [53] and can be classified in various ways. A spike raster plot for 5 minutes of spontaneous recording is shown in Figure 5.1C. Culture-wide bursts are periods of increased firing rate across most of the active electrodes (Figure 5.1C). Since, there was a clear bimodal distribution in the burst size for all tested cultures (Figure 5.1B), bursts were classified into two categories, big and small bursts (Figure 5.1C), with the threshold set at the minimum in the burst size histogram (Figure 5.1B). A burst activity matrix (BAM, see Materials and Methods) was generated for each burst by counting number of spikes on each electrode within the length of the burst using a 100 ms sliding time window (time step = 10 ms) (Figure 5.2A).

5.3.2 Stimulus-evoked responses to detect functional plasticity

Activity-dependent changes in stimulus-evoked responses as a result of a local tetanus have been used successfully to demonstrate plastic changes both *in vitro* [2, 52, 138-140] and *in vivo* [141, 142]. Such use-dependent modification of probe (single electrode stimulation) responses due to tetanic stimulation have also been demonstrated

in dissociated cortical cultures [30-32, 44]. Similar experiments, adapted from Jimbo *et al.* (1998), were performed (Materials and Methods: *Probe experiments*) on spontaneously bursting cultures to test for tetanus-induced changes in probe responses.

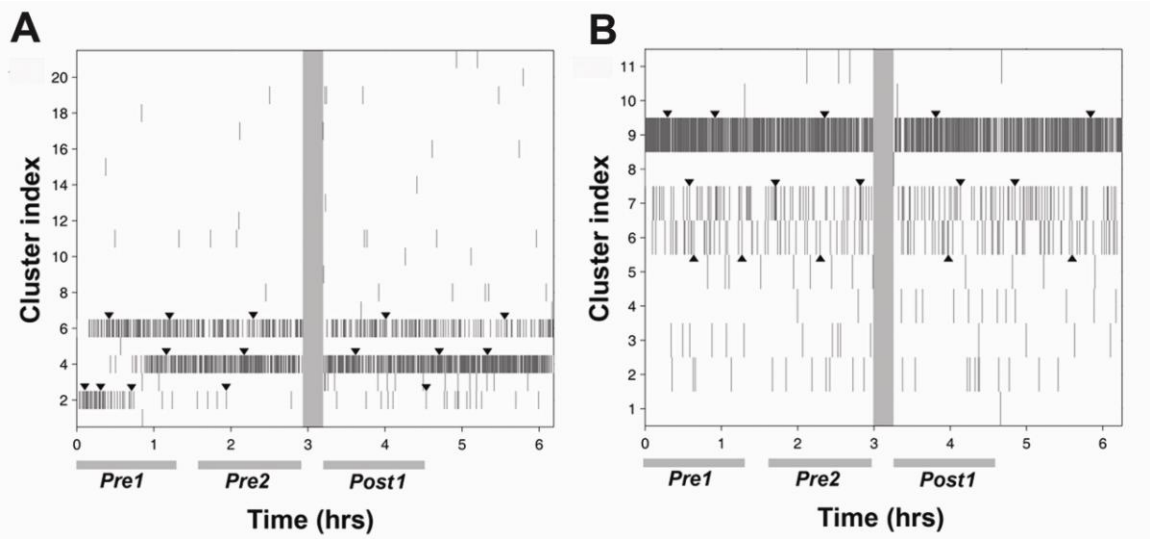

Figure 5.4: Occurrence of clusters of BAM for evoked bursts changed before and across the tetanus. **A.** Each stroke represents one *Occurrence* of a BAM cluster of small evoked bursts. **B.** Each stroke represents one *Occurrence* of a BAM cluster of big evoked bursts. This is a representative example of a *Probe experiment*. The grey bar indicates the period of tetanization. The arrowheads indicate the timing of the each individual BAM cluster shown in figure 5.5.

Since the chosen probing rate in our experiments was 0.5 Hz at a single electrode, most of the stimuli evoked bursts of activity. In addition to evoked bursts which occurred at a fixed latency after the probe, there was spontaneous bursting (not time-locked to probes) in all the tested cultures. Thus, bursts in these experiments were of additional two categories: non-time locked and evoked bursts (Materials and Methods: *Burst detection*). Since these two categories of bursts were triggered by separate mechanisms, the classification of bursts and analysis on the BAMs of bursts were performed independently for the non-time locked and evoked bursts.

The BAMs for evoked and non-time locked bursts were clustered into different groups using a correlation based clustering algorithm (Figure 5.3). Time distribution of various clusters of BAM (*Occurrence*) for small as well as big evoked bursts for one representative *Probe experiment* is shown in Figure 5.4.

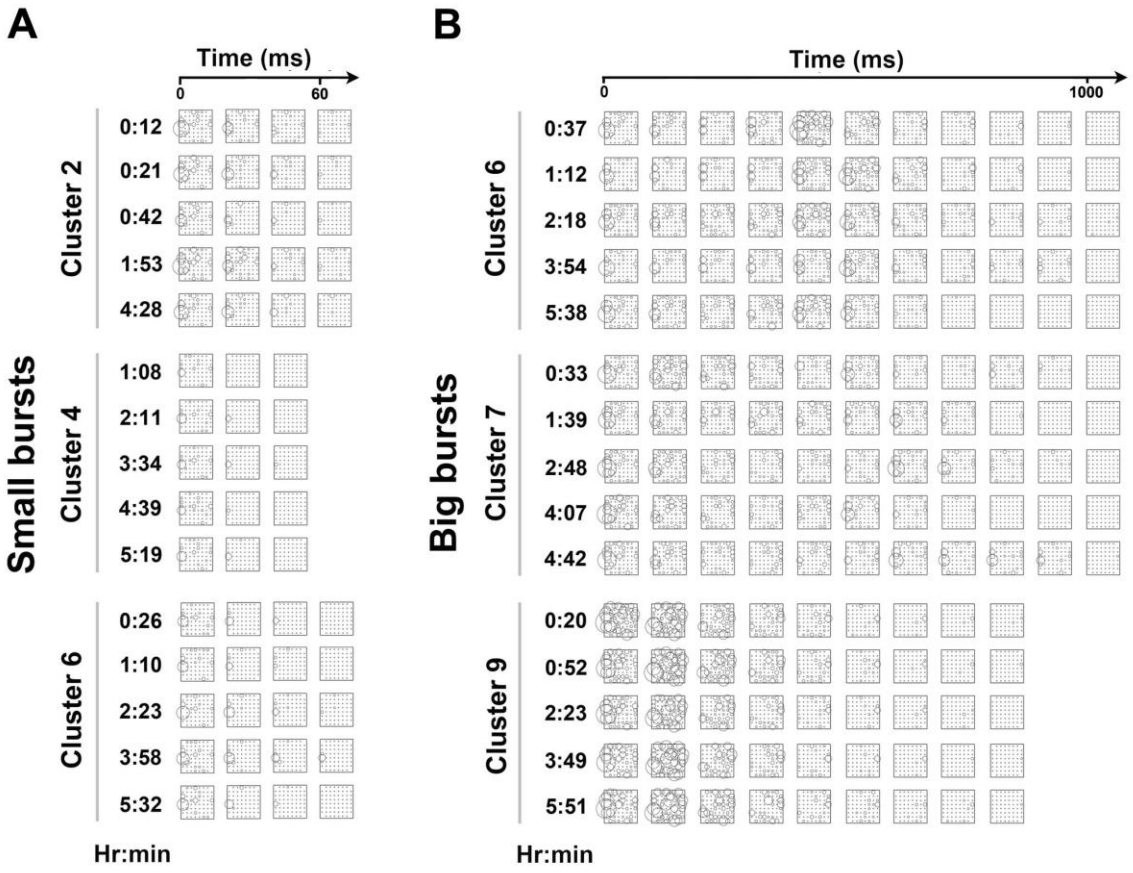

Figure 5.5: Examples of clusters of BAMs of evoked bursts. The sampled times are marked by arrowheads on Figure 5.4. **A.** Clusters of BAMs of small evoked bursts in the original coordinates of the multi-electrode array. The BAMs of each small evoked burst clusters were different from each other. Size of the circles represents the number of spikes in that particular electrode for a particular time bin. BAMs were collected every 20ms. **B.** Clusters of BAMs of big evoked bursts in the original coordinates of the multi-electrode array. The BAM of each of the big evoked burst cluster were different from each other. Size of the circles represents the number of spikes on that particular electrode for a particular time bin. BAMs were collected every 100ms since the big bursts were much longer the small bursts shown in part A.

The *Occurrence* of BAM for evoked bursts (small and big evoked bursts) changed both before and after the tetanus. To compare the BAMs of bursts within clusters,

temporally spaced BAM clusters (arrowheads in Figure 5.4) were plotted (Figure 5.5). The clusters of BAMs for evoked bursts were distinct from each other and showed high spatial and temporal similarity despite having occurred many hours apart (Figure 5.5). To determine whether the tetanus had caused a change in activity patterns greater than the ongoing intrinsic activity change (drift) in the network, the change in *Integrated Occurrence* of BAM clusters within the period before the tetanus was compared to its change across the tetanus for significance (see Materials and Methods). For N=5 *Probe experiments*, the average activity change in the period before tetanization was significantly greater ($p<0.01$, Wilcoxon's rank sum test) than the change across the tetanus for evoked bursts (Figure 5.6B). Change in the *Occurrence* of BAM clusters before the tetanus made it difficult to ascertain whether the change across the tetanus (if any) was due to the tetanus and not due to the ongoing intrinsic drift in network activity. Similar to evoked bursts, the distribution of BAM clusters for non-time locked bursts changed before and after tetanus (Figure 5.6A) but there were fewer non-time locked bursts (808 ± 273.8) as most of the bursts were evoked by the probes (2579.6 ± 473.48 evoked bursts).

5.3.3 Structure in Spontaneous bursts

Since we found considerable drift in the probe responses, we studied patterns in the spontaneous spiking activity in the culture to determine if they could be used to indicate functional plasticity in the neuronal network resulting from tetanic stimulation.

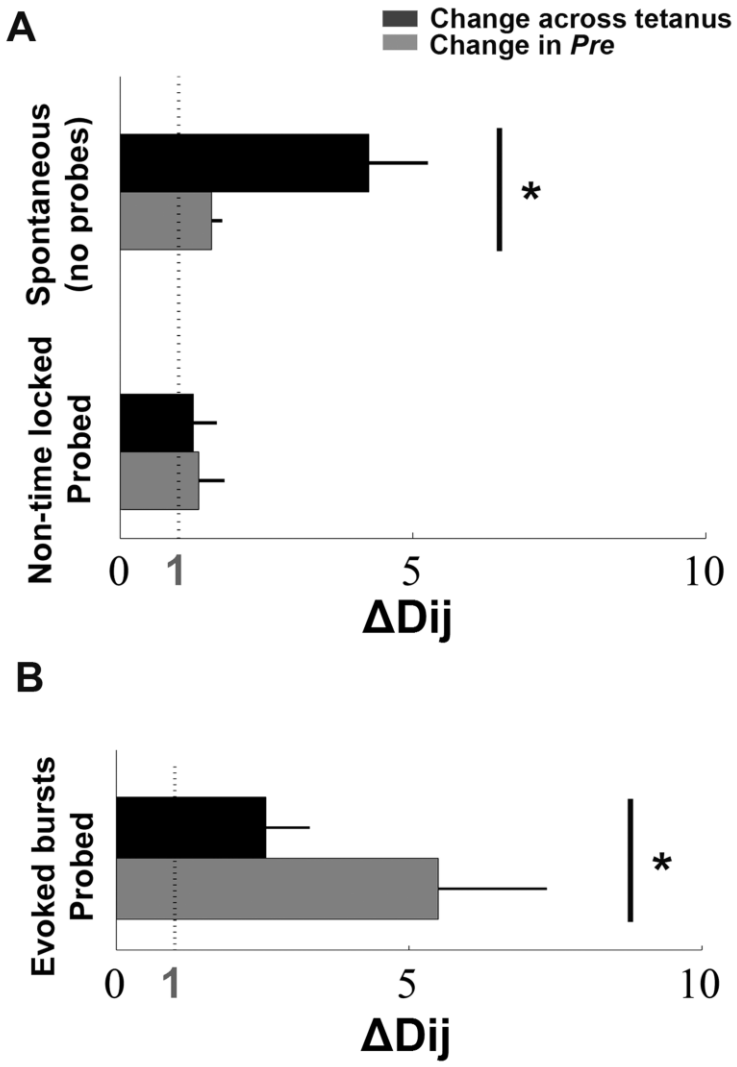

Figure 5.6: The Occurrence of spontaneous bursts in Spontaneous experiments (not probed) was changed significantly by tetanic stimulation. A. The average change in N=5 *Spontaneous experiments* across a tetanus (change across periods *Pre2* and *Post1*, ΔD_{23}) of *Occurrence* of spontaneous bursts was significantly greater ($p<0.01$) than the average drift (change across periods *Pre1* and *Pre2*, ΔD_{12}) of the *Occurrence* of spontaneous bursts. In contrast, the average change in N=5 *Probe experiments* across the tetanus and drift across periods *Pre1* and *Pre2* were not statistically different. The average change across the tetanus (change across periods *Pre2* and *Post1*, ΔD_{23}) of *Occurrence* of spontaneous bursts in *Spontaneous experiments* was greater than the average change of *Occurrence* of spontaneous bursts in *Probe experiments*. The graph compares averages from five *Spontaneous experiments* and five *Probe experiments*. $\Delta D_{ij}=1$ indicates that there was no change in the *Occurrence* between periods i and j. ΔD_{12} of spontaneous bursts in the *Spontaneous experiments* was close to 1 indicating that there was very little drift in the *Pre* period before the tetanus and the *Occurrence* of BAM of spontaneous bursts was stable for this period. **B.** The average drift (Change across periods *Pre1* and *Pre2*, ΔD_{12}) of the *Occurrence* of evoked bursts was significantly greater ($p<0.01$) than the change across the tetanus in five *Probe experiments*. Asterisk indicates $p<0.01$, Wilcoxon's rank sum test for equal medians.

To explore the presence of temporal and spatial structure within spontaneous bursts, the correlation between BAMs of all bursts in *Spontaneous experiments* was determined (see Materials and Methods) and hierarchical clustering algorithms were used to cluster the BAMs of bursts having the least distance in correlation space into groups (see Supplementary material). To visualize the clusters the correlation matrix was sorted (Figure 5.3), resulting in regions of high correlation values along the diagonal showing spontaneous bursts that exhibit high similarity in spatiotemporal structure (Figure 5.7A). In addition, the BAMs of spontaneous bursts belonging to different clusters showed high spatiotemporal fidelity over several hours of recording (Figure 5.5).

The data were shuffled in various ways to verify that the structure in spontaneous bursts was not an artifact of the clustering algorithm (see Materials and Methods). On shuffling the data, both temporally and spatially [129], the correlation values in the shuffled data were significantly lower than those in the original dataset (Figure 5.7B, $p<0.001$). Thus, the lack of high correlation values in the shuffled data shows that the original data consisted of various spatiotemporal activity patterns that have specific structure more than would be expected by chance. In 5 experiments on 4 cultures we identified an average 59.5 ± 7.9 (Mean ± SEM) clusters of small bursts and 158 ± 23.1 clusters of big bursts per culture. Also, there was an average of 4128 ± 553.28 spontaneous bursts per culture (5 experiments on 4 cultures).

5.3.4 Spontaneous bursts as indicators of tetanus-induced network plasticity

Bursts have been suggested as a reliable neural codes as they could facilitate neurotransmitter release at a synapse more reliably than could a single spike [56]. Beggs

and Plenz (2004) suggested that in order for repeatable patterns to serve as substrates of memory they should be diverse, precisely timed and possess long-term stability.

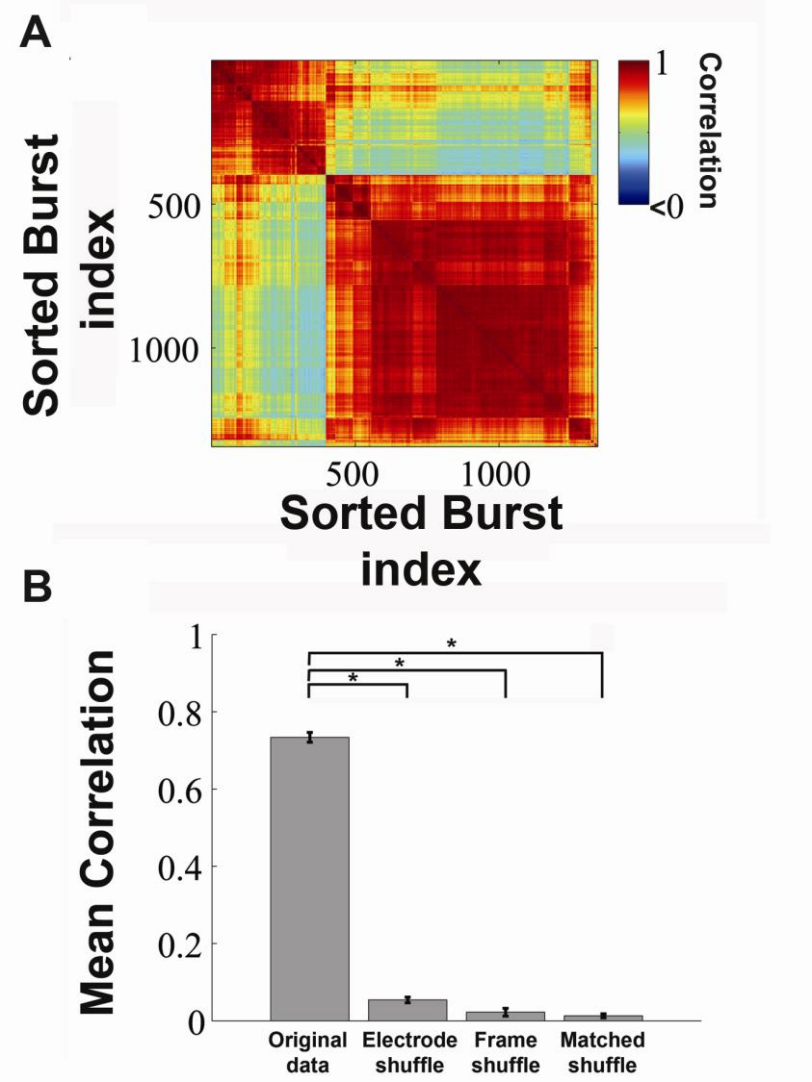

Figure 5.7: Shuffled data does not show significant structure in BAM of spontaneous bursts. **A.** Sorted correlation matrix of actual un-shuffled data for one representative *Spontaneous experiment*. There were high correlations indicating high similarity among BAM of spontaneous bursts **B.** Average correlation values between BAM clusters from N=5 *Spontaneous experiments* after "Electrode shuffle", "Temporal shuffle" and "Matched shuffle" methods showed low correlation values compared to original un-shuffled data (Asterisk indicates $p<0.001$, Wilcoxon's rank sum test for equal medians).

Motivated by these studies we sought to determine whether network-wide bursting in dissociated cortical cultures could be a potential mechanism for transfer and

storage of information in cultured networks. Other multi-electrode array studies use responses to stimulation probes [30] but we have shown that probe responses are subject to intrinsic drift (Figure 5.4). Since we found specific structure in spontaneous bursts (Figure 5.7), we sought to use changes in spatiotemporal patterns of spontaneous culture-wide bursts as a measure for detecting functional plasticity in the network.

Bursts in 3 hour periods before and after the tetanus (see Materials and Methods: *Spontaneous experiments*) were classified into big and small bursts depending on their size (Figure 5.1B) and clustered into separate types using a correlation-based clustering algorithm. This analysis showed that spontaneous bursts occurred in clusters having different spatiotemporal patterns that remained stable during the 3-hour period before the tetanus (Figure 5.8). Stability of *Occurrence* of BAM clusters for spontaneous bursts, in the absence of any stimulation, persisted for at least 9 hours (the longest experiment, not shown). Structure within temporally spaced BAM clusters of spontaneous small and big bursts (arrowheads on Figure 5.8) were conserved over time for all N=5 experiments (one representative experiment shown in Figure 5.9). Thus, not only were the spontaneous bursts repeatable, but they also occurred in precisely timed dynamic patterns that remained stable over hours.

Wagenaar *et al.* (2006) documented the presence of repeatable spatiotemporal structure in burst sequences ('superbursts') in dissociated cortical cultures, which remained stable for hours. The present study was not restricted to 'superbursts'. We found highly conserved structure for all bursts occurring during the recording period. The stability of burst patterns represents the tendency of the culture to express certain types of

bursts spontaneously and we sought to determine whether a strong (tetanic) stimulus would change this tendency.

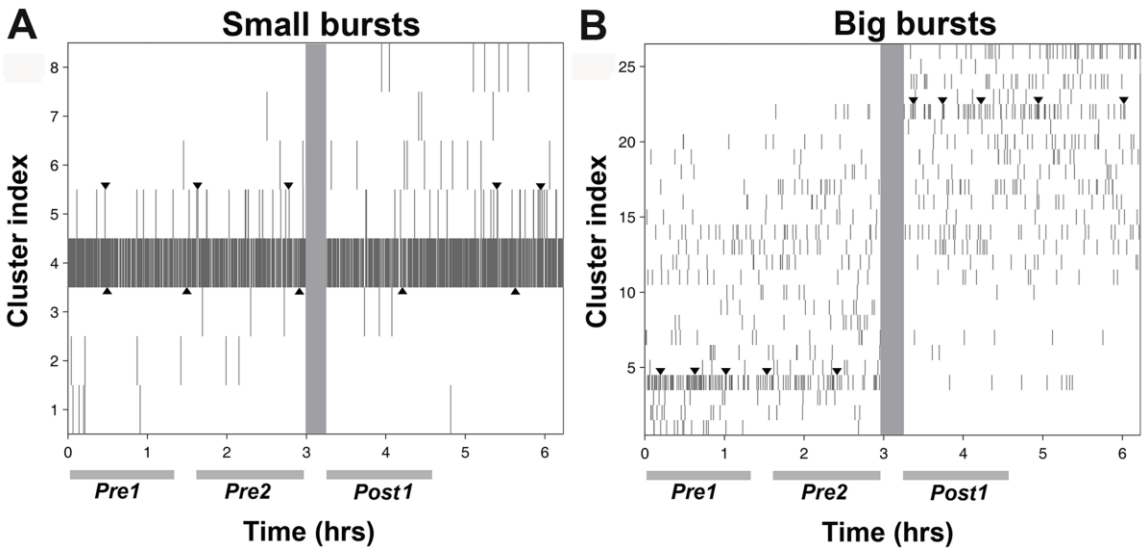

Figure 5.8: Occurrence of spontaneous bursts was stable before the tetanus and changed across the tetanus. A. Each stroke represents one *Occurrence* of a BAM cluster of small spontaneous bursts. **B.** Each stroke represents one *Occurrence* of a BAM cluster of big spontaneous bursts. This is a representative example of a *Spontaneous experiment*. The grey bar indicates period of tetanization. The arrowheads indicate the timing of the different BAM clusters shown in figure 5.9.

Any change in the *distribution* of burst clusters was quantified by the change in the *Integrated Occurrence* of BAM clusters (Figure 5.2C). Stability of *Integrated Occurrence* of BAMs of spontaneous bursts was previously determined on two 9 hour-long spontaneous recordings without any electrical stimulation. The average change in *Integrated Occurrence* of BAMs across sequential 3 hour periods in two 9 hour recordings was not significant ($p=0.17$, Wilcoxon's rank sum test).

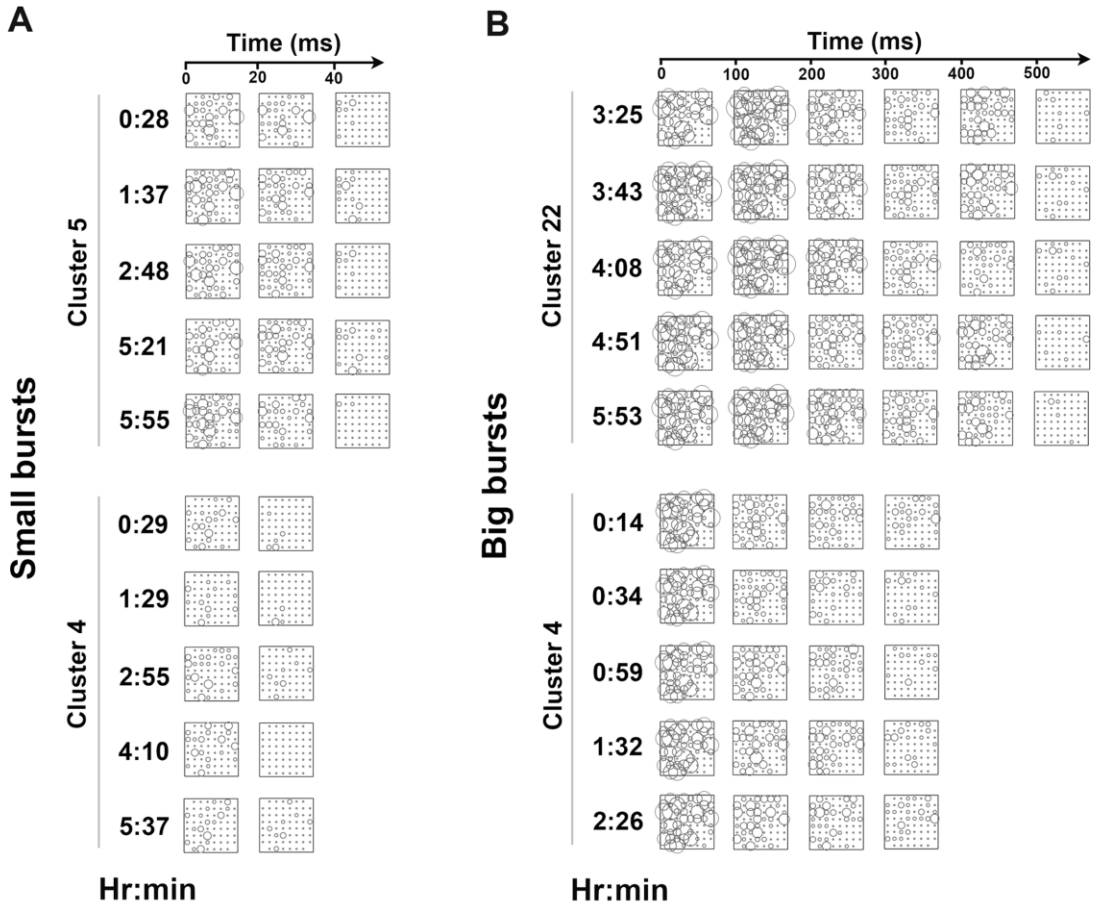

Figure 5.9: Examples of clusters for BAM of spontaneous bursts for one Spontaneous experiment. The sampled times are marked by arrows on Figure 5.8. Clusters show similarity in structure over hours but there was difference in the patterns of any two clusters. **A.** BAM clusters for small bursts in the original coordinates of the multi-electrode array. The BAM of each of the spontaneous 'small' burst clusters were different from each other. BAMs were collected every 20ms. **B.** BAM clusters for big bursts in the original coordinates of the multi-electrode array. The BAM of each of the 'big' burst clusters were different from each other. BAMs were collected every 100 ms since the big bursts were much longer the small bursts shown in A. The sizes of the circles represent the number of spikes in that particular electrode for a particular time bin.

To quantify whether the change in the distribution of burst patterns across the tetanus was more than their drift in the periods of no stimulation, the change in *Integrated Occurrence* of BAM clusters across the tetanus was compared to their change across a 'sham' period of equal duration to the tetanus (see Materials and Methods, *Statistics on Occurrence*). The burst patterns changed significantly across the tetanus but not within

the spontaneous period before it, in *Spontaneous experiments* (Figure 5.6A). The average change across the 'sham' period ($\Delta D_{12,}$ ΔD_{ij} change between *Pre1* and *Pre2* periods) for N=5 *Spontaneous experiments* was not significantly greater than 1 ($p=0.063$). $\Delta D_{ij} = 1$ indicates that the distribution of burst clusters did not change between periods *i* and *j* (see Materials and Methods). In addition, the average change in the distribution of burst patterns across the tetanus ($\Delta D_{23,}$ ΔD_{ij} change between period *Pre2* and *Post* across tetanus) for N=5 *Spontaneous experiments* was significantly greater ($p<0.01$, Wilcoxon's rank test) than the change within the period before the tetanus (Figure 5.6A).

In contrast, for N=5 *Probe experiments*, the average change in the distribution of non-time locked bursts across the tetanus was not statistically different from their average change within the period before the tetanus (Figure 5.6A). In addition, there was a significant change ($p<0.01$) in the distribution of evoked bursts in the period before the tetanus (averaged over N=5 *Probe experiments*) compared to their change across the tetanus (Figure 5.6B).

5.3.5 Spontaneous bursts can represent information in dissociated cortical networks

As shown above, spontaneous burst patterns possessed high temporal fidelity and specific spatiotemporal structure, which could be modified by tetanic stimulation (Figures 5.6 - 5.9). Thus, they satisfy many of the requirements for a memory substrate [129, 136, 143]. In an attempt to quantify the amount of information stored in burst patterns, we calculated the information modified or preserved across the tetanus (see Materials and Methods). The tetanus caused a change in network dynamics resulting in the creation or loss of an average of 70.91 ± 15.74 BAM clusters of big bursts (Mean ± SEM) and 55.33 ± 8.64 BAM clusters of small bursts for N=5 *Spontaneous experiments*.

We take this as a measure of the amount of information in bursts that was modified by the tetanus. We also quantified the amount of information retained across the tetanus as the number of BAM clusters that occurred in the *Post* period after the tetanus given that they had occurred in the *Pre* period before the tetanus. An average of 24.1 ± 14.72 BAM clusters of big bursts and 27.78 ± 14.7 BAM clusters of small bursts were retained across the tetanus in N=5 *Spontaneous experiments*. This quantity represents the fraction of clusters that were preserved across the tetanus, but does not indicate whether the temporal distribution (*Occurrence*) of the 'preserved clusters' was also retained across the tetanus. In order to quantify the stability of the 'preserved clusters' across the tetanus, the *Integrated Occurrences* of these clusters were compared for the *Pre* and *Post* periods. There was no significant change in the *Integrated Occurrence* of the 'preserved' clusters across the tetanus ($p=0.55$, Wilcoxon's rank sum test).

5.3.6 Tetanic stimulation causes changes in the locus of bursts

Typically, spontaneous bursts originate from various locations in the networks, termed as burst initiation sites, and spread to the entire network. Eytan *et al.* (2006) identified early-to-fire neurons during the start of the burst and these initiation areas were found to be characterized by high neuronal density and recurrent excitatory and inhibitory connections [144].

On quantifying the probability of neurons around any particular electrode initiating a burst, we found that this probability was stable if no external stimulation was delivered, and was changed significantly by tetanic stimulation (Figure 5.10B, $p<0.05$, rank sum test). Hence, not only did the tetanus change the spatiotemporal dynamics of

burst patterns, but also changed the locus of the neurons involved in triggering bursts, indicating that tetanic stimulation altered the connectivity in the neuronal network.

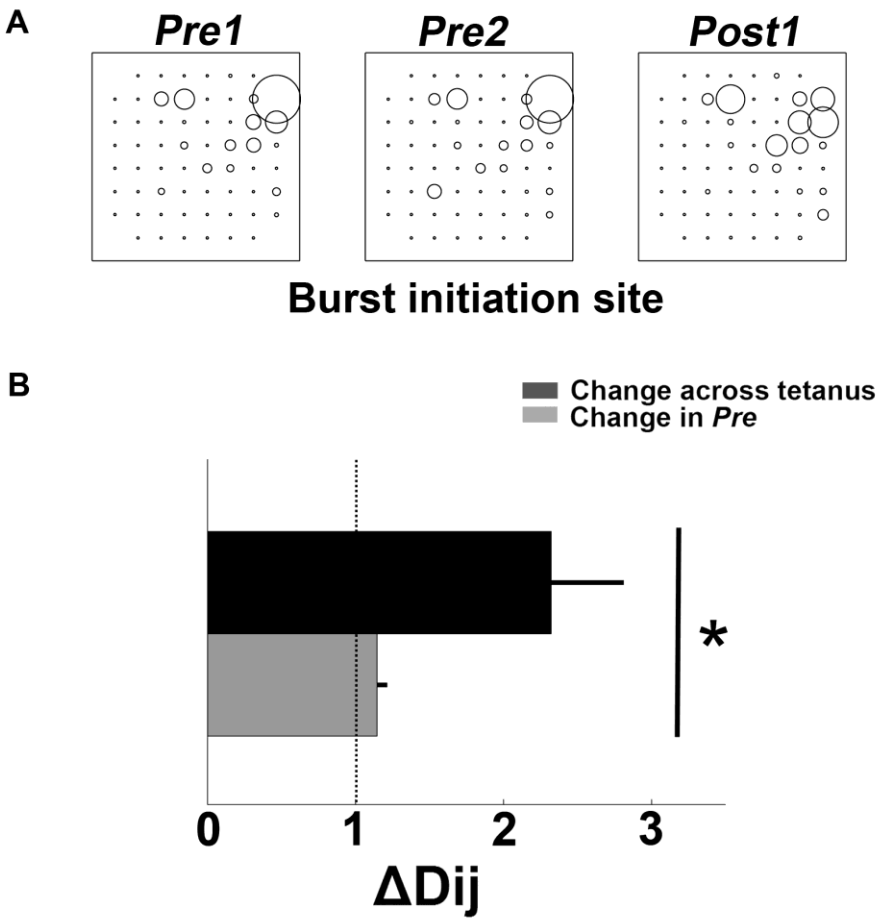

Figure 5.10: Burst initiation site was significantly changed by a strong tetanus. A. The probability of neurons around an electrode initiating a burst is shown by the different sizes of the circles. Though this probability did not change much in the spontaneous recording periods before the tetanus (*Pre1* and *Pre2*), it changed significantly across the tetanus. Figure shows a representative *Spontaneous experiment*. **B.** The average change in the probability of burst initiation changed significantly after ($p<0.05$) but not before the tetanus (N=5 *Spontaneous experiments*). Asterisk * - $p<0.05$, Wilcoxon's rank sum test. Error bars represent SEM.

5.4 Discussion

Synchronized or correlated activity within neuronal networks has been proposed as a likely mechanism for encoding information (for review see [145]). To investigate the potential of recurring burst patterns in dissociated nets as information carriers *in vitro*, we characterized spatiotemporal characteristics of spontaneous bursts expressed by dissociated cortical cultures. We demonstrated that spontaneous bursts occurred in diverse but repeatable patterns that were stable for hours in the absence of electrical stimulation, and could be altered significantly by a strong tetanus applied simultaneously on two electrodes (Figure 5.6A, $p<0.01$).

5.4.1 Comparison with previous work

Probe responses were useful for demonstrating functional plasticity in other studies [30-32, 44, 146]. The plating densities in our cultures were an order of magnitude higher than in these studies. Cultures with higher plating densities showed faster development of network activity and more synchronized bursting than cultures with lower plating densities [53]. Possibly due to higher levels of ongoing activity in our densely plated cultures, we observed that probe responses continuously change with time (Figure 5.4) making it more difficult to detect functional plasticity in probe responses than in spontaneous bursts.

Other studies on spontaneous activity in cortical slices without probe or tetanic stimulation have shown that spatiotemporal patterns of activity, termed neuronal avalanches, were stable for over 10 hours [129]. These stable repeatable patterns in local field potentials (LFPs) lasted tens of milliseconds. The spatiotemporal patterns of bursts we studied, in dissociated cortical cultures, typically last much longer (100ms–1 second)

than do avalanches in slices. Unlike neuronal avalanches, the size distributions of spontaneous bursts (defined here as the number of spikes in a specified time bin) were bimodal and did not follow a power law (Figure 5.11).

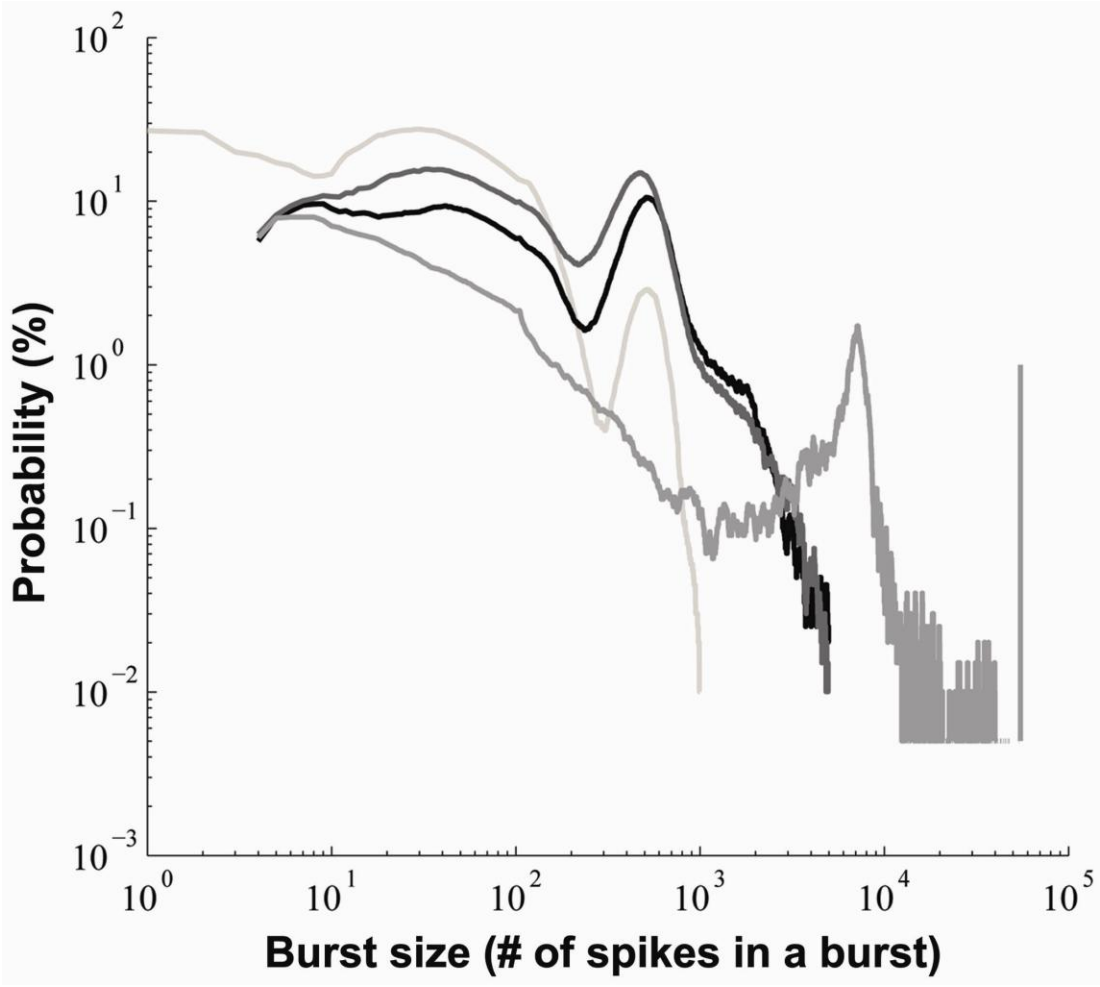

Figure 5.11 Size distributions of spontaneous bursts were bimodal and did not follow the power law. Size distribution of spontaneous bursts for N=4 *Spontaneous experiments* are plotted on log-log coordinates. Beggs and Plenz (2003, 2004) investigated recurring spontaneous patterns in local field potentials (LFPs) in acute slices of rat cortex (neuronal avalanches) and showed that the size distributions of avalanches obey the power law. The number of spikes per burst represents size of bursts here, which is similar to avalanche amplitude. For each experiment, a histogram of the number of spikes in every burst (time bin=100ms) in the experiment was plotted on a log-log scale.

In a similar dissociated culture preparation, Eytan and Marom (2006) also showed that network bursts in dissociated cortical networks follow a bimodal distribution for

burst size (number of electrodes) and burst duration. They attributed this contrast with neuronal avalanches to the conserved cortical layer organization in Beggs and Plenz's *in vitro* slice preparation [147]. Segev *et al.* (2004) have reported correlated spontaneous burst patterns in dissociated cortical networks, [148] but the study did not attempt to investigate the effects of external electrical stimulation on these patterns.

We extend the previous findings by demonstrating that the distribution of spontaneous burst clusters changed significantly after tetanic stimulation (Figure 5.6A). Though there was a change in the distribution of spontaneous bursts within a period of spontaneous activity, the effect was significantly more across the tetanus (Figure 5.6A). In contrast, our experiments using stimulus-evoked responses, showed significant drift ($p<0.01$) in the distribution of bursts evoked by stimulation in the period before the tetanus (Figure 5.6B). This suggests that the intrinsic drift in evoked activity blurs the effect of the tetanus. The methods used here are general measures of spatiotemporal activity patterns, which are not restricted to *in vitro* studies and could be applied to the analysis of spontaneous and stimulus-evoked multi-unit activity patterns *in vivo*.

5.4.2 Bursts as information-carriers in cortical networks

We found spatiotemporal activity patterns within spontaneous bursts to be stable and diverse. These patterns can be altered by tetanization suggesting that they could serve as a vehicle for information storage in cortical networks. Single neuron bursts have been proposed as reliable coding elements [56]. Recordings from area MT of macaque monkey have shown that burst rate was on average a more sensitive measure of visual stimulus direction than the total number of spikes [149]. Models of bursting in pyramidal neurons have shown that the spike count of a burst encodes the rate of increase of inputs [150].

These studies propose that bursts are a special neural code that carry information about input characteristics [151].

Spontaneous bursts observed in cultured dissociated networks could potentially store information; we have shown them to be stable over hours (Figure 5.8), diverse to encode different memories (Figure 5.9) and susceptible to functional plasticity (Figure 5.6A). These properties exhibited by spatiotemporal patterns of spontaneous bursting satisfy the requirements of a memory substrate [129]. We analyzed the *Occurrences* of spontaneous bursts in various clusters across the tetanus and showed that while some clusters were preserved across the tetanus others were modified by the tetanus. If indeed information could be transmitted through a neuronal network in the form of spontaneous bursts with different spatiotemporal structures, this study suggests that while some existing memories were preserved across the tetanus, some new memories were also created.

5.4.3 Bursts as dynamic attractors in cortical networks

Spontaneous bursts with different but stable BAM patterns could represent different intrinsic spatiotemporal tendencies of the network. Our modeling study of network activity revealed attractors in the network intrinsic state, represented by network synaptic weights, and a corresponding set of stable spontaneous bursts [59]. If the network was driven from one attractor to another (by the tetanus), the spontaneous burst pattern was also changed. In the present experiments using living networks, the change of *Occurrence* of spontaneous bursts with different BAMs after tetanus suggests that the network was driven from one attractor to a different one by the tetanus.

Precisely-timed sequences of single-unit activity were reactivated with high temporal precision in cortex *in vivo* and *in vitro* cortical slices [152]. These repeated sequences have been suggested to represent attractors in the cortex [152]. In our study, BAMs of spontaneous bursts consisting of specific sequences of network activity patterns were found to recur over hours. The robust spatiotemporal activity patterns within bursts could represent attractors in dissociated cortical cultures. The steady occurrence of different attractors over hours could correspond to a stable underlying intrinsic state of the network. This intrinsic state of the network could be modified by tetanic stimulation (or sensory input *in vivo*) resulting in a new set of attractors, which represents new information in the network.

This study of enduring patterns in dense cortical networks exhibiting both stability and activity-dependent plasticity demonstrates the usefulness of multi-electrode *in vitro* systems as a model for studying memory mechanisms in the brain.

CHAPTER 6

CONCLUSIONS AND DISCUSSION

The ultimate goal of our research is to decipher the network-level rules of learning and memory. For these studies, we use *in vitro* cultured networks because they provide easier access, allow for detailed observation and complete control over the inputs to the neurons compared to the brain *in vivo*. We have developed a model system of cultured monolayer networks of mammalian neurons that are interfaced to real-time 2-way processing systems through extracellular electrodes. Distributed patterns of electrical stimulation serve as sensory input to this model system and spatiotemporal patterns of activity represent model motor output.

Spontaneous culture-wide barrages of activity (bursts) characterize these cultured networks isolated from the cortex. We hypothesized that the persistence of spontaneous bursts of activity beyond the developmental phase, was a sign that the networks were arrested in development due to lack of afferent input. Substituting for the lack of input through electrical stimulation ceased culture-wide bursting and allowed for tonic patterns of activity. Thus, by using continuous distributed electrical stimulation paradigms we can bring *in vitro* cultures out of their 'sensory-deprived' state, which was previously the norm for *in vitro* models. We showed that cultured networks with controlled background activity are more amenable for induction and detection of functional plasticity. This control of background activity was found to be mediated by homeostatic changes in inhibitory neurotransmitter expression levels in the network. We also studied functional changes in spontaneously occurring activity patterns and suggested that they could serve

as information codes in un-stimulated intrinsically active neuronal networks. The results of this study provide tools for understanding and mapping network-level manifestations of memory, that can help connect the cellular plasticity mechanisms to behavioral level studies of learning and memory.

Feedback, or interaction with the environment, is a necessary element in the wiring of the brain. Learning can be defined as a process by which experience results in a permanent change in behavior [153]. Since our cultures are removed from the body, our lab has used hardware and software in order to re-embody them [19]. The first step to study learning in embodied closed-loop systems was to develop reliable input (stimulation) – output (reproducible patterns) mappings and derive methods to induce changes in these I/O mappings. My work provides various methods to induce stable directed plastic changes using both stimulated and spontaneous activity patterns expressed by the cultured networks. Additionally, these studies provide analytical tools that help decipher and quantify functional changes. Hence, this body of work provides the foundation for developing closed-loop systems that allow studies of adaptive behavior using embodied cultured networks.

6.1 Major findings

The major findings of this research have been deliberated upon at the end of each chapter. This section integrates these findings and discusses their collective implications in the study of learning and memory *in vitro*.

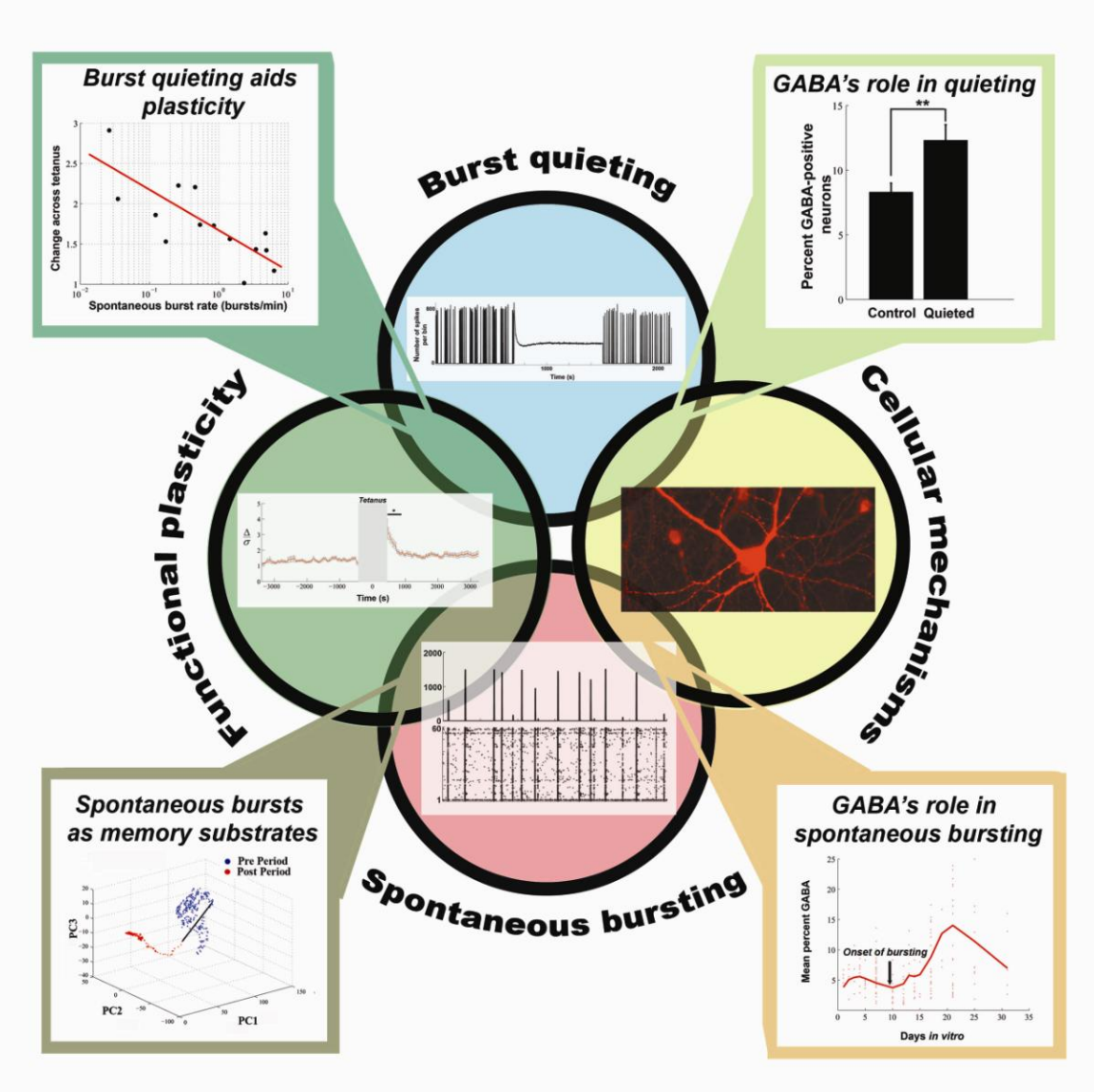

Figure 6.1: Schematic showing the relation between different aims and the major conclusions of this dissertation.

6.1.1 Control of ongoing activity allowed for greater functional plasticity

Ongoing activity patterns have been thought to affect post-synaptic responses. Most studies of plasticity in dissociated cortical networks either selected cultures that intrinsically expressed low levels of spontaneous bursting or reduced the amount of spontaneous bursting by using elevated levels of extracellular Mg^{2+}. In order to

investigate the effects of spontaneous bursting on the ability to induce plasticity in dissociated cortical networks, we quantified the amount of functional plasticity induced by tetanic stimulation on the background of varied levels of ongoing bursting activity. The levels of ongoing activity were controlled by varying the levels of spontaneous bursting using continuous distributed electrical stimulation. Hence every culture, irrespective of its spontaneous bursting rate, could be adjusted to the express a desired rate of bursting. This unbiased study of the effects of controlling levels of ongoing network activity is the first to experimentally demonstrate the role of spontaneous global bursting on the capability of cultured networks to exhibit stable functional plasticity.

The amount of tetanus-induced changes in the network was negatively correlated to the spontaneous burst rate of the network. This increased efficacy in identifying tetanus-induced change was a result of maintaining stable baseline levels of activity through distributed continuous stimulation. In addition, the absolute amount of plastic changes in burst-controlled cultures was significantly greater than in cultures with high levels of spontaneous bursting ($p<1e-4$, rank sum test) and the induced changes persisted for at least 2 hours. Hence, burst control allowed for higher efficacy of inducing long term plastic changes in dissociated neuronal networks. A novel measure of spatiotemporal activity, center of activity trajectory [59], was used to quantify the changes in stimulus-responses. Compared to other traditionally used quantitative measures of network-level plasticity like firing rate, CAT was found to be the most sensitive measure for detecting tetanus-induced change.

We hypothesized that spontaneous barrages of activity serve to interfere with tetanus-induced plasticity, by resetting synaptic weights. Hence, spontaneous bursts can

be thought to represent one of the mechanisms for 'forgetting' information. By preventing bursts, through the control of the amount of input to the network, we increased the probability of inducing robust plastic changes. This study of plasticity on the background of continuous input represents a more realistic model of the brain, in which continuous inputs are being processed in parallel to produce behaviorally relevant outputs.

Juvenile epilepsy is often accompanied by learning and cognitive disorders [101]. An understanding of the effects of global activity on network-level learning and memory could have potential applications in the treatment of cognitive deficiencies in epileptic children.

6.1.2 Homeostatic changes in GABA expression levels are involved in electrical burst-control

On demonstrating that distributed stimulation helped in controlling spontaneous bursts of activity, it was important to understand the underlying molecular mechanisms involved in this process. In the adult brain, the equilibrium between excitation and inhibition is an essential feature that must be maintained to avoid pathological consequences; blockade of inhibition can cause seizures and excess excitation can cause excitotoxicity. In order to understand the role of excitation-inhibition balance in burst control mechanisms, we conducted immunocytochemical studies to measure the fraction of inhibitory neurons to correlate the effects of burst quieting on the excitation-inhibition ratio.

In spontaneously active cultures the fraction of GABAergic neurons decreased significantly at the onset of spontaneous bursting (~1 week *in vitro*) and then increased

(after 2 weeks *in vitro*). This suggests that spontaneous bursts could be a result of low amounts of inhibition in the network. The increase in the fraction of GABAergic neurons after 2 weeks could be the result of a homeostatic response operating to counter balance for the increase in activity (bursts) by increasing inhibition. These studies in spontaneously bursting cultures strongly suggest that activity-dependent transmitter expression changes were involved in the generation of spontaneous bursting.

To test whether similar mechanisms were involved in burst-quieting, we investigated the effects chronic burst-quieting for 2 days on the fraction of GABA-expressing neurons. Chronically burst-quieted cultures showed almost a two-fold increase in the fraction of GABAergic neurons compared to spontaneously active, same aged, sister cultures. Hence, homeostatic increases in GABA levels in response to increased excitatory input (electrical stimulation) might be one of the mechanisms involved in the long term control of spontaneous bursting activity in dense neuronal networks. Further insights into the role of inhibitory networks in the origin and control of global network-level activity might require quantification of the effects of bursting on the number of GABAergic synapses or receptors.

6.1.3 Spatiotemporal patterns within spontaneous bursts are indicators of functional plasticity

Now that we can control spontaneous bursting at will, we returned to the idea that bursts could reflect information processing in cortical networks. Recurring patterns of activity have been documented in various cortical preparations both *in vitro* and in the brain and have been suggested as substrates for memory. These studies, however, did not attempt to modify these patterns by external electrical stimulation. Clustering the activity

patterns within spontaneous bursts in long periods of spontaneous recordings (9-10 hours) revealed the presence of fine, diverse, repeating spatiotemporal structures that were stable for hours. Additionally, we showed that the distributions of these structures were altered by tetanic stimulation. These properties of stability, diversity and functional malleability strongly recommend spontaneous bursts as intrinsic information-carrying mechanisms in undisturbed spontaneously active neuronal networks. We propose that these stable spatiotemporal activity patterns represent attractors in the activity space of the network and tetanic stimulation serves to drive the network state from one set of attractors to another.

Though it seems contradictory that in the previous studies, we argued that bursts interfere with functional plasticity, and here we argue for the opposite (that bursts carry information), it is important to note significant differences between these two ideas. Here we suggest intrinsic spontaneous activity patterns as memory traces in un-stimulated neuronal networks. These bursts could represent patterns replayed during sleep stages [132] implicated in memory consolidation. The continuously stimulated cultures used in the previous studies could represent the active, awake, behaving brain processing multiple inputs in parallel. In such a system receiving persistent controlled input, the presence of bursts might act as a distraction serving to disrupt stimulus-induced learning. This study also indicates that bursts affect network states, and provides additional evidence that spontaneous bursting may in fact blur the effects of external stimulation.

6.2 Future research directions

Our ultimate aim is to develop closed-loop embodied systems that could bridge the knowledge gap between synaptic plasticity observed at cellular and network levels,

and animal behavior. The present work provides both the means to induce as well as reliably detect plastic changes, which is a necessary requirement for conducting feedback studies and controlling behavior in such hybrid, embodied systems.

One of the goals of providing feedback is to 'teach' the network to do things based on its spatiotemporal patterns of activity. The simplest first step might be to modify the experiments in Chapter 3 by providing tetanus based on the whether the network showed significant functional changes after the previous tetanus. If the network exhibited significant changes to tetanic stimulation, we would continue tetanizing the same pair of electrodes, else use a different pair of tetanus electrodes from a pool of electrodes. The pool of candidate electrodes for tetanus could be determined previously as the electrodes that showed highly reliable responses to stimulation. This design would provide a means to reinforce the 'appropriate' connections in the network over inappropriate ones; the appropriate connections in this scheme would be pathways that were reinforced by tetanic stimulation. It is tempting to speculate whether such a closed-loop paradigm would allow the culture to pick the reinforcing stimulation (reward) over the weakening ones (punishment). This feedback study would create stimulus-response maps in the network; each stimulus acts to selectively strengthen specific neuronal pathways unique to that stimulus such that repeated presentations of the same stimulus would result in the further strengthening of connections. Hence, long term exposure to such closed-loop stimulation could help shape the connectivity map of the network.

Since spontaneous bursts affect our ability to induce functional plasticity, they can be used in closed-loop systems as a mechanism to erase existing memory or act as negative reinforcement. In the closed-loop experiment described above, undesired action

can result in transient termination of continuous electrical quieting stimulation (instead of tetanic stimulation at a different pair of electrodes), allowing for spontaneous bursts of activity. Similar to the paradigms described above, desired action would result in positive reinforcement of tetanic stimulation on the same pair of electrodes that had previously caused significant functional change. This design would give us a method to selectively erase certain memory traces (or stimulus-response associations) in the network by simply turning off continuous electrical stimulation and allowing spontaneous global bursting.

Spontaneous burst patterns can also function as output patterns used to control adaptive behavior in embodied systems. However, spontaneous bursts occur at an average rate of ~3-4 bursts/minute, and hence their rate is too slow for studying closed-loop behavior. For the real-time feedback embodied systems our lab is interested in studying, and for possible applications in neural prosthetics, using spontaneous bursts to detect plastic changes might be too slow as we would want to correct for behavior (motor output) in the order of seconds. However, bursts may still be useful for understanding adaptation on slower time scales in hybrots.

The stimulus-response mappings obtained from this *in vitro* model system could be applied to the design of robust sensors for implantable prosthetic devices operated directly by neural recordings [51]. Present-day motor prostheses rely on visual feedback to correct for errors in motion [154], but visual feedback has large intrinsic delays (~200ms) that make it unsuitable for rapid corrections. Patients suffering a loss of the normal, rapid proprioceptive feedback can move by relying on vision of their limbs, but the movements are typically slow, poorly coordinated and require great concentration. To reduce feedback delays, we could electrically stimulate the sensory areas directly and

mappings for proprioceptive feedback [155] could be derived from our *in vitro* model system. As an example, a variation of the feedback protocol described above could be used to correct for errors in motion in motor prostheses. Since we can input complex patterns to our MEAs, and simultaneously record the output of an ensemble of neurons, I/O mappings (recordings of spatiotemporal patterns as motor output and sensory elements as stimulation input) could be developed using MEAs. This would accelerate the design of sensory elements for adding extra features to brain-controlled prostheses [50]. For a neural prosthesis to be effective, the brain must learn to reorganize encoding and decoding mechanisms. For example, the cortical neurons connected to a robotic arm must learn to generate new patterns of motor commands to adapt to different operating conditions. Our network level studies can provide the initial clues to understand the nature of these plastic changes.

Alternatively, stimulation-response mappings that actively control unwanted (pathological) activity patterns, like those found in epilepsy and Parkinson's, can be designed using the results of this work. There are several reasons that recommend this work for potential use in the control and understanding of epileptic seizures. 1) In humans, focal stimulation in the cortex or the hippocampus has been found effective in quieting epileptic seizures [89, 90, 156]. Techniques, like distributed electrical stimulation, that reduce bursting could be of potential importance in the treatment of epilepsy. 2) Pediatric epilepsy is often accompanied by cognitive impairment [100, 101]. Our results demonstrate that global bursting affects the ability of circuits to exhibit plastic changes and provide a direct link between the global seizure-like activity and long term memory. 3) Additionally, this work provides insight into the effects of global activity

patterns on cellular-level changes in the network. Activity-dependent changes in the proportion of GABAergic neurons suggests that homeostatic mechanisms might use molecular strategies (changes in transmitter expression) to adapt to chronic abnormalities in neuronal activity. Hence, by providing knowledge on the fundamental properties of population, correlated firing in neuronal networks, this work could direct future techniques to cure aberrant activity patterns in the brain.

The research presented here provides critical tools to study robust, functional, long term plastic changes in neuronal networks by providing an insight into the cellular as well as the network level mechanisms involved. Future studies of network plasticity and closed-loop learning will use these tools as their foundation to study dynamical plastic changes in a behavioral paradigm. In addition, this study of the control of aberrant network activity could contribute towards the treatment of diseases like epilepsy.

APPENDIX A

CELL CULTURING PROTOCOL

This section details the cell culturing protocols used for the studies described in this dissertation. Though each chapter provides a brief description of culturing methods used for that particular study, a general stepwise procedure to culture dissociated cortical cells on MEAs has been detailed in this section. Formulations of various cell culture media are also listed here.

Tissue dissection

Timed-pregnant Sasco Sprague-Dawley rats (Charles River) were euthanized with isoflurane according to NIH-approved protocols. Embryos were removed and euthanized by chilling and decapitation. The embryos used were at embryonic day 18. The entire neocortex, excluding the hippocampus, was dissected in Hanks Balanced Salt solution (HBSS, Invitrogen, Carlsbad, CA) under sterile conditions. The dissected tissue was stored in Hibernate E (Brainbits) at 4°C. Though the hibernate solution is optimal for maintaining neuron viability after dissection, the yield of cells is poorer in tissue maintained for over 24 hours in hibernate. All the experiments performed for this work were prepared from freshly dissected tissue.

Cell dissociation

After enzymatic digestion in 2.5U/mL papain in Segal's medium (Table A.1) for 20 minutes in a 37°C water bath, cells were mechanically dissociated by 6-9 passes through a 1mL pipette tip, in the plating medium (Table A.2). Cells were passed through

a 40μm cell strainer (Falcon, Bedford, MA) to remove large debris and then were centrifuged at 150x*g* onto 5% bovine serum albumin (BSA) in phosphate buffered saline (PBS) to remove small debris. The resulting pellet of cells was re-suspended and the required density of cells was plated in a 20μL drop of plating medium on pre-coated MEAs. The yield of cells was determined using a 0.1μL drop of cell suspension on a haemocytometer and the suspension was diluted to 2500 cells/μL. We plate mixed cultures of neural cells without differentiating between neurons and glia. Glial cells have been shown to provide necessary trophic support for the neurons [84] and hence are critical for the long term survival of cortical cultured networks.

Coating of MEAs and cell plating

MEAs were pre-coated with polyethylene imine (PEI, Sigma, 94832) and laminin (Invitrogen, L2020) [22]. The drop of laminin was dropped carefully on the center of the MEA (area covered by electrodes). Cell suspension drops of 20μL were plated on the pre-coated MEAs. Cell density in the suspension was usually 2500 cells/μL. This resulted in a plating density of ~2500 cells/mm^2 corresponding to 50,000 cells per culture. The density of the plating was verified by visual inspection under the microscope to ensure that there were cells near each electrode. After 30 minutes of incubation at 35°C, 1mL of plating media was added to each culture dish. After 24 hours, the plating medium was replaced by 1mL of the feeding medium adapted from Jimbo *et al.* (Table A.3). Cultures were maintained in an incubator at 35°C, 65% RH, 5% CO2, and 9% O2 [83].

In some cases, propidium iodide (PI) staining was conducted before plating to determine the number of dead cells in the dissociated cell suspension. 4μg/ml of PI was added to the 1mL of cell suspension and incubated for 30 minutes. Since PI stains the

nuclei of dead cells, the live-dead ratio was determined by dividing the total number of cells by the number of PI stained (dead) cells. This ratio was >95% for a successful cell plating.

Sealed dishes

Our cultures are sealed with a lids made with Teflon membrane [22] that is permeable to O_2 and CO_2, but impermeable to water. This greatly reduces or eliminates the risk of infection in our cultures allowing us to maintain them over months. Hence, we do not add any antibiotics or antimycotics in our culture medium. Additionally, the use of sealed dishes allows us to maintain our incubators at low relative humidity (65%) making it an electronics-friendly environment. All the recordings described in this work were performed inside the incubator.

Feeding and maintaining cultures

The entire medium in the culture dish was exchanged for fresh feeding medium on the same day every week. (In some experiments, half the medium was changed twice a week.) Cell densities >60,000 cells per culture required more frequent changes in medium (full medium change, at least twice a week). Medium change was found to have profound effects on the activity levels in cultures [53] as they change the local concentration of salts near the cells. All the experiments were performed at least 1 day after the day of media change to avoid interference from effects of media swapping.

In cases where pharmacological drugs were added to the medium, the drug was prepared at 2X concentration (drug was diluted in the feeding medium) and 0.5mL of medium was replaced by 0.5mL of the drug. Recordings were taken after 10 minutes of incubation with the drug in order to eliminate any effects of medium change.

Media formulation

Segals medium for dissociation

This recipe has been adapted from Banker and Goslin, pages 309-338 [82].

Table A.1: Segals media formulation

Ingredients	Concentration mM	Formula Weight g/mol	g for 500 mL
$MgCl_2$.$6H_2O$	5.8	203.31	0.59
$CaCl_2$.$2H_2O$	0.25	147.02	0.0184
HEPES	1.6	238.3	0.191
Phenol Red	(0.001%)		0.005
Na_2SO_4.$10H_2O$	90	322.21	14.5
K_2SO_4	30	174.26	2.61
Kynurenic Acid	1	189.2	94.6
APV	0.05	197.1	0.00492

The pH was adjusted to 7.4, before and after adding APV or Kynurenic acid, using 0.1N NaOH and the final volume was brought up to 500mL. Several 50mL aliquots were prepared, quick frozen using liquid nitrogen and stored at -80°C.

Note: Kynurenic acid takes a lot of stirring to dissolve, plus a fair bit more NaOH while dissolving, to keep the pH reasonable.

Preparation of papain

200µL of papain (Roche 108014, Papain suspension) was added to 2mL of Seagals solution. The pH of the mixture was adjusted to 7.4 using 30-40µL of 0.1N NaOH. The mixture was allowed to dissolve for 30-40 minutes at room temperature and

then sterilized using a sterile filter. The papain was aliquoted in 2mL tubes, frozen using liquid nitrogen and stored at -80°C.

Plating medium

The medium was switched from plating to feeding medium 24 hours after cell plating.

Table A.2: Plating medium formulation

Ingredients	Vendor	Catalog number	Volume /100mL
Neurobasal	Invitrogen	21103-049	90mL
Horse serum	Hyclone	SH30074.03	10mL
Glutamax	Invitrogen	35050-061	250 µL (0.5mM)
B27	Invitrogen	17504-044	2mL

Feeding medium

Table A.3: Feeding medium formulation

Ingredients	Vendor	Catalog number	Volume /100mL
High-glucose DMEM w/o sodium pyruvate, glutamax	Invitrogen	9024	90mL
Horse serum	Hyclone	SH30074.03	10mL
Glutamax	Invitrogen	35050-061	250µL (0.5mM)
Sodium pyruvate	Invitrogen	11360-070	1mL (1mg/mL)
Insulin	Sigma	I5500	50µL (6 IU)

Some other studies of dissociated cultures used Neurobasal medium during electrophysiological recordings, but composition of salts in the medium reduced the resting membrane potential of the neurons [157]. Instead, we used DMEM-based medium adapted from Jimbo *et al.* (1998), which preserves the resting membrane potential (Steve Potter, personal communication), as our preferred medium for feeding and extracellular electrophysiology.

APPENDIX B

ELECTRICAL STIMULATION AND RECORDING SYSTEM

This section provides technical details of the extracellular electrophysiology set up used for this dissertation work and is aimed to serve as a guideline for constructing a similar set up.

Most labs using MEAs use the commercial software that is packaged with the recording equipment (MC_Rack). Such software is not suitable for real-time applications involving closed-loop communication between the computer and neuronal networks. Our lab uses custom built MeaBench software [112] for data acquisition, visualization of streaming data and preliminary analysis of multi-electrode data.

Electrical recording

Data acquired through MCCard (Multichannel systems) was recorded and visualized using our custom-built MeaBench software[5]. MeaBench allows us not only to record raw traces but also incorporates real-time artifact suppression and spike detection tools. Spikes were detected in real-time by identifying spikes that cross a threshold of 5X RMS noise. Since spike waveforms are often multi-phasic, it is not sufficient to identify spikes by threshold crossings. Hence, in addition to threshold crossings, the detection of false positives was reduced by looking at the waveform of the spike [112]. Post spike detection, a spike was accepted only if the detected peak was the highest peak of either polarity was within a ±1ms window. Real-time artifact suppression tools (SALPA) allowed us to detect spikes as soon as 2ms after stimulation [85], on all electrodes but the

[5] http://www.its.caltech.edu/~pinelab/wagenaar/meabench.html

stimulated electrode, making this software an ideal tool for use in real-time closed-loop systems.

MeaBench can also record simultaneously from two electrode arrays on separate preamplifiers through the 128-channel MCCard. Though there were minimum problems while using this set up with parallel spontaneous recordings, electrical stimulation to any of the two electrode arrays caused considerable artifacts on the traces recorded from the other array. The same was true for noise; if there were high noise on the recorded traces on one array, it would affect the signal-to-noise of the traces recorded from the second array. Thus, for experiments incorporating electrical stimulation, we were restricted to using only one preamplifier though the hardware allows for simultaneous recording from two preamplifiers.

Electrical stimulation on 60 electrodes

Electrical stimulation was provided through our custom-built 60-channel stimulator board (RACS) [86] which allows for stimulation on all of the 60 electrodes on the array, with rapid switching between the electrodes. The stimulator was controlled using real-time Linux and stimulus sequences were coded using C++ or Matlab. Though we only used biphasic rectangular waveforms for these studies, the stimulator is capable of generating arbitrary waveforms.

Usually the timing of each stimulus pulse was marked by sending a pulse on one of the analog channels of the MCCard. Many experiments described in this research work involved interleaved sequences of stimulation on several electrodes and it became necessary to find ways to encode information of the identity of each particular stimulus (electrode number being stimulated, what part of the experiment this stimulus a part of,

inter-stimulus interval etc.). All this relevant information about each stimulus pulse was encoded in the waveform of an analog pulse (method first implemented by Daniel Wagenaar). I encoded information about the identity of the stimulus pulse by adding preceding negative phases to the positive analog pulse sent to mark the timing of the stimulus pulse. Stimulus identity information was encoded as either width or height of the negative phase of the pulse and was decoded by reading the analog waveforms from the recorded spike file. The Matlab and C++ programs used to encode and decode the analog pulse are a part of MeaBench.

Multi-computer set up

MeaBench allows for using one dedicated computer for data acquisition and another for data analysis, thus reducing the computational load on a single computer (Figure B.1). The data acquisition (DAQ) computer and the analysis computer communicate through an Ethernet port. In addition, a third computer, operating rtlinux (real-time Linux) was used to control the stimulator. This stimulator computer also communicated to the analysis computer through the Ethernet port. Thus, the set up consisted of a DAQ computer (which has the MCCard) that acquires data from the MEA preamplifier, a data analysis computer which records data from the DAQ computer and performs detailed data analysis and a stimulator computer dedicated for sending sequences of stimuli to the electrode array. This multi-computer set up allows us to upgrade the data analysis computer without disturbing the DAQ or the stimulator computers.

For connecting to the DAQ computer, launch the MeaBench module ‘neurosock’ on the DAQ computer. It can be run without any extra arguments for 64-channel MCCard

or with *neurosock – set MC128* for 128-channel MCCard. On the data analysis computer launch the MeaBench modules 'nssrv' and specify ip address of the DAQ computer: *ip mmm.nnn.ppp.rr* in nssrv. The rest of the commands for nssrv are similar to the module 'rawsrv' [112].

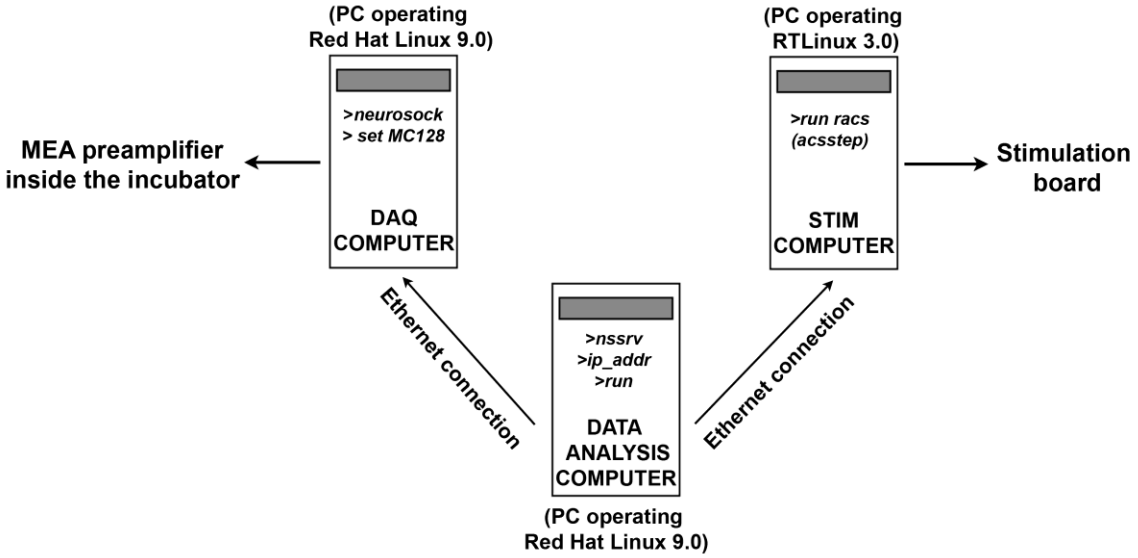

Figure B.1: Multi-computer electrophysiology set up. Schematic shows connections between various electrophysiology units and computers. The figure also shows the necessary command arguments used to communicate between the units. The DAQ and analysis computers are PCs that operate Linux Red hat 9.0, while the Stim computer could be any old PC (Pentium II or higher) that can run RTLinux.

Recording inside the incubator

The data presented here were from electrical recordings inside the incubator maintained at 35°C, 5% CO_2, 9% O_2 and 65% relative humidity. Electrical recording through the preamplifier caused ~1°C increase in temperature of the MEA relative to the ambient temperature inside the incubator. This caused some of the medium to vaporize and condense on the inside of the Teflon membrane. Condensation during long term recordings (on the scale of several hours) resulted in a considerable change in the

osmolarity of the remaining medium in the dish. Thus, it was necessary to cool the base of the MEA by ~1°C to avoid this effect.

A custom-built peltier-cooled stage was used to cool the MEA. The peltier stage consisted of peltier element sandwiched between two plates of copper. The copper plate connected to the hot side of the peltier element had a heat sink for heat dissipation. The preamplifier rested on the copper plate connected to the cold side of the peltier element. Supplying the peltier element with a constant current of ~0.9A (~1.8V) prevented condensation. The temperature of the MEA can be measured (and partially controlled) by connecting the preamplifier to the temperature control unit from Multichannel systems. This temperature control unit reads the temperature using a thermistor incorporated in the preamplifier unit.

Data visualization

Raw (entire voltage trace) as well as spike data can be recorded through MeaBench software. For most of the analysis described in this work, only spike traces were recorded since they incorporate all the information regarding the timing, location and waveforms (shape, height, width) of the spikes. Spike data recorded from MeaBench can be read into matlab using the script loadspike.m, which converts spike files into matlab-readable format. This script is incorporated as a part of MeaBench software. The attributes of gain and frequency needed by this script can be noted from the description file automatically created along with the recorded spike file. Execution of the script creates a structure containing the timing of spikes (seconds), electrodes on which spikes occurred (in hardware order from 0…63), spike height (µV) and 74 values of context (µV, at the default sampling frequency of 25kHz) around the spike. These 74 context

values can then be used to plot the waveform of the recorded spike and hence are useful for spike sorting and for determining the stimulus identity (encoded context on the analog channel). The matlab sub-directory under the MeaBench directory also contains matlab scripts to convert electrode numbers from hardware format (0…63) to the column-row arrangement of electrodes on the MEA (11…88). Once the spike stamps were read into matlab, they were used to analyze the spatiotemporal patterns in spiking activity.

APPENDIX C

IMMUNOSTAINING TECHNIQUES

This section details the general systematic procedure for conducting immunohistochemistry studies on monolayer cortical cultures.

Culture fixing and primary antibody staining

Before fixing the cultures with 4% paraformaldehyde (2g of paraformaldehyde (Sigma) mixed in 50mL of 1X PBS (Invitrogen)), the cultures were washed twice with 1X PBS to remove any floating debris. (The 4% paraformaldehyde solution was prepared in a fume hood and dissolved in 1X PBS by stirring while heating up to 60°C.) The cultures were fixed by adding 250µL of 4% paraformaldehyde to the culture for 30 minutes. The excess paraformaldehyde was removed by washing thrice with 1X PBS and the cells were permeabilized using 0.1% Triton (5µL Triton-X (Sigma) in 5mL of 1X PBS) for 20 minutes. After washing the triton (thrice with 1X PBS), the culture was blocked using 4% Goat serum (400µL goat serum (Invitrogen) in 10mL of 1X PBS) for 1.5 hours to prevent non-specific staining. The blocking solution was then replaced by 250µL of solution containing the primary antibodies in the required concentrations (as an example for 1:200 of GABA primary antibody, 5µL of GABA primary was added to 1mL of 1X PBS). It was of vital importance to stain with the right concentration of antibody to prevent partial or non-specific staining. The fixed cultures with primary antibodies added were sealed with parafilm to prevent evaporation, and kept in the refrigerator (4°C) for 12 hours. At least one other culture, functioning as control for staining, was maintained in the blocking solution without the addition of the primary

antibody. In this culture, one would expect no fluorescence, since the secondary antibody would have no primary antibody to attach to.

Secondary antibody staining

The excess of the primary antibody was removed by washing thrice with 1X PBS. This washing was carefully done to remove all excess unattached primary antibodies and reduce background fluorescence. The fixed cultures were then exposed to 250µL of solution containing the secondary antibodies in the required concentration (secondary antibody and Hoechst mixed in 1X PBS) and placed in petri-dishes covered with aluminum foil to prevent exposure to light. These petri-dishes were placed on a rocker for 1 hour at room temperature. After washing the unattached secondary antibody with 1X PBS, the dishes were filled with 1X PBS. The cultures were imaged using the appropriate filter cubes for the chosen secondary antibodies.

Details of primary and secondary antibodies used in this work

Table C.1: Primary and secondary antibodies for immunohistochemistry

Name	Vendor	Catalog #	Concentration for use
Primary antibody			
Mouse anti-MAP2 (microtubule associated protein, stringent marker for neurons)	Chemicon	MAB378	1:200
Rabbit anti-GABA (marker for GABAergic neurons)	Chemicon	AB131	1:200
Secondary antibody			

Table C.1 Continued			
Alexa Fluor 488 Goat anti-mouse	Molecular probes	A21121	1:200
Alexa Flour Goat anti-rabbit	Molecular probes	A11012	1:500
Hoechst	Molecular probes	33258	1:1000

Note: The cultures were also stained for vglut-1 (vesicular glutamate transporter 1 to identify excitatory glutamatergic neurons) using 1:500 concentration of guinea pig anti-vglut1 primary antibody (AB5905, Chemicon) [data not shown].

APPENDIX D

TESTING THE STABILITY OF PROBE RESPONSES

Most studies of network-level functional plasticity on MEAs use the responses to single-electrode stimulation (probe) to test for use-dependent changes [30, 158]. We found that the post-probe responses fluctuated considerably from trial-to-trial. In this section, I have detailed experiments aimed to reduce the inter-trial variability of post-probe responses by controlling the history of ongoing activity before the probe stimulus.

Introduction

On probing a single electrode multiple times, it was observed that its post-stimulus responses varied greatly from trial-to-trial. This inter-trial variability in responses, in the absence of plasticity-inducing stimulation, would make it difficult to determine the effects of tetanus-induced plasticity. The CA trajectories for 20 cycles of 200 probes each at a single electrode (inter-probe interval of 2s) shows that the shape of the trajectories changed enormously between multiple cycles of presentation of the same stimulus (Figure D.1). Each CA trajectory shown in the figure was an average of the CA trajectories from 200 post-probe responses (0-200ms post-probe). Different shapes of CA trajectories indicate that not only were there changes in the post-stimulus firing patterns but also different sets of electrodes were recruited in response to multiple presentations of the same stimulus.

We hypothesized that we could reduce the variability in probe responses by controlling the activity before the probe stimulus. By adding another stimulus pulse (termed ‘context’) before the probe, we could control the immediate history of activity

before the probe, possibly leading to stable post-stimulus responses. But, how soon before the probe should the context stimulus happen in order to allow for stable post-probe responses?

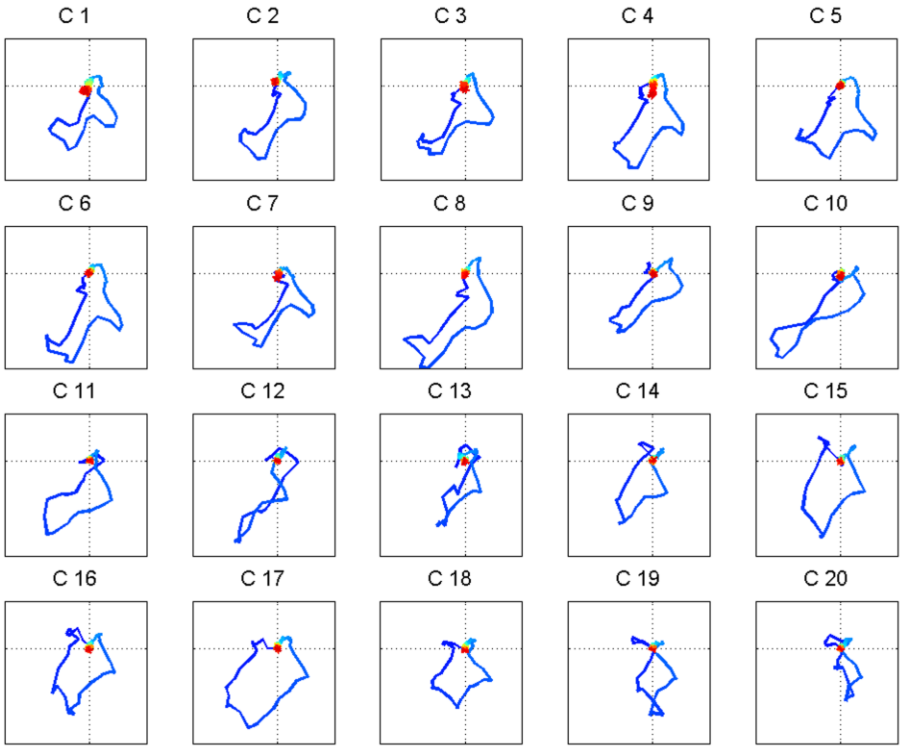

Figure D.1: Shape of CA trajectories change over multiple cycles of stimulation at the same electrode. Each cycle (C1-C20) consisted of 200 stimuli at 0.5Hz. For each cycle, the average CA trajectory over all the stimuli within the cycle is shown. Color indicates time of 0-200ms post-stimulus.

Materials and Methods

Experiment to optimize inter-pulse interval in order to reduce the variability in post-probe responses

A pair of electrodes were stimulated; the first electrode in the pair was termed 'context' (P1) while the second electrode in the pair was the probe electrode (P2). The inter-pulse interval (IPI) between P1 and P2 was 100ms-2s while the interval between P2

and the next P1 was 1-5s. An experiment consisted of 1000 pairs of stimuli at the probe and context electrodes. This experiment was repeated with four different context-probe electrode pairs. The stimulus consisted of rectangular, biphasic pulses, 400-600mV in amplitude and lasting 400μs in each phase. The probe and context electrodes were chosen from a pool of electrodes that showed post-stimulus (within 200ms after stimulus) firing rates >5X baseline firing rate before stimulus.

Analysis

For each presentation of the probe, the post-probe array-wide firing rate was determined (spikes/50ms post-stimulus). Trials with the same IPI (between context and probe stimulation) were grouped together and for each value of IPI, the mean and variance of the array-wide response were computed. Variability of the post-probe responses for each IPI was calculated as the ratio between their variance and mean.

Results and Discussion

The variability in post-probe responses was compared to the IPI between the context and the probe stimulation (Figure D.2). There was a distinct minimum in the average variability of post-probe responses at ~640ms, indicating that this value of IPI was ideal for ensuring the stability of post-probe responses. The red line shows the average curve from N=4 pairs of context-probe electrodes (Figure D.2).

Each of the gray lines indicates the relation between the IPI and post-probe variability for a context-probe pair (Figure D.2). The minima of these curves were slightly different, indicating that perhaps the ideal context-probe IPI needed to be determined separately for each pair of electrodes in an experiment. However, the IPI curves for all the electrode pairs showed a minimum IPI value between 400-700ms.

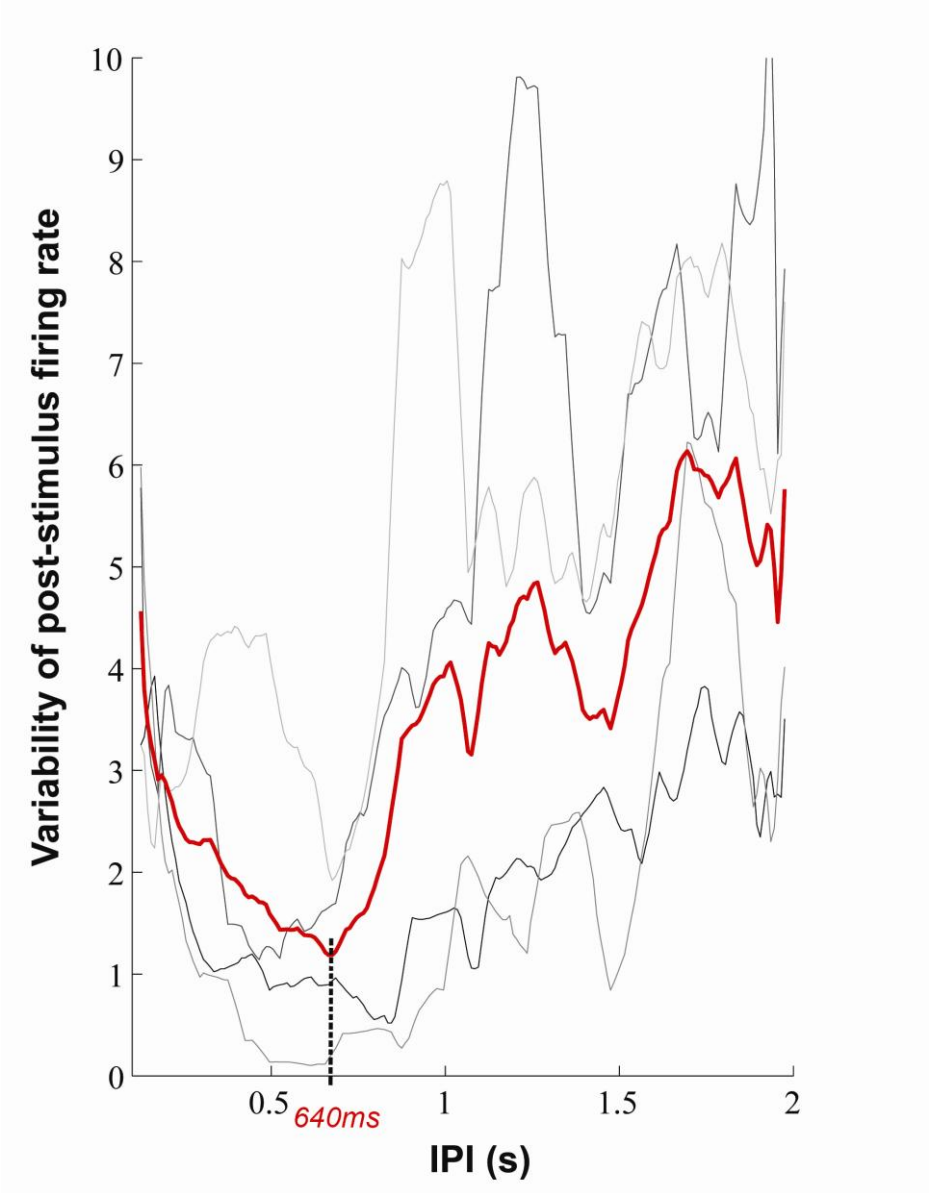

Figure D.2: Relation between the variability of post-stimulus responses and inter-pulse intervals of probe stimulation. IPI of 640ms between the context and the probe stimulus resulted in minimum variability in the post-stimulus responses. The gray curves show the individual IPI vs. variability curves for different context-probe electrode pairs. The red curve is the average of the gray curves.

In addition, it was noted that the post-probe responses were more variable if the context stimulation evoked dish-wide bursts. Thus, this indicates a relation between bursts and variability of post-stimulus responses. This aspect has been discussed in much

detail in Chapter 3. Additionally, higher IPI values (IPI >1s) could allow for more spontaneous bursting between the context and the probe stimulus. This could probably explain the increased post-probe variability at IPI values >1s.

APPENDIX E

EFFECTS OF LONG TERM ELECTRICAL BURST QUIETING

Most of the experiments described in chapters 2 and 3 involved burst-quieting stimulation delivered for short periods (minutes-hours). Chapter 4 describes the effects of long term burst quieting, delivered continuously for 2 days, on the percent of GABAergic neurons post-quieting, but it does not discuss if this chronic stimulation protocol resulted in any persistent changes in the network. More specifically, does chronic stimulation lead to permanent suppression of spontaneous bursting on the cessation of stimulation. This section describes a preliminary study aimed to investigate the effects of chronic electrical burst quieting on the spiking activity and GABAergic neuron levels 2-7 days post-quieting.

Materials and Methods

Experiment protocol

MEA cultures were burst-quieted for 2 days using distributed continuous sequential stimulation on 59 electrodes at an aggregate stimulation rate of 59Hz (inter-stimulus interval of ~17 ms). This chronic quieting protocol resulted in the successful suppression of the all the spontaneous bursts for the entire period of stimulation. Hour long recordings of spontaneous activity were obtained before the start of chronic quieting, immediately after stopping quieting stimulation and at 1, 2 and 7 days after chronic quieting. The spontaneous recording before quieting was termed as *Pre*, the 2 day-long burst-quieting period was termed *Quieted* and the subsequent days after the

chronic burst-quieting was stopped were termed as *Post1, Post2,…,Post7*. This experiment was repeated twice on two batches of sister cultures. Cultures used were between the ages of 3-4 weeks *in vitro*.

Immunostaining methods

Two sister cultures were chronically burst-quieted by multi-site electrical stimulation for 2 days, and two other sister cultures were allowed to express spontaneous bursts in parallel to serve as a *control*. The quieted cultures were then allowed to express spontaneous bursts for 2 days (*Un-quieted*), and after the 2nd day they were fixed and stained for anti-GABA and anti-MAP2 immunoreactivity [see Appendix C for more details]. The experiment was repeated twice on two batches of sister cultures. There were two *control* and two *un-quieted* cultures in each experiment. Out of the two *un-quieted* cultures, one was fixed, while the other was again recorded at 1 week (*Post 7*) after chronic quieting.

Results and Discussion

Spontaneous bursting was completely suppressed by long-term burst quieting stimulation and robust bursting resumed ~3 days after the stimulation was turned off (Figure E.1A). Although spontaneous burst rates were low in the first two days after quieting (*Post1* and *Post2*), burst rates subsequently increased in the first week post chronic quieting (Figure E.1A). At 7 days post chronic quieting, the spontaneous burst rates were much higher than in the *Pre* period.

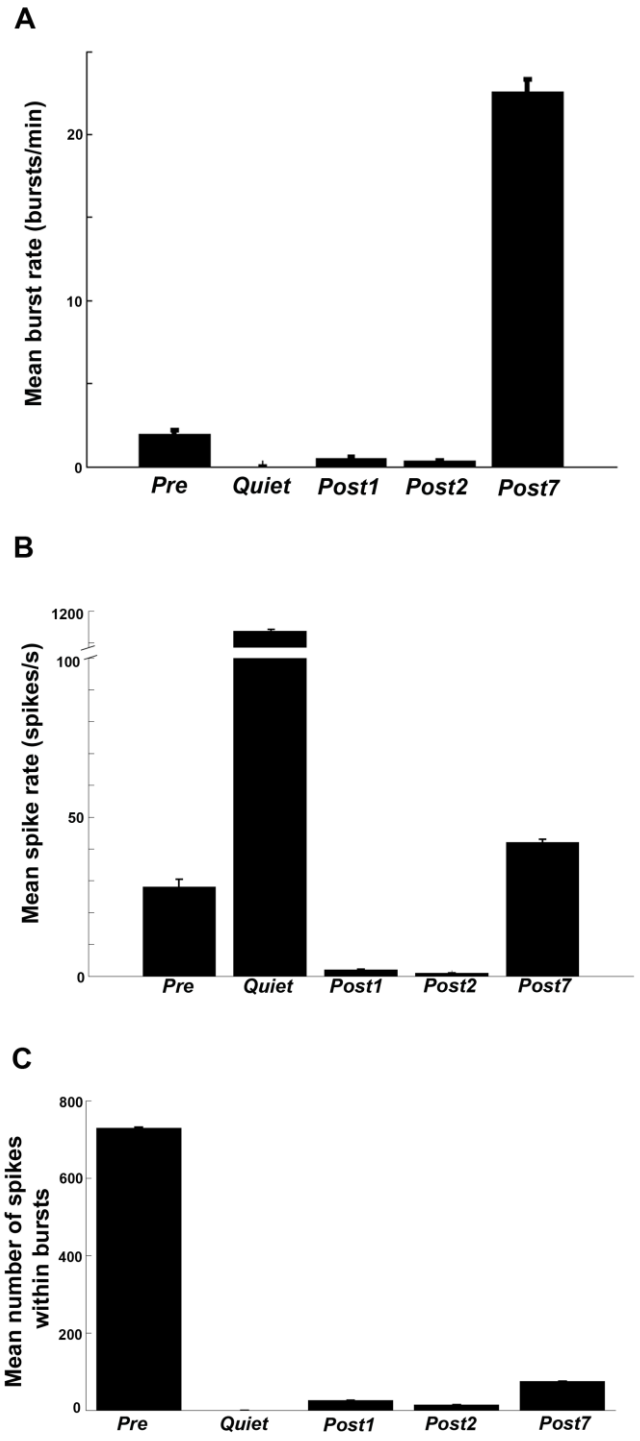

Figure E.1: Mean burst rate and mean spike rate before, during and after chronic quieting. A. Mean burst rate. Note the increase in burst rate at day 7 after quieting stimulation was stopped. These bursts observed at 7 days post chronic quieting were of shorter duration (Figure E.2).**B.** Mean spike rate. The mean spike rate (spikes per second array-wide (spsa)) during *Pre* was comparable to the mean spsa *Post7*. The spsa during quieting was much higher than during any of the spontaneous periods but none of the spikes were within bursts (Figure E.1). **C.** Mean spike rate within bursts. Data were from two cultures from two different platings.

The mean spike rate on day 7 after chronic quieting (*Post7*) was comparable to mean spike rate before the start of quieting (*Pre*) (Figure E.1B). In addition, the burst rate *Post7* was higher than the burst rate during *Pre*. However, the number of spikes within bursts was lower than at *Post7* than in *Pre* (Figure E.1C). This suggests that chronic quieting changed the properties of the culture and allowed for more dispersed activity by lowering the number of spikes within bursts (Figure E.1).

Example raster plots for various recording periods for a representative experiment are shown in figure E.2. The effects of long-term electrical burst suppression were present even after a day of quieting. Though spontaneous bursting resumed by ~1 week after chronic quieting, the burst patterns were clearly different. As shown in figure E.1C, although the number of spikes within bursts was lower in *Post7* compared to *Pre*, the burst rate was higher at *Post7* than in *Pre*. Hence, we can conclude that long-term electrical quieting affected the bursting tendencies of dissociated cultures.

The *control* cultures were stained after day 2 of the experiment (along with the *quieted* cultures) and hence there were no control cultures that were followed until *Post7* after chronic quieting. But spontaneous experiments conducted previously (Chapter 4) show that the mean spike rates and mean burst rates for non-stimulated spontaneously active cultures does not change significantly from 3-4 weeks *in vitro* (Figure 4.7). This implies that the reduction in spontaneous burst rates after chronic quieting (Figure E.1) was due to long-term stimulation rather than spontaneous changes in the culture's activity patterns.

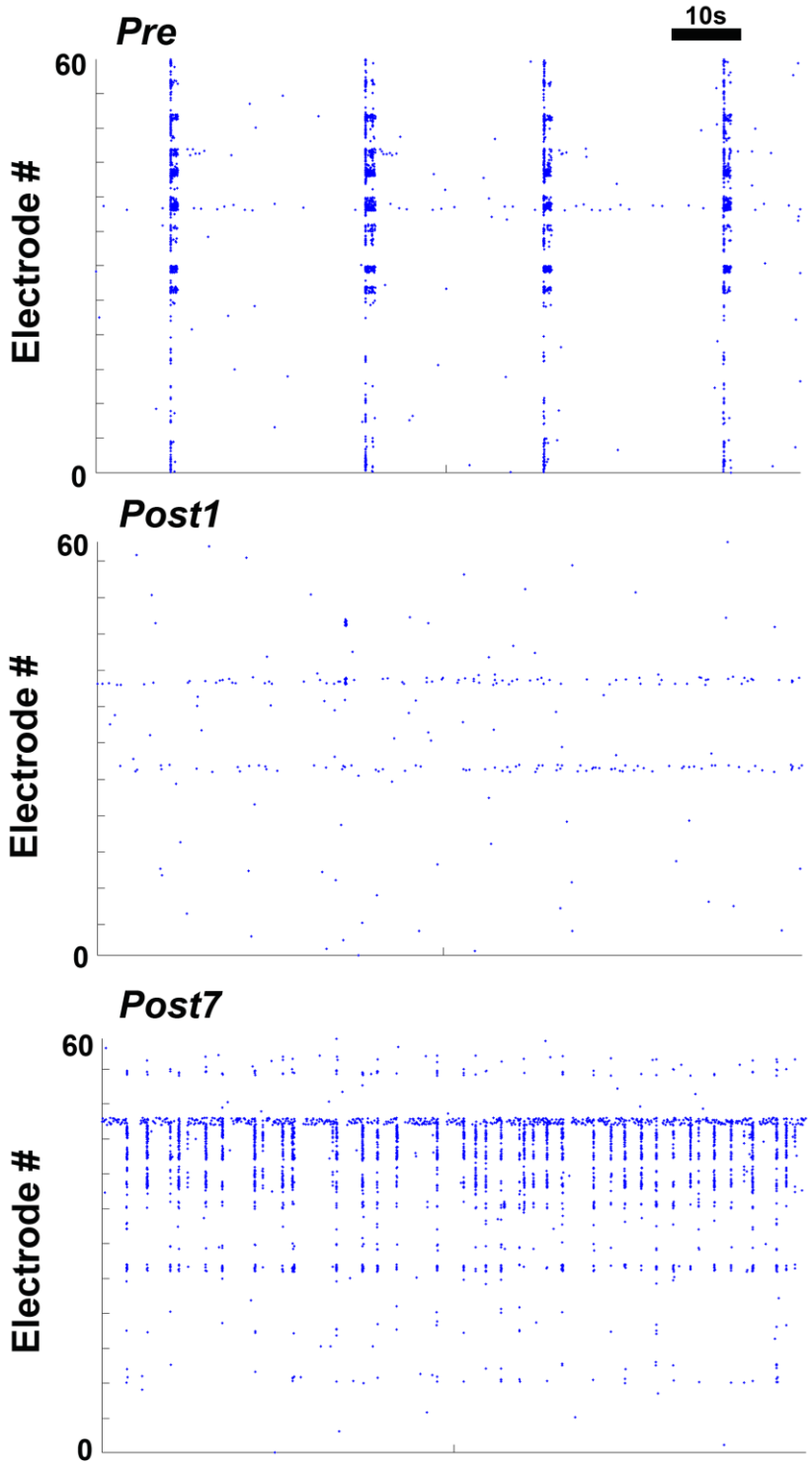

Figure E.2: Raster plots for Pre, Post1 and Post7 periods. Though the culture was dominated by spontaneous bursting before chronic burst-quieting, quieting allowed for more dispersed patterns of activity even a day after the stimulation was stopped. Spontaneous bursting resumed by a week after chronic quieting but the pattern of bursting was different.

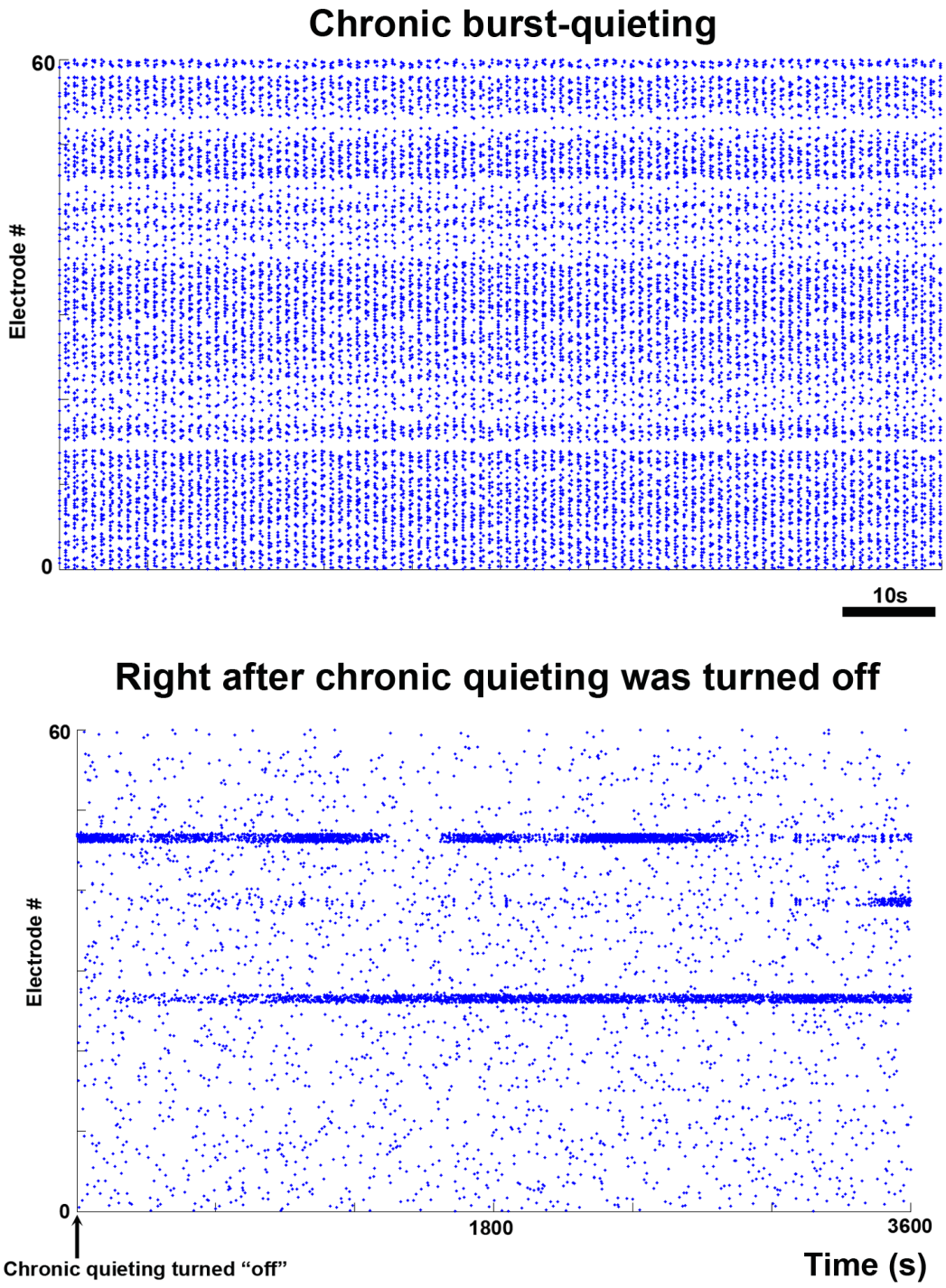

Figure E.3: Example raster plots of spiking activity during and immediately after turning off the chronic burst quieting stimulation

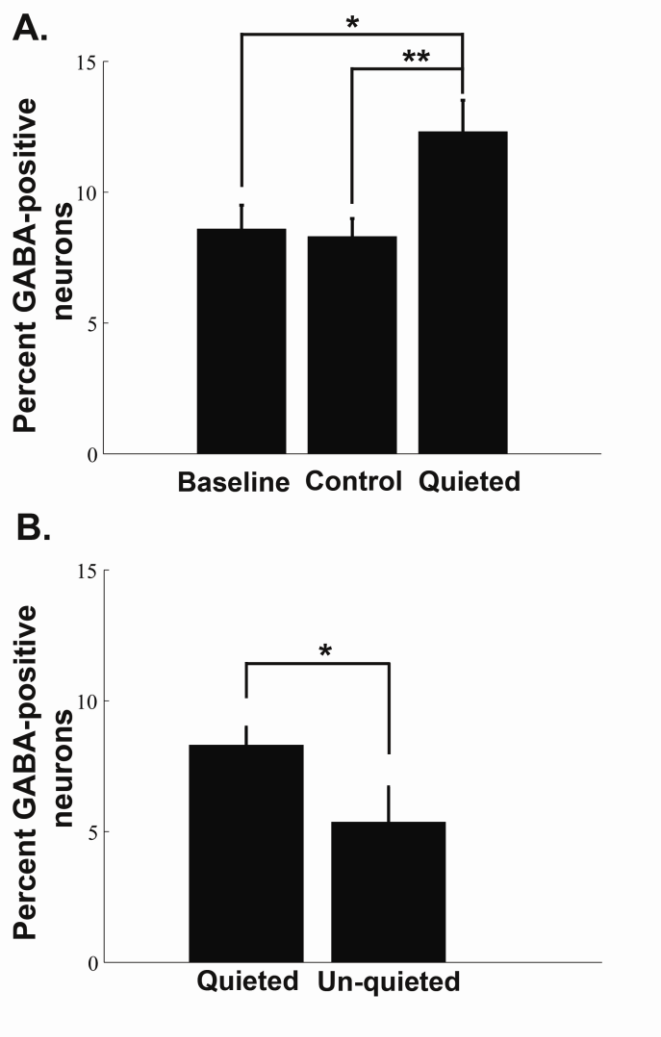

Figure E.4: Chronic burst quieting caused a significant increase in the percent of GABAergic neurons, but this percent subsequently decreased after the cessation of quieting stimulation. A. Quieted cultures (burst-quieted for 2 days) showed a significant increase in percent GABAergic neurons compared to same-age control cultures. **B.** Burst-quieted cultures allowed to spontaneously burst for 2 days after chronic quieting showed a significant decrease in the percent GABAergic neurons compared to control cultures ($p<0.05$, t-test). Asterisk ** - $p<0.005$, * - $p<0.05$

The percent of GABAergic neurons increased significantly in burst-quieted cultures compared to same age spontaneously bursting cultures (Chapter 4). On allowing the chronically quieted cultures to burst spontaneously for 2 days after chronic quieting (*un-quieted* cultures), the percent GABAergic neurons decreased significantly compared to *Control* cultures (Figure E.4, $p<0.05$, see also Immunostaining). This decrease of percent GABAergic neurons to levels below control levels may be attributed to over-

compensation by homeostatic mechanisms, caused by the sudden decrease in input (burst-quieting stimulation).

Conclusions

Long-term electrical burst quieting diminishes the tendency of the culture to burst for at least 2 days after the stimulation has been stopped (Figure E.1). Furthermore, burst-quieted cultures allowed to spontaneously burst for 2 days after long-term quieting showed a significant decrease in the percent GABAergic neurons compared to non-quieted cultures ($p<0.05$, t-test) (Figure E.4). This is a preliminary study and it would require multiple repetitions along with detailed analysis to establish the long term effects of distributed burst controlling stimulation. To ensure effective quieting of bursts, it might be attractive to repeat the above experiments with closed-loop burst-quieting stimulation [60].

REFERENCES

[1] D. O. Hebb, "The organization of behavior," New York: Wiley, 1949.

[2] G. Bi and M. Poo, "Distributed synaptic modification in neural networks induced by patterned stimulation," *Nature*, vol.401, pp. 792-6, 1999.

[3] N. A. Blum, B. G. Carkhuff, H. K. Charles, Jr., R. L. Edwards, and R. A. Meyer, "Multisite microprobes for neural recordings," *IEEE Trans Biomed Eng*, vol.38, pp. 68-74, 1991.

[4] J. Pine, "Recording action potentials from cultured neurons with extracellular microcircuit electrodes," *Journal of Neuroscience Methods*, vol.2, pp. 19-31, 1980.

[5] M. Kuperstein and H. Eichenbaum, "Unit activity, evoked potentials and slow waves in the rat hippocampus and olfactory bulb recorded with a 24-channel microelectrode," *Neuroscience*, vol.15, pp. 703-12, 1985.

[6] G. W. Gross, E. Rieske, G. W. Kreutzberg, and A. Meyer, "A new fixed-array multi-microelectrode system designed for long-term monitoring of extracellular single unit neuronal activity in vitro," *Neuroscience Letters*, vol.6, pp. 101-105, 1977.

[7] G. G. Turrigiano, "Homeostatic plasticity in neuronal networks: the more things change, the more they stay the same," *Trends Neurosci*, vol.22, pp. 221-7, 1999.

[8] G. Q. Bi and J. Rubin, "Timing in synaptic plasticity: from detection to integration," *Trends Neurosci*, vol.28, pp. 222-8, 2005.

[9] R. D. Traub, A. Bibbig, F. E. LeBeau, E. H. Buhl, and M. A. Whittington, "Cellular mechanisms of neuronal population oscillations in the hippocampus in vitro," *Annu Rev Neurosci*, vol.27, pp. 247-78, 2004.

[10] T. H. Muller, U. Misgeld, and D. Swandulla, "Ionic currents in cultured rat hypothalamic neurones," *J Physiol*, vol.450, pp. 341-62, 1992.

[11] A. Majewska and M. Sur, "Motility of dendritic spines in visual cortex in vivo: changes during the critical period and effects of visual deprivation," *Proc Natl Acad Sci U S A*, vol.100, pp. 16024-9, 2003.

[12] J. T. Trachtenberg, B. E. Chen, G. W. Knott, G. Feng, J. R. Sanes, E. Welker, and K. Svoboda, "Long-term in vivo imaging of experience-dependent synaptic plasticity in adult cortex," *Nature*, vol.420, pp. 788-94, 2002.

[13] K. Svoboda, W. Denk, D. Kleinfeld, and D. W. Tank, "In vivo dendritic calcium dynamics in neocortical pyramidal neurons," *Nature*, vol.385, pp. 161-5, 1997.

[14] J. J. Zhu and B. W. Connors, "Intrinsic firing patterns and whisker-evoked synaptic responses of neurons in the rat barrel cortex," *J Neurophysiol*, vol.81, pp. 1171-83, 1999.

[15] R. H. Britt and G. T. Rossi, "Quantitative analysis of methods for reducing physiological brain pulsations," *J Neurosci Methods*, vol.6, pp. 219-29, 1982.

[16] M. Dichter, C. Herman, and M. Selzer, "Extracellular unit analysis of the hippocampal penicillin focus," *Electroencephalogr Clin Neurophysiol*, vol.34, pp. 619-29, 1973.

[17] S. Kaech, H. Brinkhaus, and A. Matus, "Volatile anesthetics block actin-based motility in dendritic spines," *Proc Natl Acad Sci U S A*, vol.96, pp. 10433-7, 1999.

[18] S. Marom and G. Shahaf, "Development, learning and memory in large random networks of cortical neurons: lessons beyond anatomy," *Q Rev Biophys*, vol.35, pp. 63-87, 2002.

[19] S. M. Potter, D. A. Wagenaar, and T. B. DeMarse, "Closing the Loop: Stimulation Feedback Systems for Embodied MEA Cultures," in *Advances in Network Electrophysiology Using Multi-Electrode Arrays.*, M. Taketani and Baudry.M., Editors., Springer: New York. pp. 215-242., 2006.

[20] M. A. Dichter, "Rat cortical neurons in cell culture: culture methods, cell morphology, electrophysiology, and synapse formation," *Brain Res*, vol.149, pp. 279-93, 1978.

[21] J. E. Huettner and R. W. Baughman, "Primary culture of identified neurons from the visual cortex of postnatal rats," *J Neurosci*, vol.6, pp. 3044-60, 1986.

[22] S. M. Potter and T. B. DeMarse, "A new approach to neural cell culture for long-term studies," *J Neurosci Methods*, vol.110, pp. 17-24, 2001.

[23] M. Canepari, M. Bove, E. Maeda, M. Cappello, and A. Kawana, "Experimental analysis of neuronal dynamics in cultured cortical networks and transitions between different patterns of activity," *Biological Cybernetics*, vol.77, pp. 153-162, 1997.

[24] M. A. Corner, J. van Pelt, P. S. Wolters, R. E. Baker, and R. H. Nuytinck, "Physiological effects of sustained blockade of excitatory synaptic transmission on spontaneously active developing neuronal networks--an inquiry into the reciprocal linkage between intrinsic biorhythms and neuroplasticity in early ontogeny," *Neurosci Biobehav Rev*, vol.26, pp. 127-85, 2002.

[25] T. H. Murphy, L. A. Blatter, W. G. Wier, and J. M. Baraban, "Spontaneous synchronous synaptic calcium transients in cultured cortical neurons," *J Neurosci*, vol.12, pp. 4834-45, 1992.

[26] T. Opitz, A. D. De Lima, and T. Voigt, "Spontaneous development of synchronous oscillatory activity during maturation of cortical networks in vitro," *J Neurophysiol*, vol.88, pp. 2196-206, 2002.

[27] M. Meister, R. O. Wong, D. A. Baylor, and C. J. Shatz, "Synchronous bursts of action potentials in ganglion cells of the developing mammalian retina," *Science*, vol.252, pp. 939-43, 1991.

[28] R. O. Wong, M. Meister, and C. J. Shatz, "Transient period of correlated bursting activity during development of the mammalian retina," *Neuron*, vol.11, pp. 923-38, 1993.

[29] J. Streit, A. Tscherter, M. O. Heuschkel, and P. Renaud, "The generation of rhythmic activity in dissociated cultures of rat spinal cord," *Eur J Neurosci*, vol.14, pp. 191-202, 2001.

[30] Y. Jimbo, H. P. Robinson, and A. Kawana, "Strengthening of synchronized activity by tetanic stimulation in cortical cultures: application of planar electrode arrays," *IEEE Trans Biomed Eng*, vol.45, pp. 1297-304, 1998.

[31] Y. Jimbo, T. Tateno, and H. P. Robinson, "Simultaneous induction of pathway-specific potentiation and depression in networks of cortical neurons," *Biophys J*, vol.76, pp. 670-8, 1999.

[32] G. Shahaf and S. Marom, "Learning in networks of cortical neurons," *J Neurosci*, vol.21, pp. 8782-8, 2001.

[33] R. O. L. Wong, "Patterns of correlated spontaneous bursting activity in the developing mammalian retina," *Seminars in Cell & Developmental Biology*, vol.8, pp. 5-12, 1997.

[34] J. L. Puchalla, E. Schneidman, R. A. Harris, and M. J. Berry, "Redundancy in the population code of the retina," *Neuron*, vol.46, pp. 493-504, 2005.

[35] J. Demas, S. J. Eglen, and R. O. Wong, "Developmental loss of synchronous spontaneous activity in the mouse retina is independent of visual experience," *J Neurosci*, vol.23, pp. 2851-60, 2003.

[36] T. Voigt, H. Baier, and A. D. Delima, "Synchronization of neuronal-activity promotes survival of individual rat neocortical neurons in early development," *European Journal Of Neuroscience*, vol.9, pp. 990-999, 1997.

[37] E. Maeda, Y. Kuroda, H. P. Robinson, and A. Kawana, "Modification of parallel activity elicited by propagating bursts in developing networks of rat cortical neurones," *Eur J Neurosci*, vol.10, pp. 488-96, 1998.

[38] J. van Pelt, I. Vajda, P. S. Wolters, M. A. Corner, and G. J. Ramakers, "Dynamics and plasticity in developing neuronal networks in vitro," *Prog Brain Res*, vol.147, pp. 173-88, 2005.

[39] J. M. Beggs and D. Plenz, "Neuronal avalanches in neocortical circuits," *J Neurosci*, vol.23, pp. 11167-77, 2003.

[40] D. A. Wagenaar, Z. Nadasdy, and S. M. Potter, "Persistent dynamic attractors in activity patterns of cultured neuronal networks," *Phys Rev E*, vol.73, pp. 051907, 2006.

[41] F. Hofmann, E. Guenther, H. Hammerle, C. Leibrock, V. Berezin, E. Bock, and H. Volkmer, "Functional re-establishment of the perforant pathway in organotypic co-cultures on microelectrode arrays," *Brain Res*, vol.1017, pp. 184-96, 2004.

[42] G. W. Gross, A. Harsch, B. K. Rhoades, and W. Gopel, "Odor, drug and toxin analysis with neuronal networks in vitro: Extracellular array recording of network responses," *Biosensors & Bioelectronics*, vol.12, pp. 373-393, 1997.

[43] A. Stett, U. Egert, E. Guenther, F. Hofmann, T. Meyer, W. Nisch, and H. Haemmerle, "Biological application of microelectrode arrays in drug discovery and basic research," *Anal Bioanal Chem*, vol.377, pp. 486-95, 2003.

[44] M. E. Ruaro, P. Bonifazi, and V. Torre, "Toward the neurocomputer: image processing and pattern recognition with neuronal cultures," *IEEE Trans Biomed Eng*, vol.52, pp. 371-83, 2005.

[45] D. A. Wagenaar, J. Pine, and S. M. Potter, "Searching for plasticity in dissociated cortical cultures on multi-electrode arrays," *J Negat Results Biomed*, vol.5, pp. 16, 2006.

[46] G. W. Staveren, J. R. Buitenweg, E. Marani, and W. L. C. Rutten. "The Effect of Training of Cultured Neuronal Networks, Can They Learn?" presented at The 2nd International Conference on Neural Engineering, March 2005, Arlington, VA, USA, Arlington, Washington DC, 2005.

[47] C. G. Morris, "Psychology: An Introduction," New York, NY: Prentice Hall, 1973.

[48] D. J. Bakkum, A. C. Shkolnik, G. Ben-Ary, P. Gamblen, T. B. DeMarse, and S. M. Potter, "Removing some 'A' from AI: Embodied Cultured Networks.," in *Embodied Artificial Intelligence*, F. Iida, Pfeifer, R., Steels, L. and Kuniyoshi, Y., Editor., Springer: New York. pp. 130-145, 2004.

[49] T. B. DeMarse, D. A. Wagenaar, A. W. Blau, and S. M. Potter, "The Neurally Controlled Animat: Biological Brains Acting with Simulated Bodies," *Autonomous Robots*, vol.11, pp. 305-310, 2001.

[50] F. A. Mussa-Ivaldi and L. E. Miller, "Brain-machine interfaces: computational demands and clinical needs meet basic neuroscience," *Trends Neurosci*, vol.26, pp. 329-34, 2003.

[51] M. A. Nicolelis, "Brain-machine interfaces to restore motor function and probe neural circuits," *Nat Rev Neurosci*, vol.4, pp. 417-22, 2003.

[52] T. V. Bliss and T. Lomo, "Long-lasting potentiation of synaptic transmission in the dentate area of the anaesthetized rabbit following stimulation of the perforant path," *J Physiol*, vol.232, pp. 331-56, 1973.

[53] D. A. Wagenaar, J. Pine, and S. M. Potter, "An extremely rich repertoire of bursting patterns during the development of cortical cultures," *BMC Neurosci*, vol.7, pp. 11, 2006.

[54] H. Kamioka, E. Maeda, Y. Jimbo, H. P. C. Robinson, and A. Kawana, "Spontaneous periodic synchronized bursting during formation of mature patterns of connections in cortical cultures," *Neuroscience Letters*, vol.206, pp. 109-112, 1996.

[55] P. E. Latham, B. J. Richmond, S. Nirenberg, and P. G. Nelson, "Intrinsic dynamics in neuronal networks. II. experiment," *J Neurophysiol*, vol.83, pp. 828-35, 2000.

[56] J. E. Lisman, "Bursts as a unit of neural information: making unreliable synapses reliable," *Trends Neurosci*, vol.20, pp. 38-43, 1997.

[57] E. J. Furshpan and D. D. Potter, "Seizure-like activity and cellular damage in rat hippocampal neurons in cell culture," *Neuron*, vol.3, pp. 199-207, 1989.

[58] Madhavan R, Chao C, Wagenaar D.A., Bakkum D.J, and P. S.M. "Multi-site Stimulation Quiets Network-wide Spontaneous Bursts and Enhances Functional Plasticity in Cultured Cortical Networks." presented at EMBC 2006, New York City, NY, 2006.

[59] Z. C. Chao, D. J. Bakkum, D. A. Wagenaar, and S. M. Potter, "Effects of random external background stimulation on network synaptic stability after tetanization: a modeling study," *Neuroinformatics*, vol.3, pp. 263-80, 2005.

[60] D. A. Wagenaar, R. Madhavan, J. Pine, and S. M. Potter, "Controlling bursting in cortical cultures with closed-loop multi-electrode stimulation," *J Neurosci*, vol.25, pp. 680-8, 2005.

[61] O. Garaschuk, E. Hanse, and A. Konnerth, "Developmental profile and synaptic origin of early network oscillations in the CA1 region of rat neonatal hippocampus," *J Physiol*, vol.507 (Pt 1), pp. 219-36, 1998.

[62] M. J. O'Donovan, N. Chub, and P. Wenner, "Mechanisms of spontaneous activity in developing spinal networks," *J Neurobiol*, vol.37, pp. 131-45, 1998.

[63] P. Wenner and M. J. O'Donovan, "Mechanisms that initiate spontaneous network activity in the developing chick spinal cord," *J Neurophysiol*, vol.86, pp. 1481-98, 2001.

[64] Y. Ben-Ari, E. Cherubini, R. Corradetti, and J. L. Gaiarsa, "Giant synaptic potentials in immature rat CA3 hippocampal neurones," *J Physiol*, vol.416, pp. 303-25, 1989.

[65] X. Leinekugel, R. Khazipov, R. Cannon, H. Hirase, Y. Ben-Ari, and G. Buzsaki, "Correlated bursts of activity in the neonatal hippocampus in vivo," *Science*, vol.296, pp. 2049-2052, 2002.

[66] M. J. O'Donovan, "The origin of spontaneous activity in developing networks of the vertebrate nervous system," *Curr Opin Neurobiol*, vol.9, pp. 94-104, 1999.

[67] A. R. Houweling, M. Bazhenov, I. Timofeev, M. Steriade, and T. J. Sejnowski, "Homeostatic synaptic plasticity can explain post-traumatic epileptogenesis in chronically isolated neocortex," *Cereb Cortex*, vol.15, pp. 834-45, 2005.

[68] R. Madhavan, D. A.Wagenaar, C. H. Chao, and S. M. Potter. "Control of bursting in dissociated cortical cultures on multi-electrode arrays." presented at Substrate-Integrated Micro-Electrode Arrays, Denton, Texas, 2003.

[69] G. J. Ramakers, H. van Galen, M. G. Feenstra, M. A. Corner, and G. J. Boer, "Activity-dependent plasticity of inhibitory and excitatory amino acid transmitter systems in cultured rat cerebral cortex," *Int J Dev Neurosci*, vol.12, pp. 611-21, 1994.

[70] G. W. Gross, B. K. Rhoades, and J. K. Kowalski, "Dynamics of burst patterns generated by monolayer networks in culture," in *Neurobionics: An Interdisciplinary Approach to Substitute Impaired Functions of the Human Nervous System*, H.W. Bothe, M. Samii, and R. Eckmiller, Editors., North-Holland: Amsterdam. pp. 89-121, 1993.

[71] P. Darbon, L. Scicluna, A. Tscherter, and J. Streit, "Mechanisms controlling bursting activity induced by disinhibition in spinal cord networks," *Eur J Neurosci*, vol.15, pp. 671-83, 2002.

[72] R. Krahe and F. Gabbiani, "Burst firing in sensory systems," *Nat Rev Neurosci*, vol.5, pp. 13-23, 2004.

[73] R. Madhavan, D. A. Wagenaar, and S. M. Potter. "Multi-site stimulation quiets bursts and enhances plasticity in cultured networks." presented at Society for Neuroscience Meeting, New Orleans, LA, 2003.

[74] M. A. Corner and G. J. Ramakers, "Spontaneous firing as an epigenetic factor in brain development--physiological consequences of chronic tetrodotoxin and picrotoxin exposure on cultured rat neocortex neurons," *Brain Res Dev Brain Res*, vol.65, pp. 57-64, 1992.

[75] M. Ichikawa, K. Muramoto, K. Kobayashi, M. Kawahara, and Y. Kuroda, "Formation and maturation of synapses in primary cultures of rat cerebral cortical cells: an electron microscopic study," *Neurosci Res*, vol.16, pp. 95-103, 1993.

[76] K. Muramoto, M. Ichikawa, M. Kawahara, K. Kobayashi, and Y. Kuroda, "Frequency of synchronous oscillations of neuronal activity increases during development and is correlated to the number of synapses in cultured cortical neuron networks," *Neurosci Lett*, vol.163, pp. 163-5, 1993.

[77] F. van Huizen, H. J. Romijn, and A. M. Habets, "Synaptogenesis in rat cerebral cortex cultures is affected during chronic blockade of spontaneous bioelectric activity by tetrodotoxin," *Brain Res*, vol.351, pp. 67-80, 1985.

[78] T. Voigt, T. Opitz, and A. D. de Lima, "Synchronous oscillatory activity in immature cortical network is driven by GABAergic preplate neurons," *J Neurosci*, vol.21, pp. 8895-905, 2001.

[79] Y. Ben-Ari, "Developing networks play a similar melody," *Trends Neurosci*, vol.24, pp. 353-60, 2001.

[80] R. O. Wong, "Retinal waves and visual system development," *Annu Rev Neurosci*, vol.22, pp. 29-47, 1999.

[81] D. Heck, "Investigating dynamic aspects of brain function in slice preparations: spatiotemporal stimulus patterns generated with an easy-to-build multi-electrode array," *J Neurosci Methods*, vol.58, pp. 81-7, 1995.

[82] G. Banker and K. Goslin, "Culturing Nerve Cells, 2nd Edition," Cambridge, Mass.: MIT Press, 1998.

[83] G. J. Brewer and C. W. Cotman, "Survival and growth of hippocampal neurons in defined medium at low density: advantages of a sandwich culture technique or low oxygen," *Brain Res*, vol.494, pp. 65-74, 1989.

[84] E. M. Ullian, S. K. Sapperstein, K. S. Christopherson, and B. A. Barres, "Control of synapse number by glia," *Science*, vol.291, pp. 657-61, 2001.

[85] D. A. Wagenaar and S. M. Potter, "Real-time multi-channel stimulus artifact suppression by local curve fitting," *J Neurosci Methods*, vol.120, pp. 113-20, 2002.

[86] D. A. Wagenaar and S. M. Potter, "A versatile all-channel stimulator for electrode arrays, with real-time control," *J Neural Eng*, vol.1, pp. 39-45, 2004.

[87] D. A. Wagenaar, J. Pine, and S. M. Potter, "Effective parameters for stimulation of dissociated cultures using multi-electrode arrays," *J Neurosci Methods*, vol.138, pp. 27-37, 2004.

[88] J. F. Kerrigan, B. Litt, R. S. Fisher, S. Cranstoun, J. A. French, D. E. Blum, M. Dichter, A. Shetter, G. Baltuch, J. Jaggi, S. Krone, M. Brodie, M. Rise, and N. Graves, "Electrical stimulation of the anterior nucleus of the thalamus for the treatment of intractable epilepsy," *Epilepsia*, vol.45, pp. 346-54, 2004.

[89] F. Velasco, M. Velasco, A. L. Velasco, D. Menez, and L. Rocha, "Electrical stimulation for epilepsy: stimulation of hippocampal foci," *Stereotact Funct Neurosurg*, vol.77, pp. 223-7, 2001.

[90] D. S. Dinner, S. Neme, D. Nair, E. B. Montgomery, Jr., K. B. Baker, A. Rezai, and H. O. Luders, "EEG and evoked potential recording from the subthalamic nucleus for deep brain stimulation of intractable epilepsy," *Clin Neurophysiol*, vol.113, pp. 1391-402, 2002.

[91] E. J. Tehovnik, "Electrical stimulation of neural tissue to evoke behavioral responses," *J Neurosci Methods*, vol.65, pp. 1-17, 1996.

[92] B. Hu, S. Karnup, L. Zhou, and A. Stelzer, "Reversal of hippocampal LTP by spontaneous seizure-like activity: role of group I mGluR and cell depolarization," *J Neurophysiol*, vol.93, pp. 316-36, 2005.

[93] S. D. Moore, D. S. Barr, and W. A. Wilson, "Seizure-like activity disrupts LTP in vitro," *Neurosci Lett*, vol.163, pp. 117-9, 1993.

[94] M. Lynch, U. Sayin, J. Bownds, S. Janumpalli, and T. Sutula, "Long-term consequences of early postnatal seizures on hippocampal learning and plasticity," *Eur J Neurosci*, vol.12, pp. 2252-64, 2000.

[95] P. J. Thompson, "Memory function in patients with epilepsy," *Adv Neurol*, vol.55, pp. 369-84, 1991.

[96] C. Beaulieu, "Numerical data on neocortical neurons in adult rat, with special reference to the GABA population," *Brain Res*, vol.609, pp. 284-92, 1993.

[97] M. A. Kisley and G. L. Gerstein, "Trial-to-trial variability and state-dependent modulation of auditory-evoked responses in cortex," *J Neurosci*, vol.19, pp. 10451-60, 1999.

[98] G. L. Holmes, "Effects of early seizures on later behavior and epileptogenicity," *Ment Retard Dev Disabil Res Rev*, vol.10, pp. 101-5, 2004.

[99] J. W. Swann and J. J. Hablitz, "Cellular abnormalities and synaptic plasticity in seizure disorders of the immature nervous system," *Ment Retard Dev Disabil Res Rev*, vol.6, pp. 258-67, 2000.

[100] A. Kolk, A. Beilmann, T. Tomberg, A. Napa, and T. Talvik, "Neurocognitive development of children with congenital unilateral brain lesion and epilepsy," *Brain Dev*, vol.23, pp. 88-96, 2001.

[101] J. W. Swann, "The effects of seizures on the connectivity and circuitry of the developing brain," *Ment Retard Dev Disabil Res Rev*, vol.10, pp. 96-100, 2004.

[102] Y. Ben-Ari, "Excitatory actions of gaba during development: the nature of the nurture," *Nat Rev Neurosci*, vol.3, pp. 728-39, 2002.

[103] Y. Ben-Ari, "Basic developmental rules and their implications for epilepsy in the immature brain," *Epileptic Disord*, vol.8, pp. 91-102, 2006.

[104] S. H. Hendry and E. G. Jones, "Activity-dependent regulation of GABA expression in the visual cortex of adult monkeys," *Neuron*, vol.1, pp. 701-12, 1988.

[105] A. R. Kriegstein, T. Suppes, and D. A. Prince, "Cellular and synaptic physiology and epileptogenesis of developing rat neocortical neurons in vitro," *Brain Res*, vol.431, pp. 161-71, 1987.

[106] K. F. Fischer, P. D. Lukasiewicz, and R. O. Wong, "Age-dependent and cell class-specific modulation of retinal ganglion cell bursting activity by GABA," *J Neurosci*, vol.18, pp. 3767-78, 1998.

[107] E. Sernagor and N. M. Grzywacz, "Spontaneous activity in developing turtle retinal ganglion cells: pharmacological studies," *J Neurosci*, vol.19, pp. 3874-87, 1999.

[108] E. Sernagor, C. Young, and S. J. Eglen, "Developmental modulation of retinal wave dynamics: shedding light on the GABA saga," *J Neurosci*, vol.23, pp. 7621-9, 2003.

[109] S. R. Snodgrass, W. F. White, B. Biales, and M. Dichter, "Biochemical correlates of GABA function in rat cortical neurons in culture," *Brain Res*, vol.190, pp. 123-38, 1980.

[110] G. Turrigiano, L. F. Abbott, and E. Marder, "Activity-dependent changes in the intrinsic-properties of cultured neurons," *Science*, vol.264, pp. 974-977, 1994.

[111] A. D. de Lima, B. D. Lima, and T. Voigt, "Earliest spontaneous activity differentially regulates neocortical GABAergic interneuron subpopulations," *Eur J Neurosci*, vol.25, pp. 1-16, 2007.

[112] D. A. Wagenaar, T. B. DeMarse, and S. M. Potter. "MEABench: A toolset for multi-electrode data acquisition and on-line analysis." presented at 2nd International IEEE EMBS Conference on Neural Engineering, Arlington, VA, 2005.

[113] A. D. de Lima and T. Voigt, "Identification of two distinct populations of gamma-aminobutyric acidergic neurons in cultures of the rat cerebral cortex," *J Comp Neurol*, vol.388, pp. 526-40, 1997.

[114] A. D. de Lima, M. D. Merten, and T. Voigt, "Neuritic differentiation and synaptogenesis in serum-free neuronal cultures of the rat cerebral cortex," *J Comp Neurol*, vol.382, pp. 230-46, 1997.

[115] A. D. de Lima, T. Opitz, and T. Voigt, "Irreversible loss of a subpopulation of cortical interneurons in the absence of glutamatergic network activity," *Eur J Neurosci*, vol.19, pp. 2931-43, 2004.

[116] P. E. Garraghty, E. A. LaChica, and J. H. Kaas, "Injury-induced reorganization of somatosensory cortex is accompanied by reductions in GABA staining," *Somatosens Mot Res*, vol.8, pp. 347-54, 1991.

[117] L. A. Benevento, B. W. Bakkum, and R. S. Cohen, "gamma-Aminobutyric acid and somatostatin immunoreactivity in the visual cortex of normal and dark-reared rats," *Brain Res*, vol.689, pp. 172-82, 1995.

[118] K. D. Micheva and C. Beaulieu, "Neonatal sensory deprivation induces selective changes in the quantitative distribution of GABA-immunoreactive neurons in the rat barrel field cortex," *J Comp Neurol*, vol.361, pp. 574-84, 1995.

[119] L. N. Borodinsky, C. M. Root, J. A. Cronin, S. B. Sann, X. Gu, and N. C. Spitzer, "Activity-dependent homeostatic specification of transmitter expression in embryonic neurons," *Nature*, vol.429, pp. 523-30, 2004.

[120] J. J. LoTurco, D. F. Owens, M. J. Heath, M. B. Davis, and A. R. Kriegstein, "GABA and glutamate depolarize cortical progenitor cells and inhibit DNA synthesis," *Neuron*, vol.15, pp. 1287-98, 1995.

[121] D. F. Owens, X. Liu, and A. R. Kriegstein, "Changing properties of GABA(A) receptor-mediated signaling during early neocortical development," *J Neurophysiol*, vol.82, pp. 570-83, 1999.

[122] H. P. Robinson, M. Kawahara, Y. Jimbo, K. Torimitsu, Y. Kuroda, and A. Kawana, "Periodic synchronized bursting and intracellular calcium transients elicited by low magnesium in cultured cortical neurons," *J Neurophysiol*, vol.70, pp. 1606-16, 1993.

[123] C. L. Lee, J. Hannay, R. Hrachovy, S. Rashid, B. Antalffy, and J. W. Swann, "Spatial learning deficits without hippocampal neuronal loss in a model of early-onset epilepsy," *Neuroscience*, vol.107, pp. 71-84, 2001.

[124] J. W. Swann, J. T. Le, and C. L. Lee, "Recurrent seizures and the molecular maturation of hippocampal and neocortical glutamatergic synapses," *Dev Neurosci*, vol.29, pp. 168-78, 2007.

[125] R. Gutierrez, H. Romo-Parra, J. Maqueda, C. Vivar, M. Ramirez, M. A. Morales, and M. Lamas, "Plasticity of the GABAergic phenotype of the "glutamatergic" granule cells of the rat dentate gyrus," *J Neurosci*, vol.23, pp. 5594-8, 2003.

[126] R. Madhavan, Z. C. Chao, D. J. Bakkum, Wagenaar D. A., and P. S. M. "Multi-site Stimulation Quiets Network-wide Spontaneous Bursts and Enhances Functional Plasticity in Cultured Cortical Networks." presented at IEEE 2006 International Conference of the Engineering in Medicine and Biology Society, New York City, NY, 2006.

[127] D. L. Meinecke and A. Peters, "GABA immunoreactive neurons in rat visual cortex," *J Comp Neurol*, vol.261, pp. 388-404, 1987.

[128] C. S. Lin, S. M. Lu, and D. E. Schmechel, "Glutamic acid decarboxylase and somatostatin immunoreactivities in rat visual cortex," *J Comp Neurol*, vol.244, pp. 369-83, 1986.

[129] J. M. Beggs and D. Plenz, "Neuronal avalanches are diverse and precise activity patterns that are stable for many hours in cortical slice cultures," *J Neurosci*, vol.24, pp. 5216-29, 2004.

[130] Z. Nadasdy, "Spike sequences and their consequences," *J Physiol Paris*, vol.94, pp. 505-24, 2000.

[131] K. L. Hoffman and B. L. McNaughton, "Coordinated reactivation of distributed memory traces in primate neocortex," *Science*, vol.297, pp. 2070-3, 2002.

[132] Z. Nadasdy, H. Hirase, A. Czurko, J. Csicsvari, and G. Buzsaki, "Replay and time compression of recurring spike sequences in the hippocampus," *J Neurosci*, vol.19, pp. 9497-507, 1999.

[133] M. A. Wilson and B. L. McNaughton, "Reactivation of hippocampal ensemble memories during sleep," *Science*, vol.265, pp. 676-9, 1994.

[134] Y. Ikegaya, M. Le Bon-Jego, and R. Yuste, "Large-scale imaging of cortical network activity with calcium indicators," *Neurosci Res*, vol.52, pp. 132-8, 2005.

[135] R. Cossart, Y. Ikegaya, and R. Yuste, "Calcium imaging of cortical networks dynamics," *Cell Calcium*, vol.37, pp. 451-7, 2005.

[136] S. J. Martin, P. D. Grimwood, and R. G. M. Morris, "Synaptic plasticity and memory: An evaluation of the hypothesis," *Annual Review of Neuroscience*, vol.23, pp. 649-711, 2000.

[137] G. W. Gross and J. M. Kowalski, "Origins of activity patterns in self-organizing neuronal networks in vitro," *Journal of Intelligent Material Systems and Structures*, vol.10, pp. 558-564, 1999.

[138] M. A. Castro-Alamancos, J. P. Donoghue, and B. W. Connors, "Different forms of synaptic plasticity in somatosensory and motor areas of the neocortex," *J Neurosci*, vol.15, pp. 5324-33, 1995.

[139] A. Kirkwood and M. F. Bear, "Hebbian synapses in visual cortex," *J Neurosci*, vol.14, pp. 1634-45, 1994.

[140] R. L. Berry, T. J. Teyler, and T. Z. Han, "Induction of LTP in rat primary visual cortex: tetanus parameters," *Brain Res*, vol.481, pp. 221-7, 1989.

[141] A. B. Mulder, M. P. Arts, and F. H. Lopes da Silva, "Short- and long-term plasticity of the hippocampus to nucleus accumbens and prefrontal cortex pathways in the rat, in vivo," *Eur J Neurosci*, vol.9, pp. 1603-11, 1997.

[142] C. M. Werk and C. A. Chapman, "Long-term potentiation of polysynaptic responses in layer V of the sensorimotor cortex induced by theta-patterned tetanization in the awake rat," *Cereb Cortex*, vol.13, pp. 500-7, 2003.

[143] S. J. Martin and R. G. M. Morris, "New life in an old idea: The synaptic plasticity and memory hypothesis revisited," *Hippocampus*, vol.12, pp. 609-636, 2002.

[144] O. Feinerman, M. Segal, and E. Moses, "Identification and dynamics of spontaneous burst initiation zones in unidimensional neuronal cultures," *J Neurophysiol*, vol.97, pp. 2937-48, 2007.

[145] F. Rieke, "Spikes: exploring the neural code," Cambridge, Mass.: MIT Press, 1997.

[146] T. Tateno and Y. Jimbo, "Activity-dependent enhancement in the reliability of correlated spike timings in cultured cortical neurons," *Biol Cybern*, vol.80, pp. 45-55, 1999.

[147] D. Eytan and S. Marom, "Dynamics and effective topology underlying synchronization in networks of cortical neurons," *J Neurosci*, vol.26, pp. 8465-76, 2006.

[148] R. Segev, I. Baruchi, E. Hulata, and E. Ben-Jacob, "Hidden neuronal correlations in cultured networks," *Phys Rev Lett*, vol.92, pp. 118102, 2004.

[149] W. Bair, C. Koch, W. Newsome, and K. Britten, "Power spectrum analysis of bursting cells in area MT in the behaving monkey," *J Neurosci*, vol.14, pp. 2870-92, 1994.

[150] A. Kepecs, X. J. Wang, and J. Lisman, "Bursting neurons signal input slope," *J Neurosci*, vol.22, pp. 9053-62, 2002.

[151] A. Kepecs and J. Lisman, "How to read a burst duration code," *Neurocomputing*, vol.58-60, pp. 1-6, 2004.

[152] Y. Ikegaya, G. Aaron, R. Cossart, D. Aronov, I. Lampl, D. Ferster, and R. Yuste, "Synfire chains and cortical songs: temporal modules of cortical activity," *Science*, vol.304, pp. 559-64, 2004.

[153] C. G. Morris, "Psychology: An Introduction," New York 1973.

[154] P. R. Kennedy, R. A. Bakay, M. M. Moore, K. Adams, and J. Goldwaithe, "Direct control of a computer from the human central nervous system," *IEEE Trans Rehabil Eng*, vol.8, pp. 198-202, 2000.

[155] D. Duncan, "Implanting Hope," *Technology review*, vol.108, pp. 48-54, 2005.

[156] K. Vonck, P. Boon, E. Achten, J. De Reuck, and J. Caemaert, "Long-term amygdalohippocampal stimulation for refractory temporal lobe epilepsy," *Ann Neurol*, vol.52, pp. 556-65, 2002.

[157] M. S. Evans, M. A. Collings, and G. J. Brewer, "Electrophysiology of embryonic, adult and aged rat hippocampal neurons in serum-free culture," *J Neurosci Methods*, vol.79, pp. 37-46, 1998.

[158] E. Maeda, H. P. Robinson, and A. Kawana, "The mechanisms of generation and propagation of synchronized bursting in developing networks of cortical neurons," *J Neurosci*, vol.15, pp. 6834-45, 1995.

VITA

Radhika was born in New Delhi, India. She received her B.S in Electrical Engineering from the Maharaja Sayajirao University, Vadodara, India and was awarded two gold medals for securing the highest grades in her graduating class. She was placed in the top 50 students in India in the nationwide tests conducted to secure admission into prestigious graduate programs across the country. Radhika went on to pursue her Masters in Biomedical Engineering at the Indian Institute of Technology (IIT), Bombay, India. During her Masters at IIT Bombay, Radhika was supported by the Government of India and was involved in developing a low-cost myoelectric prostheses for lower elbow amputees currently being made available to hospitals across India. She joined the Georgia Institute of Technology in 2002 to pursue a PhD in Bioengineering. During her PhD, Radhika has presented her research work at various conferences around the country, both in the form of posters as well as talks. She is a recipient of the Faculty of the Future grant from the Schlumberger Foundation, which encourages the participation of women in Science and Engineering. Radhika's future plans include hiking the Himalayas and spending more time with her family back in India, before getting back to an academic career in Neuroscience.